

12-1-2010

An impaired 20S proteasome contributes to the accumulation of oxidized proteins in multiple sclerosis and its animal model

Jianzheng Zheng

Follow this and additional works at: https://digitalrepository.unm.edu/biom_etds

Recommended Citation

Zheng, Jianzheng. "An impaired 20S proteasome contributes to the accumulation of oxidized proteins in multiple sclerosis and its animal model." (2010). https://digitalrepository.unm.edu/biom_etds/27

This Dissertation is brought to you for free and open access by the Electronic Theses and Dissertations at UNM Digital Repository. It has been accepted for inclusion in Biomedical Sciences ETDs by an authorized administrator of UNM Digital Repository. For more information, please contact disc@unm.edu.

Jianzheng Zheng

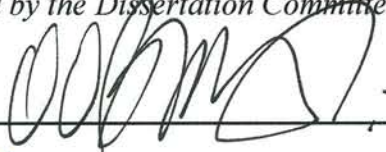
Candidate

cell biology and physiology

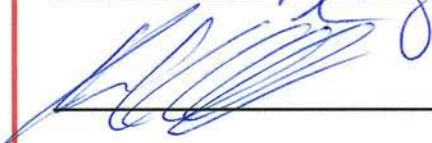
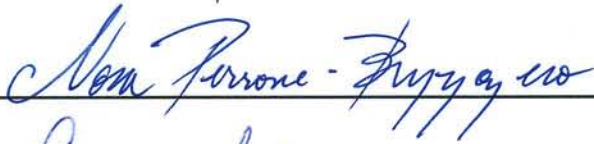
Department

This dissertation is approved, and it is acceptable in quality and form for publication:

Approved by the Dissertation Committee:



, Chairperson



**AN IMPAIRED 20S PROTEASOME CONTRIBUTES TO
THE ACCUMULATION OF OXIDIZED PROTEINS IN
MULTIPLE SCLEROSIS AND ITS ANIMAL MODEL**

BY

JIANZHENG ZHENG

B.S., Southern Medical University, 2003
M.S., Guangzhou Medical University, 2006

DISSERTATION

Submitted in Partial Fulfillment of the
Requirements for the Degree of

**Doctor of Philosophy
Biomedical Science**

The University of New Mexico
Albuquerque, New Mexico

December 2010

Acknowledgements

This dissertation would not have been possible without the help of so many people in so many ways.

My deepest gratitude is to my advisor, Dr. Oscar Bizzozero, for all the years of patience and guidance throughout my graduate studies. As an outstanding mentor, he impresses me most by his rigorous scholarship qualities, prompt and thoughtful mind on science, and considerable contributions that keep me progressing in my studies. His guidance and professional style will remain with me as I continue my career. I am thankful to Dr. Nora Perrone-Bizzozero for the productive discussions and for helping me to setup the astrocyte cell culture and to analyze the immunofluorescence microscopy data. I thank the other members of my committee, Dr. Kevin Caldwell and Dr. Erin Milligan for their constant support, valuable recommendations pertaining to this study and assistance in my professional development. I would like to acknowledge Ms. Tamara Howard for her help with tissue fixation and slicing techniques. I would also like to thank all my labmates in Dr. Bizzozero's laboratory, especially Amelia Hilgart, Anushka Dasgupta and Suzanne Smerjac. They helped me, supported me and cheered me up during difficult times. I am indebted to the personnel from the Rocky Mountain MS Center (Englewood, CO) and the UCLA Human Brain and Spinal Fluid Resource Center (Los Angeles, CA) who provided the control and MS tissues for my study. Lastly, none of this work would have been possible without grant support from the National Institute of Neurological Disorders and Stroke.

On the personal side, none of this would have been possible without the love and patience of my family - my dear husband Shijie Liang and my precious daughter Lydia Liang. I would like to express my heart-felt gratitude to them for their continued love, concern, support and strength all these years. Finally, I thank all my classmates; my Chinese friends and American friends; program managers, directors and all the members of the Department of Cell Biology and Physiology and the Department of Neurosciences.

**AN IMPAIRED 20S PROTEASOME CONTRIBUTES TO
THE ACCUMULATION OF OXIDIZED PROTEINS IN
MULTIPLE SCLEROSIS AND ITS ANIMAL MODEL**

BY

JIANZHENG ZHENG

ABSTRACT OF DISSERTATION

Submitted in Partial Fulfillment of the
Requirements for the Degree of

**Doctor of Philosophy
Biomedical Science**

The University of New Mexico
Albuquerque, New Mexico

December 2010

An impaired 20S proteasome contributes to the accumulation of oxidized proteins in multiple sclerosis and its animal model

BY

JIANZHENG ZHENG

B.S., Southern Medical University, China, 2003

M.S., Guangzhou Medical University, China, 2006

Ph.D., University of New Mexico, Health Science Center, 2010

ABSTRACT

Carbonylated (oxidized) proteins are known to accumulate in the brain of patients with multiple sclerosis (MS) and in the spinal cord of rats with acute experimental autoimmune encephalomyelitis (EAE). Yet, our knowledge regarding mechanism(s) underlying the build-up of protein carbonyls in these inflammatory demyelinating disorders is quite limited. The objectives of this dissertation were (1) to measure the changes in protein carbonylation during disease progression, and to identify the target cells and modified proteins in the cerebellum of EAE animals, prepared by active immunization of C57/BL6 mice with MOG₃₅₋₅₅ peptide, (2) to determine if the accumulation of carbonylated proteins in the CNS of these animals is due to a defect in the degradation of the modified proteins and (3) to establish if a similar mechanism underlies the build-up of carbonylated proteins in the cerebral white matter (WM) and gray matter

(GM) of MS patients. Initial studies using double immunofluorescence microscopy showed that carbonyls accumulate mostly in white matter astrocytes of EAE mice, both in the acute and chronic phase. Two-dimensional oxyblot and mass spectrometry analysis identified β -actin, β -tubulin, GFAP and HSC-71 as the major carbonylation species throughout disease. Using a pull-down/western blot method I also discovered that the proportion of carbonylated cytoskeletal proteins is elevated in chronic EAE, suggesting that as disease progresses from the inflammatory to the neurodegenerative phase there may be an inappropriate removal of these species. This idea was subsequently tested by identifying the 20S proteasome as the proteolytic system responsible for the elimination of oxidized cytoskeletal proteins in cultured astrocytes and by demonstrating that the proteasomal activities were reduced in chronic EAE. These findings were finally extended to the human disease, where I found a profound decrease in proteasomal activity both in the normal-appearing GM and WM of MS patients. Collectively, the studies presented in this dissertation demonstrate that an impaired 20S proteasome in the central nervous system of chronic EAE mice and MS patients significantly contributes to the accumulation of carbonylated (and potentially toxic) proteins. This work may provide the foundation for future studies aimed at developing new approaches to treat MS.

Table of Contents

Acknowledgements	i
Table of Contents	viii
List of Figures	xi
List of Tables	xiv
1. General Introduction	1
1.1 Multiple Sclerosis and its animal model experimental autoimmune encephalomyelitis (EAE)	1
1.2 Oxidative stress and protein carbonylation in MS/EAE	2
1.2.1 Oxidative stress plays a major role in the pathogenesis of MS/EAE and protein carbonylation is one of the most significant chemical modification from severe and/or prolonged oxidative stress.....	2
1.2.2 Direct oxidation by ROS is the major process for producing protein carbonyls in glutathione-depleted rat brain slices and EAE cerebellum.....	4
1.2.3 Protein carbonyls accumulate in MS/EAE CNS tissue	6
1.3 Possible mechanisms underlying the accumulation of carbonylated cytoskeletal proteins inside cerebellar astrocytes in chronic EAE	7
1.4 The peptidolytic activities of 20S proteasome are also impaired in the cerebrum of MS.	12
1.5 Goal of thesis	12
2 Accumulation of protein carbonyls within cerebellar astrocytes in murine experimental autoimmune encephalomyelitis	16
2.1 Abstract.....	17
2.2 Introduction	18
2.3 Materials and Methods.....	20
2.3.1 Induction of Experimental Autoimmune Encephalomyelitis (EAE)	20
2.3.2 Biochemical determination of oxidative markers.....	21
2.3.3 Two-dimensional oxyblots of cerebellar proteins	22
2.3.4 Identification of major carbonylated proteins by mass-spectrometry.....	22
2.3.5 Quantification of carbonylation levels in specific proteins.....	23
2.3.6 Immunohistochemical detection of protein carbonyls	23
2.3.7 Statistical Analysis.....	25
2.4 Results	25
2.4.1 Characteristics of EAE mice.....	25
2.4.2 Increase oxidative stress in acute and chronic EAE	26
2.4.3 Protein carbonyls accumulate within astrocytes present at the lesion's sites.....	27

2.4.4	Identification of the major protein targets of carbonylation in EAE	28
2.4.5	Accumulation of carbonylated cytoskeletal proteins in chronic EAE.	29
2.5	Discussion.....	30
2.6	Reference	43
3	Reduced proteasomal activity may contribute to the accumulation of carbonylated proteins in chronic experimental autoimmune encephalomyelitis	46
3.1	Abstract.....	47
3.2	Introduction	47
3.3	Materials and Methods.....	50
3.3.1	Astrocyte culture.....	50
3.3.2	Induction of Experimental Autoimmune Encephalomyelitis (EAE)	51
3.3.3	Protease activity assays.....	52
3.3.4	Western blots	53
3.3.5	Quantification of carbonylation levels in specific proteins.....	53
3.3.6	Immunohistochemical localization of poly-ubiquitinated proteins in cerebellum.....	54
3.3.7	Statistical Analysis.....	55
3.4	Results	55
3.4.1	Differentiation of C6 cells into astrocytes and induction of oxidative stress with LPS..	55
3.4.2	Proteasome inhibition leads to accumulation of carbonylated proteins in cultured astrocytes	56
3.4.3	Proteasomal proteolytic activity is reduced in chronic EAE	58
3.4.4	Carbonylated cytoskeletal proteins prepared from acute and chronic EAE tissues are equally sensitive to proteasomal degradation in cell-free system.....	60
3.4.5	Ubiquitinated proteins build-up in cerebellar astrocytes in chronic EAE.....	61
3.5	Discussion.....	61
3.6	Reference	77
4	Reduced Proteasomal Activity in the Cerebral White Matter and Gray Matter of Patients with Multiple Sclerosis.....	81
4.1	Abstract.....	82
4.2	Introduction	83
4.3	Materials and Methods.....	85
4.3.1	Tissue Specimens	85
4.3.2	Protease activity assays.....	86
4.3.3	Western blot analysis	87

4.3.4	Statistical Analysis.....	88
4.4	Results	88
4.4.1	Proteasomal peptidase activities are decreased in MS-WM and MS-GM	88
4.4.2	Levels of 20S proteasome α , β 1, β 2 and β 5 subunits are not reduced in MS tissue.	89
4.4.3	PA28 α and PA700 levels are also diminished in MS.....	90
4.4.4	Calpain activity and expression are significantly upregulated in MS brains	91
4.4.5	Lysosomal proteolytic activity is slightly increased in MS gray matter.....	92
4.4.6	Levels of Lon protease are unaltered in MS	92
4.5	Discussion.....	93
4.6	References.....	106
5	General Discussion.....	109
5.1	Major Conclusions	109
5.2	The proteasome may play an important role in the pathophysiology of EAE/MS.	112
5.3	Future directions	117
5.3.1	Carbonylation may affect the major properties of cytoskeletal proteins like GFAP.	117
5.3.2	Possible mechanisms underlying proteasome impairment in chronic EAE and MS.	120
5.4	Scientific Impact.....	125
Appendix A	126
Appendix B	153
Appendix C	154
Appendix D	155
Appendix E	156
Appendix F	157
Abbreviations	159
References	162

List of Figures

Figure 1.1 Mechanisms of formation of protein-bound carbonyls.....	5
Figure 1.2 Protein oxidative modifications and maintenance systems.....	8
Figure 1.3 Different forms of proteasome system.....	10
Figure 2.1 Clinical course and cerebellar pathology of EAE in C57BL/6 female mice.....	36
Figure 2.2 Levels of oxidative stress markers in the cerebellum of acute and chronic EAE mice.....	37
Figure 2.3 High levels of carbonyls in cerebellar white matter of acute and chronic EAE mice....	38
Figure 2.4 Colocalization of carbonyls and GFAP in the cerebellum of acute and chronic EAE mice.....	39
Figure 2.5 Carbonyl staining in the cerebellum of chronic EAE mice colocalizes mostly with astrocytes and some microglial cells..	40
Figure 2.6 β -Actin, β -tubulin, GFAP and HSC-71 are the major carbonylated proteins in EAE cerebellum.....	41
Figure 2.7 GFAP, β -actin and β -tubulin are more carbonylated in chronic than in acute EAE.	42
Figure 3.1 Differentiation of C6 glioma cells into astrocytes.....	68
Figure 3.2 Levels of nitrosative/oxidative stress markers in control and LPS-stimulated astrocytes.....	69
Figure 3.3 Only the proteasome inhibitor epoxomicin causes a build-up of carbonylated proteins in cultured astrocytes.	70
Figure 3.4 The proportion of carbonylated GFAP, β -actin and β -tubulin in LPS-stimulated astrocytes increases upon incubation with the proteasome inhibitor epoxomicin... ..	71
Figure 3.5 The chymotrypsin-like and caspase-like activities of the 20S proteasome are significantly reduced in chronic EAE.....	72
Figure 3.6 The amount of 20S proteasome is not altered in chronic EAE.....	73
Figure 3.7 Neither cathepsin B nor calpain activity is decreased in chronic EAE..	74
Figure 3.8 Carbonylated GFAP from acute and chronic EAE animals are sensitive to proteasomal degradation in a cell-free system.....	75

Figure 3.9 Ubiquitinated proteins build-up inside cerebellar astrocytes of mice with chronic EAE.	76
Figure 4.1 Proteasome peptidase activities are greatly reduced in MS.	98
Figure 4.2 - Proteins containing Lys-48-linked poly-ubiquitin accumulate in MS-WM and MS-GM..	99
Figure 4.3 The amount of 20S proteasome α subunits is not diminished in MS.....	100
Figure 4.4 Levels of 20S proteasome β 1, β 2 and β 5 subunits are not decreased in MS.....	101
Figure 4.5 Changes in the levels of the proteasomal regulators 11S and 19S in MS.	102
Figure 4.6 Calpain activity and levels are increased in MS.	103
Figure 4.7 Cathepsin B activity is increased in MS-WM and MS-GM.	104
Figure 4.8 Levels of the mitochondrial LON protease are unchanged in MS.....	105
Figure 5.1 The solubility of GFAP in DEM-treated astrocytes augmented upon incubation of KCl..	119
Figure 5.2 Possible mechanisms underlying proteasomal impairment.	125
Figure A.1 Chemical structure of the various carbonyl-trapping agents used in this study.....	142
Figure A.2 Ability of carbonyl scavengers to trap various RCS in a cell-free system.....	143
Figure A.3 Effect of carbonyl scavengers on DEM-induced protein carbonylation.	144
Figure A.4 Detection of RCS-protein adducts in control and GSH-depleted brain slices.....	145
Figure A.5 Effect of hydralazine on protein-bound carbonyl groups.....	146
Figure A.6 Effect of increasing concentrations of hydralazine on DEM-induced protein carbonylation and hydrogen peroxide production.....	147
Figure A.7 Effect of hydralazine on hydrogen peroxide and lipid hydroperoxide stability.	148
Figure A.8 Effect of NADPH oxidase and MAO inhibitors on DEM-induced protein carbonylation.	149
Figure B Lymphocytes accumulate in cerebellar white matter of EAE mice..	153
Figure C Colocalization of carbonyls and GFAP in the cerebellum of acute EAE mice.....	154
Figure D Stimulation of astrocytes with LPS.....	155

Figure E The proportion of carbonylated GFAP in cultured astrocytes increases upon incubation
with DEM..... 156

Figure F The solubility of β -actin in DEM-treated astrocytes is elevated upon incubation of
KCl.....157

List of Tables

Table 4.1 Brian samples from control and MS patients.....	97
Table 5.1 Summary of protein carbonyl levels in acute and chronic EAE	111

1. General Introduction

1.1 Multiple Sclerosis and its animal model experimental autoimmune encephalomyelitis (EAE)

Multiple sclerosis (MS) is an inflammatory, demyelinating disease of the central nervous system (CNS) affecting approximately 1 in 700 young adults, and thereby representing a major burden for their families and communities in North America and Europe (Trapp and Syts, 2009). The pathological changes that contribute to neurological disability in MS include inflammation, demyelination, gliosis, oligodendrocyte death and axonal degeneration (Kornek and Lassmann, 1999). In most patients, MS presents as a biphasic disease characterized initially by remittent, acute neurological dysfunction followed by a progressive increase in disability (Gonsette, 2008). It is believed that different pathological mechanisms take place in the relapsing-remitting (RR) and in the secondary progressive (SP) stages; the RR phase being associated with transient, immune mediated inflammatory reactions and the SP phase with steady, neurodegenerative processes (Gonsette, 2008).

Experimental autoimmune (allergic) encephalomyelitis (EAE) recapitulates a number of clinical and pathological features of MS, and is routinely employed to study the mechanistic bases of disease and to test therapeutic approaches (Gold *et al.*, 2000). EAE can be induced in a variety of mammalian species by active immunization with myelin-specific antigens or by adoptive transfer of T-cells from immunized animals into naïve recipients. Depending on the nature of the autoantigen and the strain of the animals utilized, EAE can be made acute,

chronic monophasic or chronic relapsing, to model the course of the experimental disorder to the various types of MS. The studies in this thesis employed the chronic monophasic EAE model in female C57BL/6 mice produced by active immunization with myelin oligodendrocyte glycoprotein (MOG) peptide 139-151. This animal model is characterized by acute inflammation (without demyelination) throughout the CNS at the peak of disease and by neurodegeneration (extensive demyelination and axonal damage with minor inflammation) during the chronic phase (Kuertten *et al.*, 2007). These features make this an ideal model to study the pathophysiological mechanisms underlying disease progression.

1.2 Oxidative stress and protein carbonylation in MS/EAE

1.2.1 Oxidative stress plays a major role in the pathogenesis of MS/EAE and protein carbonylation is one of the most significant chemical modification from severe and/or prolonged oxidative stress.

Oxidative stress (OS) is a condition in which the cellular antioxidant defenses are insufficient to keep the levels of reactive oxygen species (ROS) below a toxic threshold (Mancuso *et al.*, 2009). Clearly, OS may be induced by increased ROS, decreased antioxidant defenses or both. During the course of MS and EAE, an excessive amount of several ROS including hydrogen peroxide (H_2O_2), superoxide ($\text{O}_2^{\cdot-}$), hypochlorous acid (HClO) and peroxynitrite (ONOO^-) are extracellularly and intracellularly generated in the CNS (Bizzozero, 2009). The major ROS produced extracellularly come from infiltrating phagocytes and activated microglia while intracellular ROS (mostly $\text{O}_2^{\cdot-}$ and H_2O_2) are largely

produced by dysfunctional mitochondria, which may result from glutamate excitotoxicity, axonal depolarization, and glutathione depletion (Bizzozero, 2009). In addition, cellular antioxidant defense systems in MS are weakened as inferred from (1) reduced plasma levels of antioxidants (e.g. ubiquinone, vitamin E) and antioxidant enzymes (e.g. catalase and glutathione peroxidase), and (2) low levels of antioxidants like glutathione, α -tocopherol and uric acid in MS plaques (Bizzozero, 2009). Furthermore, various antioxidant treatments including N-acetylcysteine, bilirubin, uric acid and catalase, were found to be effective on ameliorating EAE (Bizzozero, 2009). Together the above studies suggest that oxidative stress plays a major role in the development of tissue injury in MS/EAE. More specifically, oxidative stress has been implicated as a mediator of demyelination and axonal damage in MS and EAE (Gilgun-sherki *et al.*, 2004).

The principal outcome of oxidative stress is the chemical transformation of lipid, proteins, and nucleic acid by ROS. Among these, protein carbonylation is one of the most significant chemical modifications (Bizzozero, 2009), due to the high susceptibility of most amino acids to oxidation and its irreversible nature. Carbonylation affects the biological activity of important structural and enzymatic polypeptides. For example, carbonylation of tubulin can lead to microtubule disassembly and instability, while actin filaments are also easily depolymerized upon carbonylation (Yan and Sohal, 1998). Thus, protein carbonyls (PCOs) are likely to play an important role in the pathophysiology of disorders in which there is considerable OS, such as in neurodegenerative and chronic inflammatory diseases (Bizzozero, 2009).

1.2.2 Direct oxidation by ROS is the major process for producing protein carbonyls in glutathione-depleted rat brain slices and EAE cerebellum

Carbonyl groups are introduced into proteins by two different mechanisms (Figure 1.1). The first one involves the direct metal ion-catalyzed oxidation of side-chains of proline, arginine, lysine, and threonine through Fenton chemistry. A small portion of the protein carbonyls may also arise from decomposition of side-chain hydroperoxides of Val and Leu. The second mechanism involves the reaction of the nucleophilic centers in cysteine, histidine, or lysine residues with reactive carbonyl species (RCS) derived from the oxidation of lipids [e.g., 4-hydroxynonenal (4-HNE), malondialdehyde (MDA), acrolein (ACR)], and carbohydrates [(e.g., glyoxal (GO), methylglyoxal (MGO)] (Bizzozero, 2009). These non-oxidative processes of carbonyl formation are termed lipoxidation and glycooxidation, respectively. Despite of much work done in this field, there is still controversy as to the relative contribution of oxidative (direct) and non-oxidative (indirect) pathways to the total amount of carbonyls present in a protein. While directly oxidized amino acids have been found as the major modified species in rat liver and human brain proteins, inhibition of lipid peroxidation (indirect pathway) is also known to reduce protein carbonyls in diseased tissues. To identify the major pathway of carbonylation with the goal to provide possible therapeutic strategies by preventing it, I used glutathione-depleted rat brain slices. Acute depletion of GSH, accomplished with dimethyl maleate (DEM), significantly increases mitochondrial production of superoxide and hydrogen peroxide (Zheng and Bizzozero, 2009), leading to oxidative stress. Interestingly, RCS including 4-

HNE, MDA and ACR were barely detectable in these tissues and traditional RCS scavengers failed to prevent the carbonylation of brain proteins. These findings clearly suggest that the direct oxidation by ROS, is the major process in this paradigm (see appendix A). More importantly, RCS were also barely detectable in EAE tissues, indicating that lipoxidation and glycooxidation are unlikely to produce protein carbonyls in inflammatory demyelinating diseases (see chapter 2).

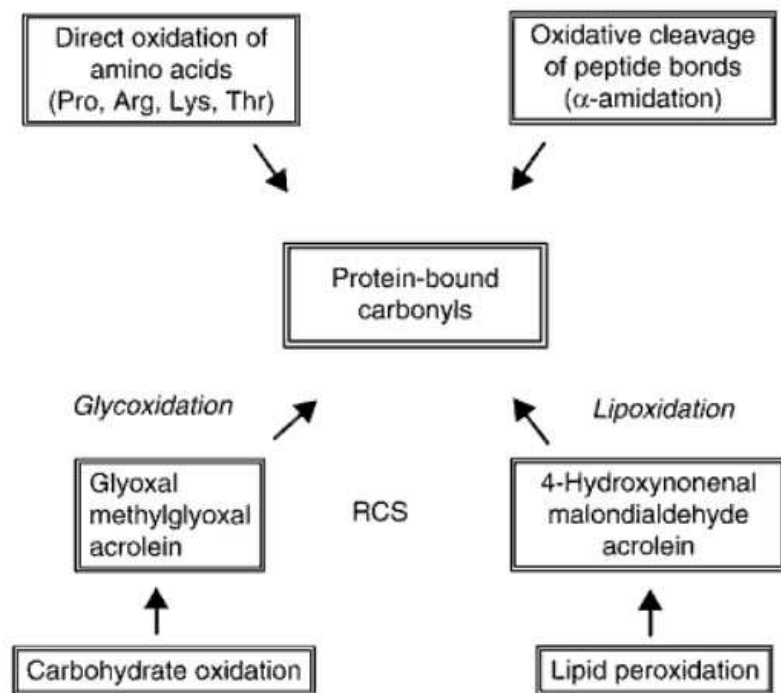


Figure 1.1 Mechanisms of formation of protein-bound carbonyls. (From Bizzozero O.A., Protein carbonylation in neurodegenerative and demyelinating CNS disease. **Handbook of neurochemistry and Molecular Neurobiology**. 2009. pp, 543-562)

1.2.3 Protein carbonyls accumulate in MS/EAE CNS tissue

Accumulation of protein carbonyls has been implicated in the etiology and/or progression of several neurodegenerative disorders such as Alzheimer's disease (Aksenov *et al.*, 2001), Parkinson's disease (Floor and Wetzel 1998), and amyotrophic lateral sclerosis (Ferrante *et al.*, 1997). Our lab recently showed that protein carbonyls also accumulate in the brain of patients with multiple sclerosis (MS) (Bizzozero *et al.*, 2005) and in the spinal cord of rats with acute experimental autoimmune encephalomyelitis (EAE) (Smerjac and Bizzozero, 2008), suggesting that this type of chemical modification may play a critical pathophysiological role in inflammatory demyelinating diseases as well. However, little efforts have been devoted until now to investigate protein carbonyl accumulation during disease progression in EAE. The primary targets of oxidative stress can vary depending on the cell type, the absolute level and the half-life of the oxidant produced, the chemical nature and site of ROS generation (intra- vs. extra-cellular), and the proximity of the oxidant to a specific cellular substrate (Dalle-Donne, 2006). Consequently, my work was initially geared to identify the target cells and the modified proteins in the cerebellum of animals during the acute and chronic phases of EAE. As described in chapter 2, β -actin, β -tubulin, glial fibrillary acidic protein (GFAP) and heat shock cognate-71 (HSC-71) were identified as the major targets of carbonylation, and most of the carbonyls were found inside astrocytes in both phases of EAE animals. Moreover, I observed that as disease progresses the proportion of the carbonylated forms

of the cytoskeletal proteins including β -actin, β -tubulin and GFAP was notably increased.

1.3 Possible mechanisms underlying the accumulation of carbonylated cytoskeletal proteins inside cerebellar astrocytes in chronic EAE

The level of oxidized proteins is determined by rates of generation and degradation of carbonyls, as well as the addition of newly synthesized macromolecules (Figure 1.2). Currently, proteolytic degradation is considered to be the only physiological mechanism for elimination of carbonylated proteins since there is no evidence for enzymatic reduction of protein-bound carbonyls to alcohols (Bizzozero, 2008). Therefore, since protein carbonyls cannot be repaired and since there is less oxidative stress in chronic than in acute EAE (Zheng and Bizzozero, 2010), it is fair to propose that the accumulation of carbonylated cytoskeletal proteins in cerebellum of chronic EAE mice may be due to their impaired degradation. The build-up of carbonylated cytoskeletal proteins could be caused by reduced activity of the degradation system and/or by decreased susceptibility of the oxidized proteins to proteolysis.

In order to maintain homeostasis, all cells must continually degrade proteins in an efficient and reliable manner (Figure 1.2). Mammalian cells contain four major proteolytic systems including the cathepsins inside lysosomes, the mitochondrial Lon protease, the calpains and the 20S/26S proteasomes, the latter localized in the cytosol, nuclei, and endoplasmic reticulum (Grune, 2001).

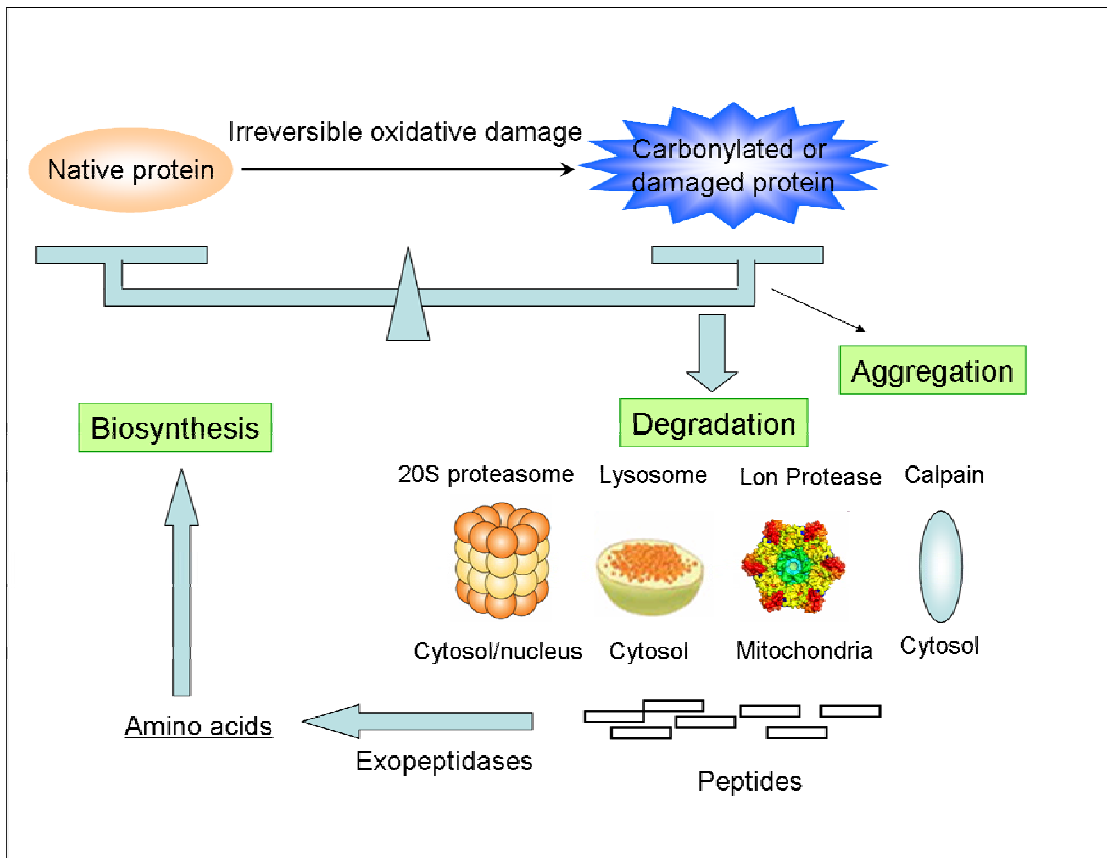


Figure 1.2 Protein oxidative modifications and maintenance systems. (Adapted from Farout and Friguet (2006) Proteasome function in aging and oxidative stress: implications in protein maintenance failure. Antioxidants & redox signaling. 8:205-216)

Proteasomes are large complexes that carry out the majority of proteolysis occurring in the cytosol and nucleus of eukaryotic cells, and thereby, perform crucial roles in cellular regulation and homeostasis (Rechsteiner *et al.*, 2005). The proteasomal system consists of the so-called 20S 'core' proteasome and several regulatory components that affect its proteolytic activity (Grune, 2000). The catalytic heart of these complexes, the 20S proteasome (670–700 kDa) is a barrel-shaped structure, made up of two outer (α) and two inner (β) rings. Three of the β subunits carry the proteolytic activity of the proteasome, classified as

caspase-like ($\beta 1$), trypsin-like ($\beta 2$), and chymotrypsin-like ($\beta 5$) activity, which cleave proteins on the carboxyl side of acidic, basic and hydrophobic amino acids, respectively (Kappahn RJ, 2007). Two activators, named 19S (PA700) and 11S (PA28), are known to bind to the 20S proteasome on both ends, forming different complexes (Figure 1.3). The 26S proteasome consisting of the 19S and 20S particles degrades proteins in an ubiquitin- and ATP-dependent fashion, whereas the 11S activator probably allows the 11S/20S complex to degrade only peptides. Indeed, the binding of the 11S regulator to the 20S proteasome results in a 3- to 25-fold increase in the degradation of fluorogenic peptides (Grune, 2000). The binding sites for the 11S and the 19S regulator seem to be distinct and the competition for the core proteasome under in vitro conditions seems to result in the formation of the 26S proteasome (Hoffmann and Rechsteiner, 1994).

It has been shown that degradation of carbonylated proteins is carried out in an ATP- and ubiquitin-independent manner by the 20S proteasome, which selectively recognizes and digests partially unfolded (denatured) oxidized proteins. For example, oxidized actin is removed by the 20S proteasome during myocardial ischemia/reperfusion (Divald A, 2005). This notion is further supported by the finding that the pharmacological inhibition of the 20S proteasome results in accumulation of carbonylated protein in cell culture (Divald and Powell, 2006). It is believed that the proteins are presumably targeted to the 20S proteasome via their increased hydrophobicity.

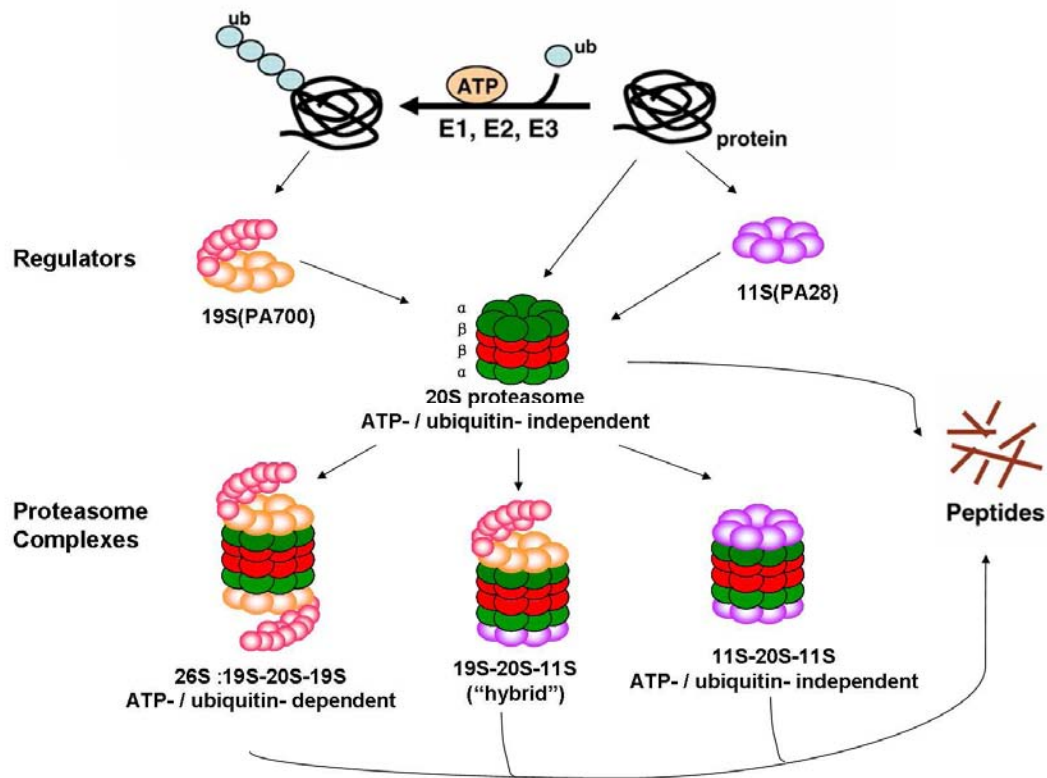


Figure 1.3 Different forms of proteasome system. Adapted from Luo *et al.*, Protein degradation systems in viral myocarditis leading to dilated cardiomyopathy Cardiovasc Res (2010) 85: 347-356)

The calcium-dependent cysteine protease calpain is located close to the cytoskeleton and mostly degrades cytoskeletal proteins and membrane proteins. In cell free systems, calpain has been shown to preferentially degrade oxidized neurofilament over non-oxidized protein (Troncoso *et al.*, 1995). There is also evidence suggesting that moderately or heavily oxidized proteins are taken up via chaperone mediated autophagy by lysosomes, where in some cases they are incompletely degraded and accumulate resulting in the formation of lipofuscin-like, autofluorescent aggregates (Dunlop *et al.*, 2009). Ubiquitin-dependent

lysosomal degradation of proteins modified 4-hydroxynonenal (HNE) which is one type of carbonylation, was also observed in lens epithelial cells (Marques *et al.*, 2004). Finally, Lon protease preferentially degrades oxidized mitochondrial protein like aconitase by an ATP-stimulated mechanism.

The efficacy of proteolysis of carbonylated protein likely depends on the specific protein being carbonylated as well as the level of oxidative damage (Smerjac and Bizzozero, 2008). While in general proteins become more susceptible to degradation by cellular proteases upon carbonylation of one or more residues, heavily oxidized proteins and cross-linked protein aggregates are not only more resistant to proteolysis but they also inhibit the activity of proteases that degrade them (Bizzozero, 2009). Thus, accumulation of carbonylated species may be the result of deficient proteolytic systems and also of decreased susceptibility of the oxidized proteins to digestion.

Although a number of *in vitro* experiments have suggested that the four major proteolytic systems mentioned above are responsible for removing oxidized proteins, it is not clear that they actually perform this function *in vivo* or that they all have a role in removing of carbonylated cytoskeletal proteins in EAE. For this reason, the ability of these major proteolytic systems to degrade carbonylated proteins was tested in LPS-stimulated astrocytes. These studies employed three relatively specific protease inhibitors. As described in Chapter 3, only the inhibitor epoxomicin leads to a build-up of carbonylated proteins in cultured astrocytes, suggesting that carbonylated proteins are mostly removed by the proteasome. Furthermore, the various proteasomal activities but not calpain

and lysosomal cathepsin B activities were reduced in chronic EAE. In addition, the carbonylated cytoskeletal proteins from acute and chronic EAE are equally sensitive to proteasomal degradation. Overall, this work provides the evidence that the accumulation of carbonylated cytoskeletal proteins in chronic phase of EAE likely results from reduced proteasomal activity.

1.4 The peptidolytic activities of 20S proteasome are also impaired in the cerebrum of MS.

The decreased proteasomal activities, which likely contribute to the accumulation of carbonylated cytoskeletal proteins in chronic EAE, raised the question of whether this is also occurring in MS. Therefore, the next set of studies was designed to determine the activities of the four major proteolytic systems in the normal-appearing white matter and gray matter of MS patients. As presented in chapter 4, the three proteolytic activities of 20S proteasome in MS patients were reduced to ~45% of control values without significant reduction in proteasome levels. Significant elevations in the activities of both total and soluble calpain were observed in MS patients and are due to the up-regulation of calpain expression. Interestingly, the lysosomal activity is increased only in the MS-gray matter as compared to controls. The mechanisms underlying the impaired proteasomal activity in MS is currently being investigated in our lab.

1.5 Goal of thesis

My work builds on previous findings in our laboratory that demonstrated an accumulation of protein carbonyls in the brain of patients with multiple sclerosis

(MS) and in the spinal cord of rats with acute experimental autoimmune encephalomyelitis (EAE). The objectives of this thesis were to identify the target cells and modified proteins of carbonylation in the cerebellum of EAE animals, and to uncover the mechanisms underlying the accumulation of carbonylated proteins occurring in the chronic phase of EAE and in MS patients.

The studies described in Chapter 2 are aimed to identify the target cells and the carbonylated proteins in the cerebellum of animals during the disease course using a chronic model of EAE. I first demonstrated that carbonyls accumulate in white matter astrocytes, and to a lesser extent in microglia/macrophages, both in the acute and chronic phase. Next, I identified β -actin, β -tubulin, GFAP and HSC-71 as the major targets of carbonylation throughout disease. Using a pull-down/western blot method I found a significant increase in the proportion of carbonylated β -actin, β -tubulin and GFAP in the chronic phase but not in the acute phase. These results suggest that as disease progresses from the inflammatory to the neurodegenerative phase there may be an inappropriate removal of oxidized proteins.

Experiments in Chapter 3 were designed to uncover the mechanisms underlying the accumulation of carbonylated proteins occurring in chronic phase of EAE. These studies examined the hypothesis that impairment of proteasome activity may contribute to accumulation of carbonylated cytoskeletal proteins within cerebellar astrocytes in chronic EAE. To test this hypothesis I first identified the proteolytic system involved in the removal of carbonylated proteins employing LPS-stimulated astrocytes and several protease inhibitors. The results

showed that only the proteasome inhibitor epoxomicin leads to a build-up of carbonylated proteins within these cells. I then discovered an increase of chymotrypsin-like proteasome activity (responsible for degradation of oxidized proteins) in acute EAE followed by a decline in chronic EAE, while neither lysosomal or calpain activity was impaired in chronic EAE. The accumulation of poly-ubiquitinated proteins within cerebellar astrocytes observed in the same animals also confirmed these results. Further, carbonylated cytoskeletal proteins from acute and chronic EAE were found to be equally sensitive to proteasomal degradation. All of these results support the notion that diminished proteasomal activity may be a major contributor to the accumulation of carbonylated cytoskeletal proteins in the chronic phase of EAE. The mechanism underlying the decline in proteasome activity will be investigated in future studies.

The diminished proteasomal activity in chronic EAE raised the question of whether the proteasome activity is also decreased in MS patients. Chapter 4 was designed to test the activities of four major proteolytic systems in MS patients. My data showed that the three enzymatic activities of the proteasome in the normal-appearing gray matter and white matter from MS cerebra are greatly diminished while the activities of calpain and lysosome in the same samples are elevated. This similar pattern of proteasomal impairment in chronic EAE and MS suggests the involvement of this particle in inflammatory demyelinating diseases. These are the first studies showing proteasomal impairment in chronic EAE and MS.

Chapter 5 seeks to bring my thesis work together. In this chapter, I discuss

some of the findings presented in the previous chapters and present several important future directions. My preliminary data in chapter 5 shows some functional consequences of protein carbonylation. I found that the oxidized form of cytoskeletal proteins including GFAP, β -actin and β -tubulin increase their solubilities to high concentrations of salt. These preliminary observations provide evidences of functional disturbance in cytoskeletal proteins under oxidative stress. A more detailed functionality study should be performed in the future. Furthermore, this chapter addresses how proteasome may be affected in chronic EAE/MS, and look at the possibility of preventing proteasomal failure or activating proteasomal activity for treating these disorders.

Taken together, these publications should lead to future scientific work on the mechanism underlying the accumulation of oxidized proteins in chronic EAE and MS. The finding of proteasomal impairment will help us to better understand the pathophysiology of EAE/MS, and may provide valuable knowledge on which to base future therapeutic intervention to MS patients.

2 Accumulation of protein carbonyls within cerebellar astrocytes in murine experimental autoimmune encephalomyelitis

Jianzheng Zheng and Oscar A. Bizzozero

Department of Cell Biology and Physiology

University of New Mexico School of Medicine

Albuquerque, NM 87131

(Published in J Neurosci Res. 2010; 88:3376-85)

2.1 **Abstract**

Recent work from our laboratory has implicated protein carbonylation in the pathophysiology of multiple sclerosis (MS) and experimental autoimmune encephalomyelitis (EAE). The present study was designed to determine the changes in protein carbonylation during the disease progression, and to identify the target cells and modified proteins in the cerebellum of EAE animals, prepared by active immunization of C57/BL6 mice with MOG35-55 peptide. In this model, protein carbonylation was maximal at the peak of the disease (acute phase) to decrease thereafter (chronic phase). Double immunofluorescence microscopy of affected cerebella showed that carbonyls accumulate in white matter astrocytes, and to a lesser extent in microglia/macrophages, both in the acute and chronic phase. Surprisingly, T cells, oligodendrocytes and neurons were barely stained. By 2D-oxyblot and mass spectrometry, β -actin, β -tubulin, GFAP and HSC-71 were identified as the major targets of carbonylation throughout disease. Using a pull-down/western blot method we found a significant increase in the proportion of carbonylated β -actin, β -tubulin and GFAP in the chronic phase but not in the acute phase. These results suggest that as disease progresses from the inflammatory to the neurodegenerative phase there may be an inappropriate removal of oxidized cytoskeletal proteins. Additionally, the extensive accumulation of carbonylated GFAP in the chronic phase of EAE may be responsible for the abnormal shape of astrocytes observed at this stage.

2.2 Introduction

Multiple sclerosis (MS) is an inflammatory demyelinating disease of the human CNS and a major cause of neurological disability among young adults in North America and Europe (Trapp and Syts, 2009). The pathological changes that contribute to neurological disability in MS include inflammation, demyelination, oligodendrocyte death and axonal degeneration (Kornek and Lassmann, 1999). Experimental autoimmune encephalomyelitis (EAE) is a well-established animal model for CNS autoimmune disorder, recapitulating a number of clinical and pathological features of MS (Gold *et al.*, 2000). Several EAE models have been developed throughout the years that reflect the different clinical courses of MS. MOG35-55 peptide-induced EAE in the C57BL/6 mouse, the animal model used in this study, is characterized by the presence of inflammatory (non-demyelinated) lesions throughout the CNS at the peak of disease and extensive demyelination with minor inflammation during the chronic phase (Kuerten *et al.*, 2007). These features make this an ideal model to study the pathophysiological mechanisms underlying disease progression.

There is substantial amount of data indicating that oxidative stress plays a major role in the pathogenesis of both MS and EAE. Excessive production of reactive oxygen species (ROS), primarily by activated microglia/macrophages and astrocytes, leads to severe oxidative stress, which contributes significantly to tissue damage (Gilgun-Sherki *et al.*, 2004). The principal outcome of oxidative stress is the chemical transformation of lipids, proteins, and nucleic acids by ROS. Of these, proteins are the major target for oxidants as the result of their

abundance and their high reaction rate constants (Davies, 2005). While the polypeptide backbone and the side chains of most amino acids are susceptible to oxidation, the non-enzymatic introduction of aldehyde or ketone functional groups to specific amino acid residues (i.e. carbonylation) constitutes the most common oxidative alteration of proteins (Bizzozero, 2009). Protein carbonyls can be introduced in proteins directly via metal ion-catalyzed oxidation of certain amino acid residues (Requena *et al.*, 2001) or indirectly by the attachment of bi-functional reactive carbonyl species (e.g. 4-hydroxynonenal, acrolein, malondialdehyde, glyoxal) (Esterbauer *et al.*, 1991). In either case, carbonylation often leads to loss of protein function and the formation of toxic cross-linked protein aggregates (Bizzozero, 2009).

Accumulation of protein carbonyls has been implicated in the etiology and/or progression of several neurodegenerative disorders including Alzheimer's disease (Aksenov *et al.*, 2001), Parkinson's disease (Floor and Wetzel, 1998), and amyotrophic lateral sclerosis (Ferrante *et al.*, 1997). Our recent discovery that protein carbonyls accumulate in the brain of MS patients (Bizzozero *et al.*, 2005; Hilgart and Bizzozero, 2008) and in the spinal cord of rats with acute EAE (Smerjac and Bizzozero, 2008), suggests that this type of chemical modification may also play a critical pathophysiological role in inflammatory demyelinating diseases. The present study was designed to assess the levels of protein carbonylation and to identify the target cells and the modified proteins in the cerebellum of EAE mice during the course of the disease. The results show that most of the carbonyls accumulate in white matter astrocytes, and to a lesser

extent in microglia/macrophages, present at the site of inflammatory lesions both at the peak of disease and during the chronic phase. Surprisingly, T cells, oligodendrocytes and neurons were barely stained. At all disease stages, the major carbonylated proteins were identified as β -actin, β -tubulin, GFAP and heat shock cognate-71 (HSC-71). While both oxidative stress and total protein carbonylation decrease later in the disease, we observed that the proportion of the carbonylated forms of the cytoskeletal proteins was notably higher in the chronic animals. This suggests impairment in the removal of oxidized proteins as disease progresses. A preliminary account of this work has been presented in abstract form (Zheng and Bizzozero, 2009).

2.3 Materials and Methods

2.3.1 Induction of Experimental Autoimmune Encephalomyelitis (EAE)

Housing and handling of the animals as well as the euthanasia procedure were in strict accordance with the NIH Guide for the Care and Use of Laboratory Animals, and were approved by the Institutional Animal Care and Use Committee. Eight-week-old female C57BL/6 mice were purchased from Harlan Bioproducts (Indianapolis, IN) and housed in the UNM-animal resource facility. To induce EAE, animals received a subcutaneous injection into the lower back area of 200 μ l of MOG35-55 peptide (200 μ g) (AnaSpec, San Jose, CA) in saline mixed with complete Freund's adjuvant (CFA) supplemented with 4 mg/ml of heat killed Mycobacterium tuberculosis H37Ra (Chondrex Inc; Redmond, WA). Control animals were given CFA without MOG peptide. Two-hours and 48h after EAE induction, all animals received an i.p. injection of 0.3 μ g of pertussis toxin (List

Biological Laboratories; Campbell, CA) in 100 µl of saline. Seven days after disease induction mice received a second immunization with the MOG peptide in CFA. Animals were weighed and examined daily for the presence of neurological signs. At prescribed days post-immunization (DPI), EAE mice and CFA-injected controls were euthanized by decapitation. The cerebellum was removed and either fixed with methacarn (methanol : chloroform : acetic acid, 60 : 30 : 10 by vol) or homogenized in PEN buffer (20 mM sodium phosphate, pH 7.5, 1 mM EDTA, and 0.1 mM neocuproine) containing 2 mM 4,5 dihydroxy-1,3 benzene disulfonic acid and 1 mM dithiothreitol (DTT). Protein homogenates were stored at -20°C until use. Protein concentration was assessed with the Bio-Rad DC™ protein assay (Bio-Rad Laboratories; Hercules, CA) using bovine serum albumin as standard.

2.3.2 Biochemical determination of oxidative markers

The amount of non-protein thiols, of which > 90% is reduced glutathione (GSH) was determined with 5,5'-dithiobis-(2-nitrobenzoic acid) (Bizzozero *et al.*, 2006). Lipid peroxidation was assessed by measuring the amount of thiobarbituric acid reactive substances (TBARS) in the tissue homogenates (Ohkawa *et al.*, 1979). The relative amount of protein carbonyls was measured with the OxyBlot™ protein oxidation detection kit (Intergen Co., Purchase, NY) as described elsewhere (Bizzozero *et al.*, 2006).

2.3.3 Two-dimensional oxyblots of cerebellar proteins

Cerebellar proteins (5 µg) were first incubated with 2,4-dinitrophenylhydrazine (DNPH) to convert the carbonyl groups into 2,4-dinitrophenyl (DNP) hydrazone derivatives, and were then analyzed by 2D-gel electrophoresis (Smerjac and Bizzozero, 2008). After electrophoresis, proteins were blotted to polyvinylidene difluoride (PVDF) membranes. DNP-containing proteins were detected using rabbit anti-DNP antiserum (1:5000) and goat anti-rabbit IgG conjugated to horseradish peroxidase (1:2000). Blots were developed by enhanced chemiluminescence (ECL) using the Western Lightning ECL™ kit from Perkin-Elmer (Boston, MA). Blots were stripped and re-probed with antibodies against specific cytoskeletal proteins including β-tubulin (1:1000, mouse monoclonal; Sigma, St Louis, MO), GFAP (1:1000, mouse monoclonal; Sigma) and β-actin (1:1000, mouse monoclonal; GeneTex, Irvine, CA). As before, blots were developed by ECL.

2.3.4 Identification of major carbonylated proteins by mass-spectrometry

Spot matching between the 2D-oxyblots and the coomassie blue stained 2D-gels was performed using the Discovery Series PDQuest 2-D Analysis Software Version 7.0.1 (Bio-Rad). Protein spots were excised from the gel and subjected to in situ digestion with trypsin (Bizzozero *et al.*, 2002). Before mass-spectrometry, peptides were cleaned-up and concentrated using C-18 Zip-tips (Millipore Corp., Billerica, MA) and mixed with -cyano-4-hydroxycinnamic acid. Mass spectra were acquired on a Biosystems 4700 Proteomics Analyzer (TOF/TOF) (Applied Biosystems/MDX Sciex, Foster City, CA) in positive ion

reflection mode and using a S/N threshold of 30. Monoisotopic peak lists were generated employing a GPS Explorer™ software (v3.5, Applied Biosystems) and were submitted to the MASCOT search tool for protein identities. For all searches, precursor ion mass tolerance was 100 ppm. Protein identification was considered significant with a Mascot score corresponding to $p < 0.05$.

2.3.5 Quantification of carbonylation levels in specific proteins

The extent of protein carbonylation was determined using a pull-down/western blot method (Bizzozero *et al.*, 2006). Briefly, protein carbonyls were biotinylated by reaction with biotin hydrazide in the presence of cyanoborohydride. A small aliquot of these protein homogenates was saved for western blotting and the rest was processed to isolate the biotinylated proteins using streptavidin-agarose. Proteins were eluted from the beads with SDS-sample buffer and analyzed by western blotting on 10% polyacrylamide gels. Blots were probed with antibodies against individual protein species and developed by ECL as described above. Films were scanned in a Hewlett Packard Scanjet 4890 and the images were quantified using the NIH Image 1.63 imaging analysis program. Band intensities from the total and streptavidin-eluted fractions were used to calculate the percent of protein modified by carbonylation.

2.3.6 Immunohistochemical detection of protein carbonyls

Tissue specimens were fixed overnight in methacarn and then mounted in paraffin. Tissue was sectioned in the sagittal plane (6- μ m thick) and mounted on Vectabond™-treated slides (Vector Laboratories, Burlingame, CA). Sections

were deparafinized with xylenes and a graded alcohol series, and then rinsed with phosphate-buffered saline (PBS) solution for 10 min. Lesions were detected by staining with hematoxylin and eosin (H&E). Adjacent sections were incubated for 30 min with 1 mg/ml DNPH prepared in 2 N HCl to convert carbonyl groups into DNP-hydrazones. Sections were rinsed three times with PBS, blocked with 10% (v/v) normal goat serum and incubated overnight with rabbit anti-DNP antibody (1:1000) (Sigma). After removing the primary antibody with PBS containing 0.1% Triton X-100, sections were incubated for 3 h with Alexa Fluor® 647 goat anti-rabbit antibody (1:100, Molecular Probes, Eugene, OR). Sections were rinsed twice with PBS containing 0.1% Triton X-100, once with PBS, and then mounted in a buffered glycerol solution containing p-phenylenediamine as anti-fade reagent. Images were captured with a Zeiss 200m microscope (Carl Zeiss MicroImaging Inc., Thornwood, NY) equipped with a Hamamatsu C4742-95 digital camera (Hamamatsu Corp., Bridgewater, NJ).

For double immunofluorescence, DNPH-treated sections were incubated with the mixture of two primary antibodies overnight at 4°C, followed by incubation with the corresponding fluorescent secondary antibodies (Alexa Fluor® 488 and Alexa Fluor® 647, 1:100, Molecular Probes). After washing, the sections were cover slipped with anti-fade fluorescent mounting medium. The various cell types were detected by using antibodies against GFAP (1:500, mouse monoclonal; Sigma), Iba1 (1:250, mouse monoclonal, Santa Cruz Biotechnology, Santa Cruz, CA), CD3 (1:100, mouse monoclonal, Santa Cruz), adenomatous polyposis coli protein C-terminal (1:125, mouse monoclonal,

Chemicon, Temecula, CA) and NeuN (1:250, mouse monoclonal, Chemicon). To quantify the percentage of each cell type that shows positive carbonyl deposits, slide-mounted sections were scanned at a 60X magnification and were digitalized with a MagnaFire Camera (Optronics, Galeta, CA). Images were imported into Image J software to obtain merged pictures. Three fields (100µm x 75µm) per slide and three slides per animal were chosen for quantification.

2.3.7 Statistical Analysis

Results were analyzed for statistical significance with ANOVA utilizing GraphPad Prism® program (GraphPad Software Inc., San Diego, CA).

2.4 Results

2.4.1 Characteristics of EAE mice

EAE in female C57BL/6 mice was induced by active immunization with MOG35-55 peptide as described under Materials and Methods. Symptoms were graded according to the following scale: 0, no symptoms; 1, tail weakness; 1.5, clumsy gait; 2, hind limb paresis; 2.5, partial hind limb dragging; 3, hind limb paralysis; 3.5, hind limb paralysis with fore limb paresis; 4, complete paralysis; and 5, moribund. In this EAE model, neurological symptoms begin at 14 DPI (7 days after the boost with MOG peptide) reaching a peak at 30 DPI, and most animals remain ill (score 3.0-3.5) throughout the entire experimental period (60 DPI) (Figure 2.1A). Acute disease was defined as having maximal neurological symptoms of EAE without any improvement for at least three consecutive days. At this stage the cerebellar pathology is characterized perivenular infiltration of

inflammatory cells mostly within the white matter (Figure 2.1C). Chronic EAE was defined arbitrarily as animals that remain in the stationary phase of the disease for 30 days (60 DPI). At this stage there is reduced perivascular and parenchymal inflammation, and lessened transmigration of inflammatory cells into the cerebellum (Figure 2.1D). CFA-injected animals, which were sacrificed at 30DPI (control young) and 60DPI (control old), did not exhibit any neurological sign or cerebellar pathology (Figure 2.1B). Western blot analysis of cerebellar proteins using antibodies against several myelin proteins, neurofilament proteins and GFAP revealed that cerebella from acute EAE animals have increased gliosis without apparent demyelination or axonal injury. In contrast, chronic EAE cerebellar tissue has reduced gliosis and augmented demyelination and axonal damage (data not shown). These results are in agreement with the current notion that acute EAE is mainly an inflammatory disorder while chronic EAE is mostly a demyelinating/neurodegenerative disorder (Kuerten *et al.*, 2007).

2.4.2 Increase oxidative stress in acute and chronic EAE

As shown in Figure 2.2A, GSH levels in EAE cerebella was 73% and 85% of control values at the peak of disease and in the chronic phase, respectively. This indicates that the CNS of the affected animals is indeed subjected to considerable oxidative stress. Interestingly, the amount of TBARS, a marker of lipid peroxidation, in EAE animals was similar to that in controls both at peak of the disease and in the chronic phase (Figure 2.2B). Quantitative analysis of the oxyblots revealed a significant enhancement in protein carbonyl levels in the acute phase with little or no changes in the chronic phase of EAE (Figure 2.2C).

2.4.3 Protein carbonyls accumulate within astrocytes present at the lesion's sites

Immunohistochemical localization of carbonyls groups was carried out after derivatizing these moieties with DNPH (Figure 2.3). Validation of this technique was performed by omitting the DNPH-treatment, the anti-DNP antibody or the secondary anti-rabbit IgG antibody (not shown). We also carried out a positive control in which carbonyls were generated by incubating cerebellar sections with FeSO₄/H₂O₂ (Figure 2.3E) and a specificity control in which endogenous carbonyls were removed by incubation with NaBH₄ (Figure 2.3F). Using this technique we found that carbonyl staining in the cerebellum of both acute (Figure 2.3B) and chronic EAE mice (Figure 2.3D) is highly intense in the white matter, where the majority of inflammatory lesions are present. As expected from the biochemical data shown in Figure 2.3C, there is higher density of carbonyl staining in the acute phase than in chronic phase. In addition, the morphology of most carbonyl-positive cells appears to be that of astrocytes. This was confirmed by immunostaining carbonyls and GFAP simultaneously (Figure 2.4). It is worth noting that, in the acute tissue, astrocytes have normal morphology and show colocalization with GFAP and carbonyl in their distal processes, while in the chronic tissue, astrocytes exhibit an abnormal morphology. Indeed, some astrocyte processes are completely retracted.

Double immunofluorescence with antibodies against DNP and different cell-specific markers was used to identify other major cell targets of carbonylation. As depicted in Figure 2.5, the majority of astrocytes (~90%) present at the site of inflammatory lesions in chronic EAE showed positive carbonyls staining, and

similar results were found in acute EAE (data not shown). A significant proportion of microglial cells/macrophages (40%) also showed carbonyl staining, while <10% of T cells (CD3+), <5% of oligodendrocytes (APC+) and <10% of neurons (NeuN+) were stained with the anti-DNP antibody.

2.4.4 Identification of the major protein targets of carbonylation in EAE

Two-dimensional-oxyblot of cerebellar proteins from acute EAE mice shows the presence of 4 major carbonylated polypeptides and several minor species that become visible at much longer exposure times (Figure 2.6). These major oxidized species were also present in oxyblots of cerebellar proteins from chronic EAE animals (not shown). This particular 2D-pattern of carbonyls was somewhat reminiscent to that of found in the spinal cord of EAE rats, where cytoskeletal proteins are the major targets of carbonylation (Smerjac and Bizzozero, 2008). Thus, identification of carbonyl-containing proteins was initially carried out by spot matching DNP-labeled proteins on a 2D-oxyblot with those of specific cytoskeletal elements. Using this approach we identified three of the major carbonylated spots as β -actin, β -tubulin and GFAP. The other major spot in the 2D-oxyblot did not correspond to any of the other cytoskeletal species and was identified by mass-spectrometry as HSC-71 (P63017; mascot score= 208).

Experiments were also conducted to ascertain the chemical nature of the carbonyls. Western blot analysis using antibodies against acrolein, 4-hydroxynonenal and malondialdehyde failed to detect the presence of any modified protein in either control or EAE mice (data not shown), suggesting that

reactive carbonyl species-protein adducts are not formed in this disease. Thus, most carbonyl groups present in the oxidized proteins are likely to be α -aminoadipic semialdehyde and glutamic semialdehyde, which are formed by direct, metal-ion catalyzed, oxidative deamination of the amino acid side chain of proline, arginine and lysine (Requena *et al.*, 2001).

2.4.5 Accumulation of carbonylated cytoskeletal proteins in chronic EAE.

Quantification of the extent of carbonylation of individual proteins was performed using a pull-down/western blot procedure. To this end, protein carbonyl moieties from control and EAE cerebellar homogenates were first converted into biotinylated residues by reaction with biotin-hydrazide. Biotin-containing proteins were then isolated with streptavidin-agarose and analyzed by western blotting employing antibodies against the β -tubulin, β -actin and GFAP. HSC-71 was not studied due to the lack of an appropriate antibody. A number of preliminary studies were carried out to ascertain (1) the concentration of biotin hydrazide and time necessary for complete blockage of carbonyl groups, (2) the amount of streptavidin-agarose necessary for complete binding of biotinylated proteins, and (3) the composition and number of rinses that ensure the proper removal of non-biotinylated proteins from the agarose beads before elution. Also, no material was recovered from the streptavidin agarose when either the biotin hydrazide was omitted from the derivatization step or when the carbonyl groups were eliminated by pre-incubation with sodium borohydride, indicating that the procedure for isolating carbonylated proteins is indeed specific. Figure 2.7 shows the percentage of individual proteins that is modified by carbonylation in control

and EAE animals, which was calculated from the amount of each protein in the bound and total fractions. Surprisingly, the proportion of oxidized β -actin, β -tubulin and GFAP did not increase in acute EAE as compared to young control mice. The reason for the apparent discrepancy between these findings and those obtained with the 2D-oxyblots (Figure 2.6) is due to the fact that there is more β -actin and GFAP in the cerebellum of acute EAE than in control animals. In contrast, there is a five-fold increase in the proportion of carbonylated GFAP and a two-fold increase in the proportion of carbonylated β -actin and β -tubulin in chronic EAE mice relative to its control. These results suggest that as disease progresses from the inflammatory to the neurodegenerative phase there may be an inappropriate removal of the carbonylated forms of these cytoskeletal proteins.

2.5 Discussion

This is the first study on the accumulation of oxidized CNS proteins during the course of chronic EAE. We focused our research on the cerebellum since this CNS region is commonly affected in MS (Ramasamy *et al.*, 2009) and in MOG peptide-induced EAE (MacKenzie-Graham *et al.*, 2009). Furthermore, the pathophysiological changes in the cerebellum remain largely unexplored when compared to the spinal cord, the CNS area most studied in EAE. Using classical immunocytochemical techniques, we found that the majority of the carbonyl groups are localized within astrocytes located in the vicinity of inflammatory lesions both at the peak of the disease and during the chronic phase. A number of microglial cells/macrophages were also found to contain detectable levels of carbonyls in EAE, while T cells, oligodendrocytes and neurons were mostly

unstained. This result is not totally unexpected since upon inflammatory activation both microglia and astrocytes produce large amounts of ROS (Keller *et al.*, 1999) that could generate significant amounts of carbonyls within these cells. Furthermore, microglial cells contain higher levels of glutathione and antioxidant enzymes (superoxide dismutase, catalase, glutathione peroxidase and glutathione reductase) than astrocytes (Dringen, 2005), which may protect the former from a more severe oxidative damage. Nonetheless, it was somewhat surprising to find that neurons and oligodendrocytes do not have extensive carbonyl staining, particularly when these two cell types are considered by many investigators to be highly susceptible to oxidative stress (Halliwell, 2006; Benarroch, 2009). Interestingly, the notion that astrocytes are less sensitive to oxidative damage than other CNS cells has been recently challenged. It has been found that cerebellar astrocytes in the unperturbed mouse contain significantly lower levels of reduced glutathione than neurons and oligodendrocytes (Miller *et al.*, 2009). Another possibility to explain the selective oxidation of cells in our model is that the ROS generated by activated microglia/macrophages and astrocytes are short lived and do not reach other cell targets. Finally, oligodendrocytes and neurons may have a more efficient proteolytic machinery to remove oxidized proteins thus reducing the build up of carbonylated proteins in these cells. This may be also the case for T cells, whose proteasomal activity is enhanced during inflammation (Mattingly *et al.*, 2007).

Another significant finding in this study was the identification of β -actin, β -tubulin, GFAP and HSC-71 as major targets of protein carbonylation in the

cerebellum of both acute and chronic EAE. It should be noted that the detection and identification of oxidized species using a 2D-oxyblot is biased toward abundant cell proteins and that longer exposure times reveals the presence of other modified species. However, many proteins are as abundant as β -actin, β -tubulin and GFAP and yet they have minimal carbonylation (e.g. spectrin) or their oxidation does not change in EAE (e.g. vimentin), which suggests specificity. Indeed, metal ion-catalyzed oxidation of *Escherichia coli* proteins seems to be highly selective with most carbonylation sites present in RKPT-enriched regions that are exposed to the solvent (Maisonneuve *et al.*, 2009). It has been known for some time that in neurodegenerative disorders cytoskeletal proteins are particularly susceptible to carbonylation (Aksenov *et al.*, 2001; Muntané *et al.*, 2006). Furthermore, previous work from our lab has also identified β -actin, β -tubulin and GFAP as significant targets of carbonylation in the brain of MS patients (Hilgart and Bizzozero, 2008) and in the spinal cord of rats with acute EAE (Smerjac and Bizzozero, 2008).

Carbonylation of cytoskeletal proteins has been reported to cause loss of function. For instance, actin filaments and microtubules both destabilize and disassemble upon oxidation of their protein components (Dalle-Donne *et al.*, 2001; Neely *et al.*, 2005). Oxidative damage of GFAP has been described in Alzheimer's disease (Korolainen *et al.*, 2005; Pamplona *et al.*, 2005), aceruloplasminaemia (Kaneko *et al.*, 2002), Pick's disease (Muntané *et al.*, 2006) and MS (Hilgart and Bizzozero, 2008). Whether the accumulation of oxidized GFAP is associated with loss of function, as demonstrated for the other

cytoskeletal proteins, is not known. Because GFAP is a main intermediate filament of cytoskeleton that modulates astrocyte stability and shape, it is possible that the accumulation of oxidized GFAP may have an effect on astrocyte morphology. Interestingly, carbonyl-positive astrocytes in chronic EAE, where the proportion of oxidized GFAP is relatively high, have very short processes and there is redistribution of this protein from the processes to the soma. In contrast, normal morphology of activated astrocytes with long processes was observed at the peak of the disease where, despite the large excess of GFAP, the proportion of oxidized protein is just above control values. Carbonylation may also affect other GFAP properties such as the anchoring of the glutamate transporter GLAST to the plasma membrane of astrocytes, which seems to play an important role in protecting the brain against glutamate-mediated excitotoxicity (Sullivan *et al.*, 2007). Significant carbonylation of HSC-71 was detected in both EAE and control cerebella, suggesting that this chaperone is highly susceptible to oxidation. HSC-71 is a constitutively expressed and multifunctional chaperone protein present in both neurons and activated astrocytes (Kanninen *et al.*, 2004). Based on its involvement in the structural maintenance of the proteasome and conformational recognition of misfolded proteins by proteases, HSC-71 expression has been proposed as a defensive mechanism of response to unfavorable conditions. While our study is the first to describe carbonylation of HSC-71, other chaperones are known to exhibit an age-associated increase in carbonylation including BiP/Grp78, protein disulfide isomerase, and calreticulin (Rabek *et al.*, 2003).

In present study, the total amount of carbonylated protein at the peak of disease is significantly increased compared to that of control animals, while little change is found during the chronic phase of EAE. This is likely due to the lower number/activity of inflammatory lesions, the site where protein carbonyls build-up, in the chronic phase of EAE. Indeed, immunohistochemical studies revealed that carbonyls accumulate in the diseased white matter in both phases of EAE (Fig. 3). Moreover, the percentage of oxidized GFAP, β -tubulin and β -actin in the chronic phase are considerably higher than those in the acute phase. While the proportion of carbonylated cytoskeletal proteins measured in the cerebellum homogenate of chronic animals seems low (~2% for GFAP), one has to consider that these oxidized molecules may be distributed heterogeneously. Thus, the proportion of modified cytoskeletal proteins in cells near inflammatory foci may be much higher than that determined in the pull-down assays from the entire tissue. The amount carbonylated protein is determined by the rate of generation and degradation of carbonyls. Proteolysis is considered the only physiological mechanism for elimination of carbonylated proteins since there is no evidence for enzymatic reduction of protein-bound carbonyl groups to alcohols (Bizzozero, 2009). Therefore, since protein carbonyls cannot be repaired and since there is less oxidative stress in chronic than in acute EAE, it is fair to conclude that the accumulation of carbonylated cytoskeletal proteins in the cerebellum of chronic EAE mice may be due to impaired degradation. This, in turn, could be caused by reduced activity of the degradation system and/or by decreased susceptibility of the oxidized proteins to proteolysis. Degradation of carbonylated proteins is

thought to be carried out in an ATP- and ubiquitin-independent manner by the 20S proteasome, which selectively recognizes and digests partially unfolded oxidized proteins (Rivett, 1985; Grune *et al.*, 1995). Interestingly, preliminary studies in our laboratory discovered a significant decrease in proteasome activity in chronic EAE, which might explain the accumulation of oxidized proteins as disease progresses (Zheng and Bizzozero, 2010). At this time, however, we cannot exclude that oxidized cytoskeletal proteins are also less susceptible to digestion by the proteasome and other cellular proteases as previously proposed (Friguet *et al.*, 1994). Studies in our laboratory are underway to examine this possibility.

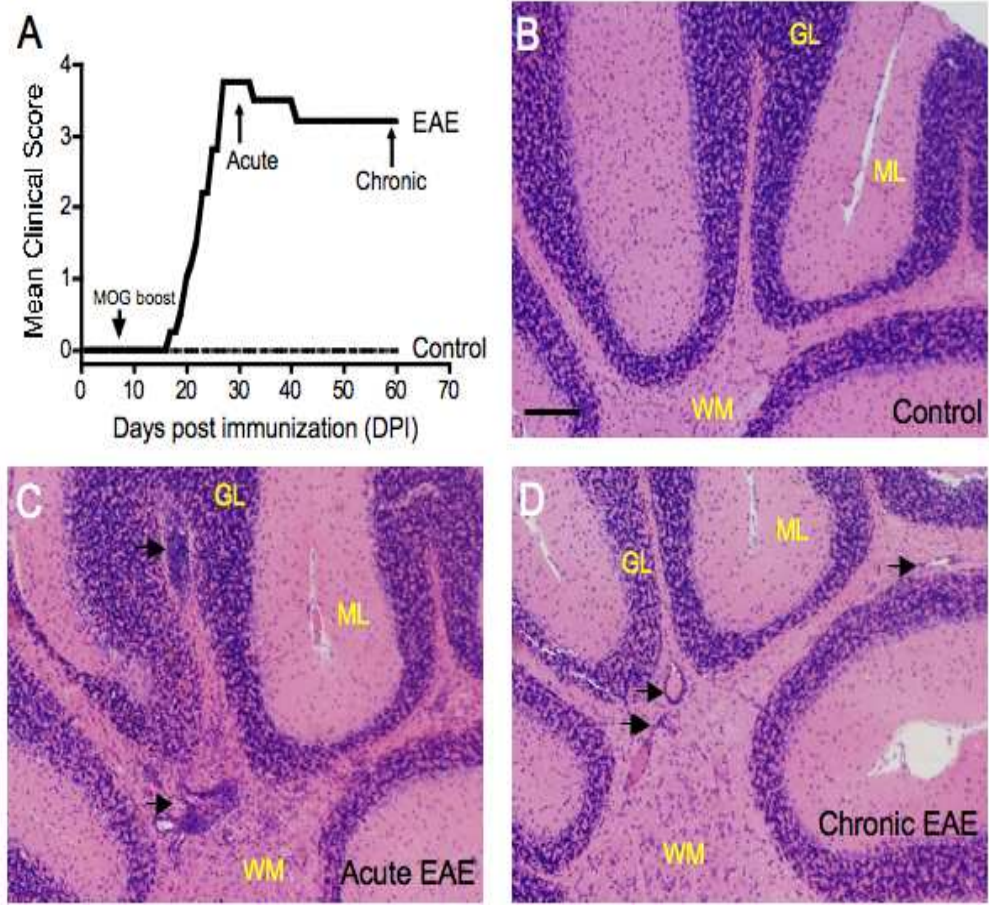


Figure 2.1 Clinical course and cerebellar pathology of EAE in C57BL/6 female mice. EAE was induced by active immunization with MOG35-55 peptide as described under Materials and Methods. Animals were monitored daily for signs of clinical disease and scored as indicated in the text. Clinical scores represent the mean of 6 control and 10 EAE mice (panel A). Panels B-D depict representative H&E-stained cerebellar sections from control, acute EAE and chronic EAE mice, respectively. GL, granule cells layer; ML, molecular layer; WM, white matter. In panel C, arrows point to perivenular white matter lesions with abundant lymphocyte infiltration in the acute EAE. In panel D, arrows point to perivenular white matter lesions in chronic EAE that show reduced inflammatory activity. Bar= 300µm.

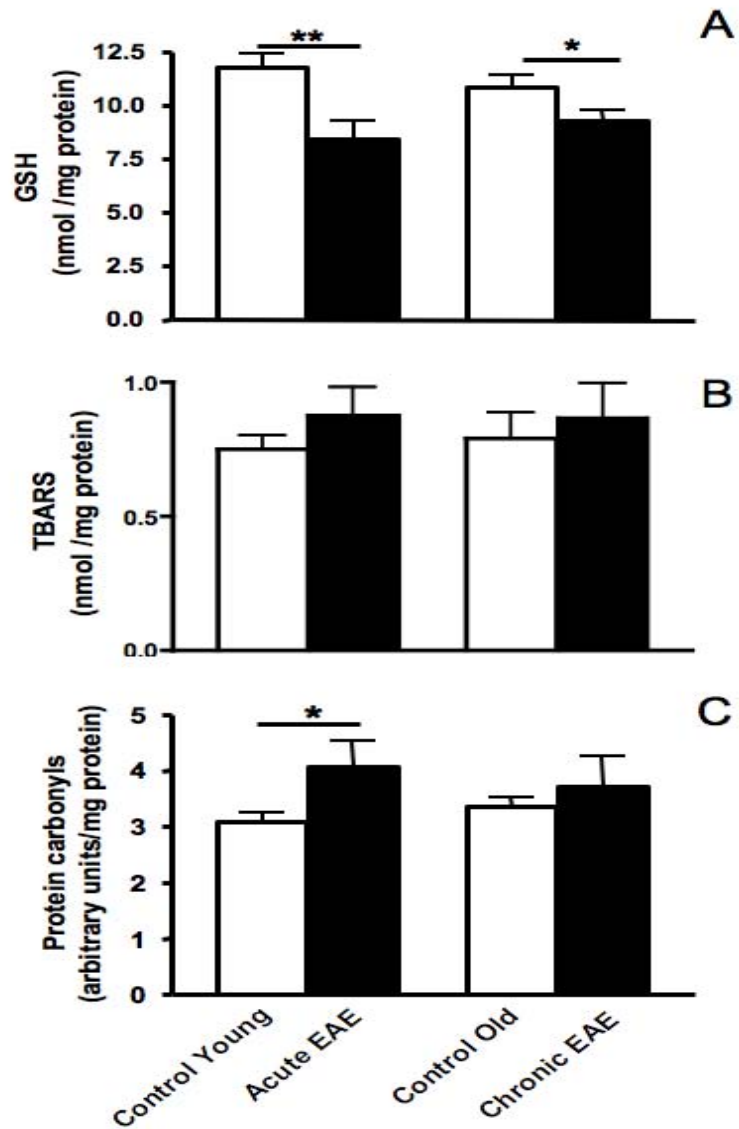


Figure 2.2 Levels of oxidative stress markers in the cerebellum of acute and chronic EAE mice. Aliquots of cerebellar homogenates from control and EAE mice were used to determine the levels of reduced glutathione (panel A), TBARS (panel B) and protein carbonyls (panel C) as described in Materials and Methods. Values represent the mean \pm SEM of 5 animals in each experimental group. Asterisks denote values that are statistically different ($p < 0.05$) from their respective controls.

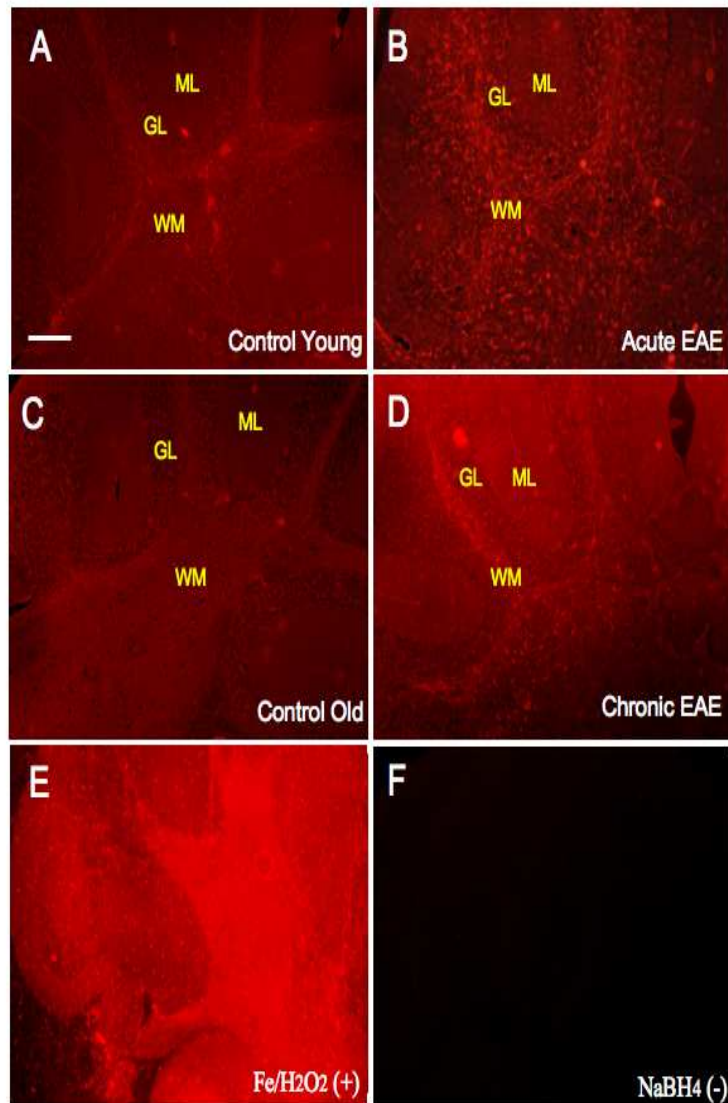


Figure 2.3 High levels of carbonyls in cerebellar white matter of acute and chronic EAE mice. Cerebellar sections (6 μ m-thick) from control, acute EAE and chronic EAE mice were incubated with DNPH to convert carbonyls into DNP-derivatives, which were detected by sequential incubation with rabbit anti-DNP and Alexa Fluor® 647 (red) goat anti-rabbit antibodies as described under Materials and Methods (panels A-D). Panels E and F show cerebellar sections from control animals that were pretreated with Fe/H₂O₂ to generate carbonyls (positive control) and with NaBH₄ to remove endogenous carbonyls (negative control), respectively. Bar= 300 μ m. Other abbreviations are as in Fig 1.

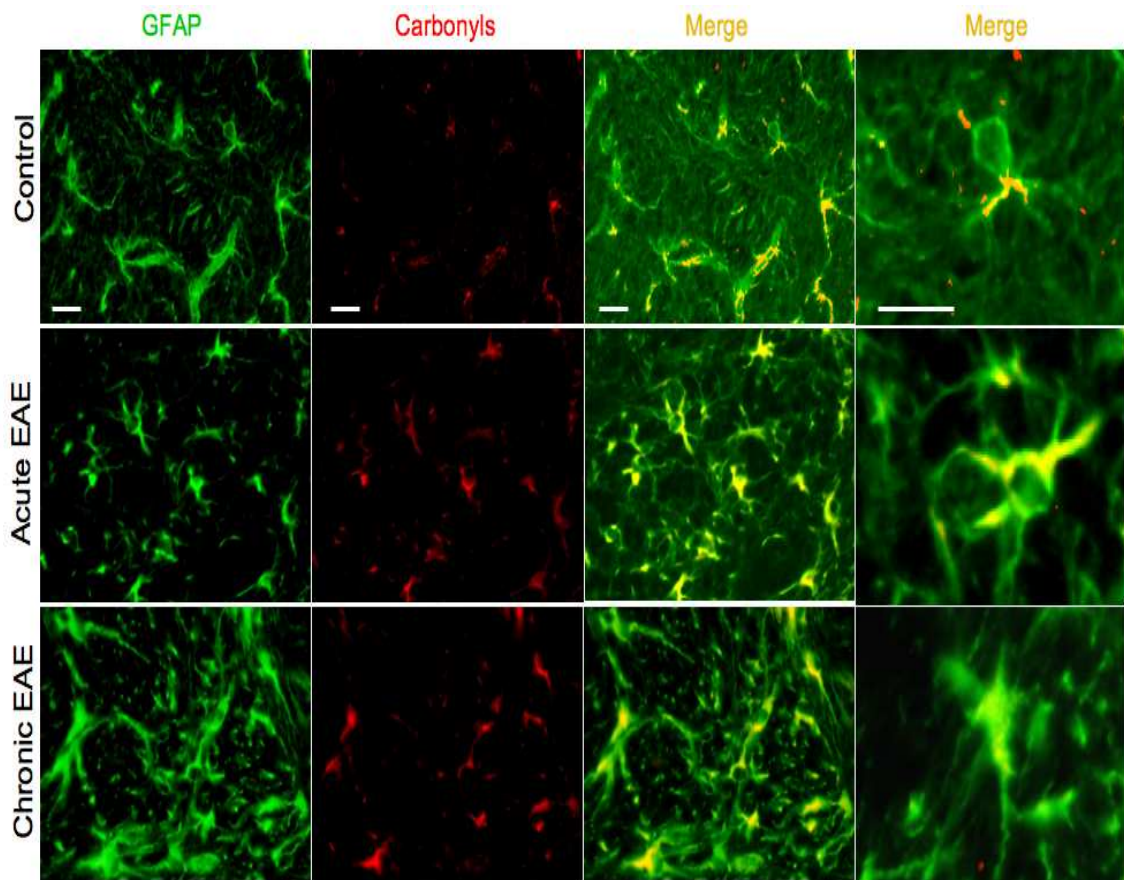


Figure 2.4 Colocalization of carbonyls and GFAP in the cerebellum of acute and chronic EAE mice. Double immunofluorescence analysis was performed as described in Methods and Materials. Green channel is for GFAP-positive astrocytes while red channel is for carbonyls. Immunofluorescent images show that the majority of white matter astrocytes in the cerebellum of acute and chronic EAE mice contain significant amounts of carbonyls. In acute EAE, cerebellar astrocytes have normal morphology and show colocalization of GFAP and carbonyl staining in their distal processes. In chronic EAE, cerebellar astrocytes exhibit abnormal morphology including the retraction of some processes. Bar= 50 μ m.

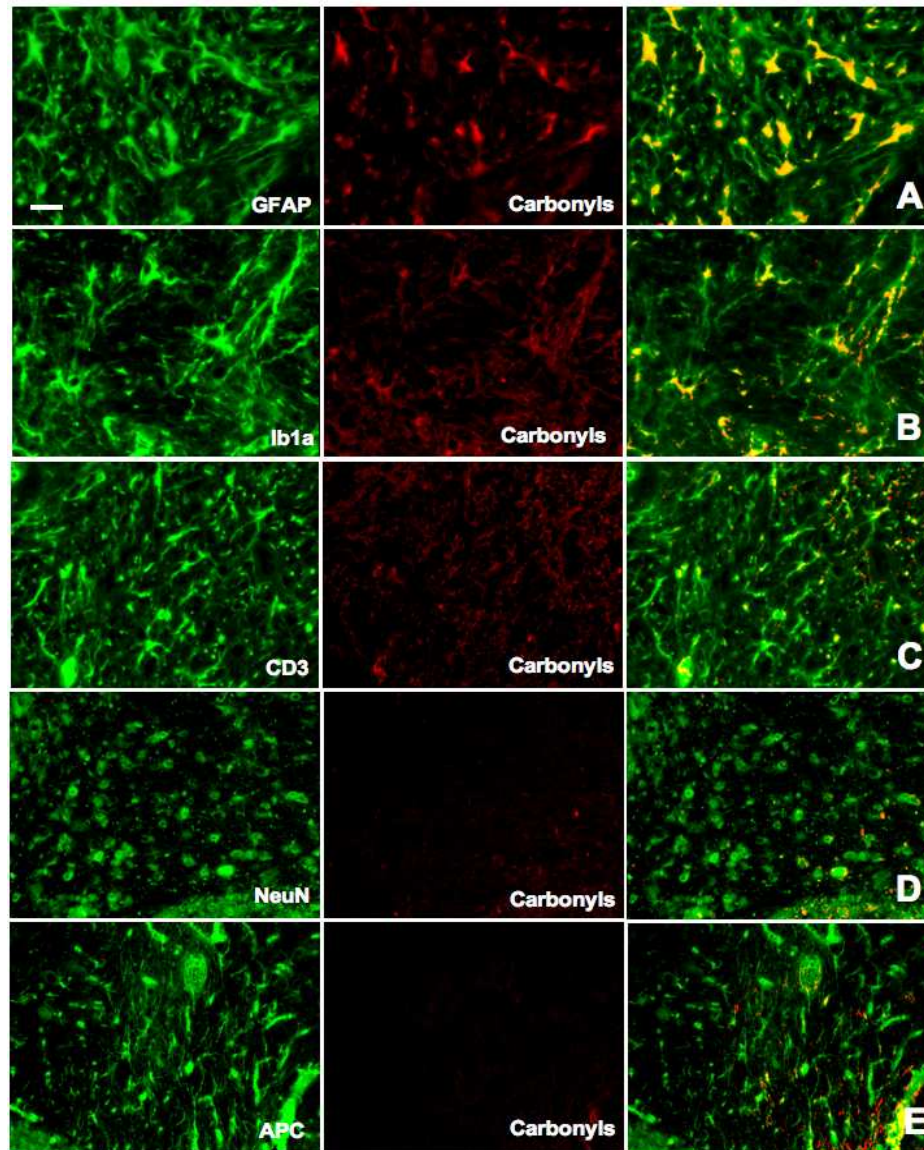


Figure 2.5 Carbonyl staining in the cerebellum of chronic EAE mice colocalizes mostly with astrocytes and some microglial cells. Double immunofluorescence analysis was performed as described in Methods and Materials. Green channel is for the various cell markers while red channel is for carbonyls. Immunofluorescent images show that the majority of cerebellar astrocytes (GFAP+) (panel A) and a significant proportion of microglia/macrophages (Ib1a+) in chronic EAE mice (panel B) are positive for carbonyls. In contrast, only a few CD3+-Tcells (panel C), NeuN-expressing neurons (panel D) and APC+-oligodendrocytes (panel E) show positive carbonyl staining. Bar= 50µm.

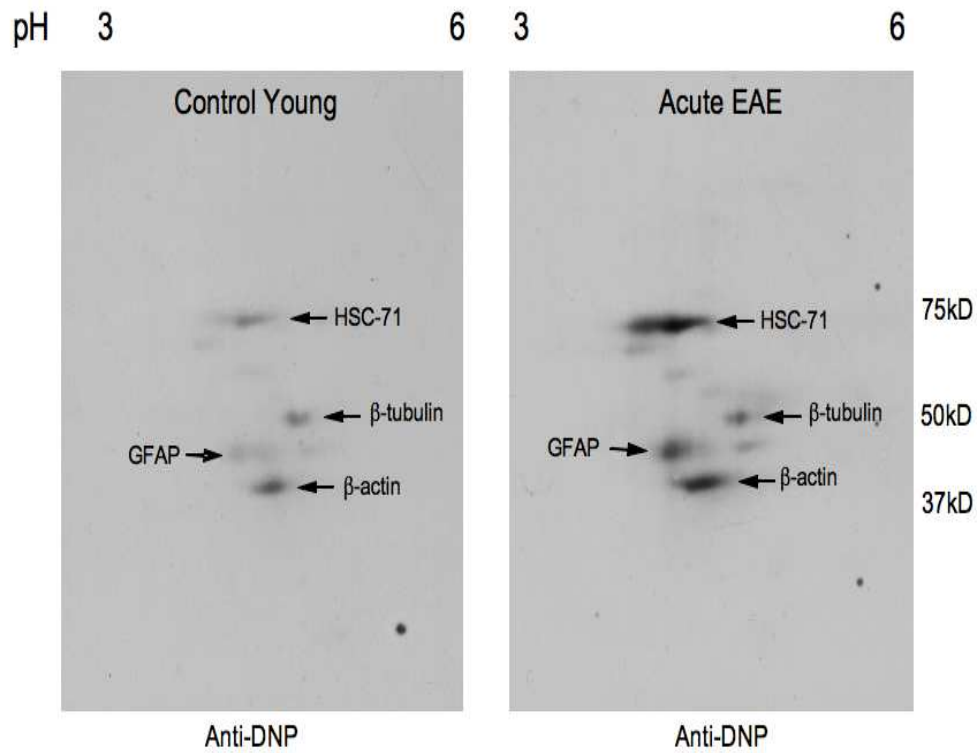


Figure 2.6 β -Actin, β -tubulin, GFAP and HSC-71 are the major carbonylated proteins in EAE cerebellum. Cerebellar proteins from control and EAE mice were derivatized with 2,4-dinitrophenylhydrazine. Proteins were separated by 2-D-gel electrophoresis and blotted to PVDF membranes. Membranes were immunostained with anti-DNP, then stripped and re-probed with antibodies against the major cytoskeletal proteins. β -Actin, β -tubulin and GFAP on the oxyblots were identified by spot matching. HSC-71 was identified by mass spectrometry as described in Materials and Methods. Only the pH 3-6 region of the oxyblots is shown since the pH 6-10 region was devoid of visible carbonyl-positive spots.

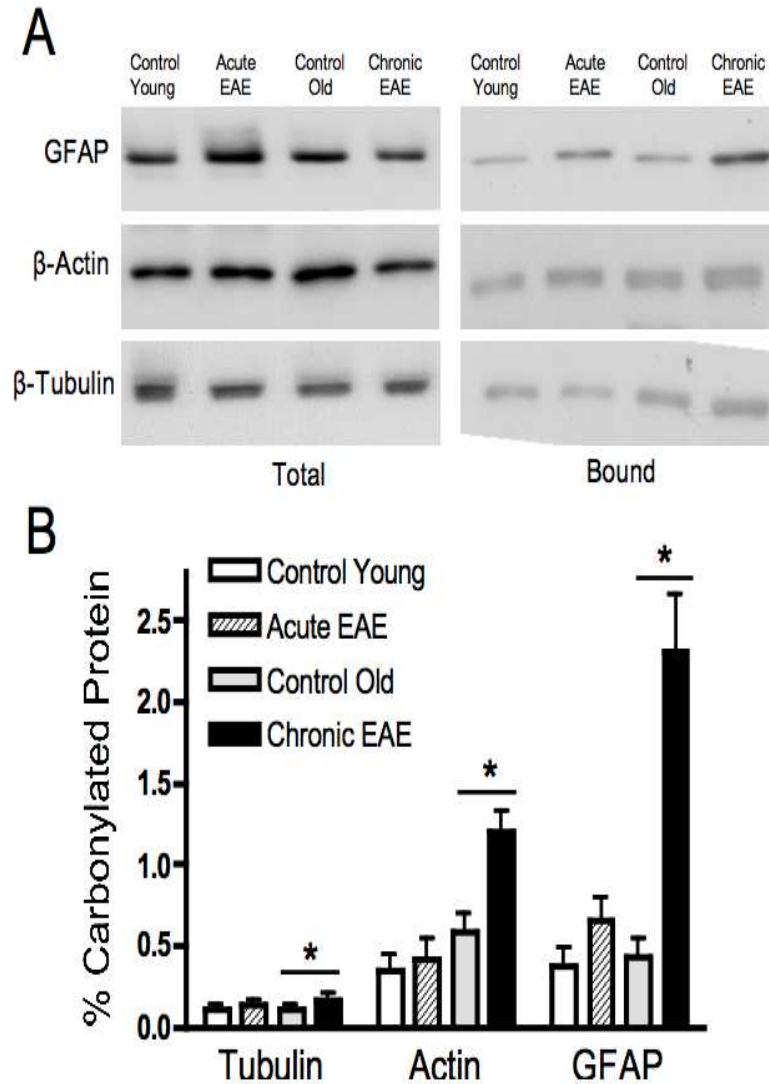


Figure 2.7 GFAP, β -actin and β -tubulin are more carbonylated in chronic than in acute EAE. Carbonylated proteins were converted into biotinylated proteins and were isolated using streptavidin-agarose as described under Materials and Methods. Aliquots of the starting material (total) and the streptavidin-purified fraction (bound) were separated on SDS-gels and transferred to PVDF membrane. Blots were probed with antibodies against various proteins and were developed by ECL (panel A). Densitometric scans were obtained to calculate the proportion of each protein that is carbonylated (panel B). Values represent the mean \pm SEM of five animals. * $p < 0.05$.

2.6 Reference

- Aksenov MY, Aksenova MV, Butterfield DA, Geddes JW, Markesbery WR. 2001. Protein oxidation in the brain in Alzheimer's disease. *Neuroscience* 103: 373 – 383.
- Benarroch EE. 2009. Oligodendrocytes: Susceptibility to injury and involvement in neurologic disease. *Neurology* 72: 1779-1785.
- Bizzozero OA, Malkoski SP, Mobarak C, Bixler HA, Evans J. (2002) Mass-spectrometric analysis of myelin proteolipids reveals new features of this family of palmitoylated membrane proteins. *J Neurochem* 81: 636-645.
- Bizzozero OA. 2009. Protein carbonylation in neurodegenerative and demyelinating CNS diseases. In "Handbook of Neurochemistry and Molecular Neurobiology" (Lajtha A, Banik N, Ray S, eds) Springer, pp. 543-562
- Bizzozero OA, DeJesus G, Callahan K, Pastuszyn A. 2005. Elevated protein carbonylation in the brain white matter and gray matter of patients with multiple sclerosis. *J Neurosci Res* 81: 687 – 695.
- Bizzozero OA, Ziegler JL, De Jesus G, Bolognani F. 2006. Acute depletion of reduced glutathione causes extensive carbonylation of rat brain proteins. *J Neurosci Res* 83: 656-667.
- Dalle-Done I, Rossi R, Giustarini D, Gagliano N, Lusini L, Milzani A, Di Simplicio P, Colombo R. 2001. Actin carbonylation: from a simple marker of protein oxidation to relevant signs of severe functional impairment. *Free Rad Biol Med* 31: 1075-1083.
- Davies MJ. 2005. The oxidative environment and protein damage. *Biochim Biophys Acta* 1703: 93-109.
- Dringen R. 2005. Oxidative and antioxidative potential of brain microglial cells. *Antiox and Redox Signaling* 7: 1223-1233.
- Esterbauer H, Schaur RJ, Zollner H. 1991. Chemistry and biochemistry of 4-hydroxynonenal, malonaldehyde and related aldehydes. *Free Radic Biol Med* 11: 81–128.
- Ferrante RJ, Browne SE, Shinobu LA, Bowling AC, Baik MJ, MacGarvey U, Kowall NW, Brown RH, Beal MF. 1997. Evidence of increased oxidative damage in both sporadic and familial amyotrophic lateral sclerosis. *J Neurochem* 69: 2064 – 2074.
- Floor E, Wetzel MG. 1998. Increased protein oxidation in human substantia nigra pars compacta in comparison with basal ganglia and prefrontal cortex measured with an improved dinitrophenylhydrazine assay. *J Neurochem* 70: 268 – 275.
- Friguet B, Szweda LI, Stadtman ER. 1994. Susceptibility of glucose-6-phosphate dehydrogenase modified by 4-hydroxy-2-nonenal and metal-catalyzed oxidation to proteolysis by the multicatalytic protease. *Arch Biochem Biophys* 311: 168 – 173.
- Gilgun-Sherki Y, Melamed E, Offen D. 2004. The role of oxidative stress in the pathogenesis of multiple sclerosis: the need for effective antioxidant therapy. *J Neurol* 251: 261 – 268.

- Gold R, Hartung HP, Toyka KV. 2000. Animal models for autoimmune demyelinating disorders of the nervous system. *Mol Med Today* 6: 88 - 91.
- Grune T, Reinheckel T, Joshi M, Davies KJ. 1995. Proteolysis in cultured liver epithelial cells during oxidative stress. Role of the multicatalytic proteinase complex, proteasome. *J Biol Chem* 270: 2344-2351.
- Halliwell B. 2006. Oxidative stress and neurodegeneration: where are we now? *J Neurochem* 97:1634-1658.
- Hilgart AA, Bizzozero OA. (2008) Carbonylation of major cytoskeletal proteins in multiple sclerosis. *J Neurochem* 104 (Suppl.1) PTW06-03.
- Kanninen K, Goldsteins G, Auriola S, Alafuzoff I, Koistinaho J. 2004. Glycosylation changes in Alzheimer's disease as revealed by a proteomic approach. *Neurosci Lett* 367: 235-240.
- Kaneko K, Nakamura A, Yoshida K, Kametani F, Higuchi K, Ikeda S. 2002. Glial fibrillary acidic protein is greatly modified by oxidative stress in aceruloplasminemia brain. *Free Radic Res* 36: 303-306
- Keller JN, Hanni KB, Gabbita SP, Friebe V, Mattson MP, Kindy MS. 1999. Oxidized lipoproteins increase reactive oxygen species formation in microglia and astrocyte cell lines. *Brain Res* 830: 10-15.
- Kornek B, Lassmann H. 1999. Axonal pathology in multiple sclerosis: a historical note. *Brain Pathol* 9: 651-656.
- Korolainen MA, Auriola S, Nyman TA, Alafuzoff I, Pirttila T. 2005. Proteomic analysis of glial fibrillary acidic protein in Alzheimer's disease and aging brain. *Neurobiol Dis* 20: 858-870.
- Kuerten S, Kostova-Bales DA, Frenzel LP, Tigno JT, Tary-Lehmann M, Angelov DN, Lehmann PV. 2007. MP4- and MOG:35-55-induced EAE in C57BL/6 mice differentially targets brain, spinal cord and cerebellum. *J Neuroimmunol* 189: 31-40.
- MacKenzie-Graham A, Tiwari-Woodruff SK, Sharma G, Aguilar C, Vo KT, Strickland LV, Morales L, Fubara B, Martin M, Jacobs RE, Johnson GA, Toga AW, Voskuhl RR. 2009. Purkinje cell loss in experimental autoimmune encephalomyelitis. *Neuroimage* 48: 637-651.
- Maisonneuve E, Ducret A, Khoeiry P, Lignon S, Longhi S, Talla E, Dukan S. 2009. Rules governing selective protein carbonylation. *PLoS One* 4: e-7269.
- Mattingly LH, Gault RA, Murphy WJ. 2007. Use of systemic proteasome inhibition as an immune-modulating agent in disease. *Endocrine, Metabolic & Immune Disorders - Drug Targets* 7: 29-34.
- Miller VM, Lawrence DA, Mondal TK, Seegal RF. 2009. Reduced glutathione is highly expressed in white matter and neurons in the unperturbed brain - Implication for oxidative stress associated with neurodegeneration. *Brain Res* 1276: 22-30.
- Muntané G, Dalfó E, Martínez A, Rey MJ, Avila J, Pérez M, Portero M, Pamplona R, Ayala V, Ferrer I. 2006. Glial fibrillary acidic protein is a major target of glycoxidative and lipoxidative damage in Pick's disease. *J Neurochem* 99:177-185.

- Neely MD, Boutte A, Milatovic D, Montine TJ. 2005. Mechanisms of 4-hydroxynonenal-induced neuronal microtubule dysfunction. *Brain Res* 1037: 90-98.
- Ohkawa H, Ohishi N, Yagi K. 1979. Assay for lipid peroxides in animal tissues by thiobarbituric acid reaction. *Anal Biochem* 95: 351 - 358.
- Pamplona R, Dalfó E, Ayala V, Bellmunt MJ, Prat J, Ferrer I, Portero-Otin M. 2005. Proteins in human cortex are modified by oxidation, glycooxidation, and lipoxidation. *J Biol Chem* 280: 21522–21530.
- Rabek JP, Boylston WH, Papaconstantinou J. 2003. Carbonylation of ER chaperone proteins in aged mouse liver. *Biochem Biophys Res Commun* 305: 566-572.
- Ramasamy DP, Benedict RH, Cox JL, Fritz D, Abdelrahman N, Hussein S, Minagar A, Dwyer MG, Zivadinov R. 2009. Extent of cerebellum, subcortical, and cortical atrophy in patients with MS: a case-control study. *J Neurol Sci* 282: 47-54.
- Requena JS, Chao CC, Levine R, Stadtman ER. 2001. Glutamic and aminoadipic semialdehydes are the main carbonyl products of metal-catalyzed oxidation of proteins. *Proc Natl Acad Sci USA* 98: 69-74.
- Rivett AJ. 1985. Preferential degradation of the oxidatively modified form of glutamine synthetase by intracellular mammalian proteases. *J Biol Chem* 260: 300-305.
- Smerjanc SM, Bizzozero OA. 2008. Cytoskeletal protein carbonylation and degradation in experimental autoimmune encephalomyelitis. *J Neurochem* 105: 763-772.
- Sullivan SM, Lee A, Björkman ST, Miller SM, Sullivan RK, Poronnik P, Colditz PB, Pow DV. 2007. Cytoskeletal anchoring of GLAST determines susceptibility to brain damage: an identified role for GFAP. *J Biol Chem* 282: 29414-29423.
- Trapp BD, Syts PK. 2009. Virtual hypoxia and chronic necrosis of demyelinated axons in multiple sclerosis. *Lancet Neurol* 8: 280-291.
- Zheng J, Bizzozero OA. 2009. Accumulation of protein carbonyls within cerebellar astrocytes in chronic experimental autoimmune encephalomyelitis. *J Neurochem* 108 (Suppl. 1) PTW06-22.
- Zheng J, Bizzozero OA. 2010. Reduced proteasomal activity contributes to accumulation of carbonylated proteins within cerebellar astrocytes in chronic EAE. *Trans Am Soc Neurochem* PTW07-07.

3 Reduced proteasomal activity may contribute to the accumulation of carbonylated proteins in chronic experimental autoimmune encephalomyelitis

Jianzheng Zheng and Oscar A. Bizzozero

Department of Cell Biology and Physiology

University of New Mexico - Health Sciences Center

Albuquerque, NM 87131

(Journal of Neurochemistry, In press)

3.1 Abstract

We have recently shown that several carbonylated proteins, including GFAP, β -actin and β -tubulin, accumulate within cerebellar astrocytes during the chronic phase of MOG35-55 peptide-induced EAE in C57BL/6 mice. Since protein carbonyls cannot be repaired and there is less oxidative stress in chronic than in acute EAE, we hypothesized that the accumulation of carbonylated proteins in the former animals may be due to a defect in the degradation of the modified proteins. Alternatively, oxidized proteins in chronic EAE mice may be more resistant to proteolysis. Using LPS-stimulated astrocytes and several protease inhibitors we identified the 20S proteasome as the proteolytic system responsible for the elimination of most oxidized proteins. We also discovered that the chymotrysin-like and caspase-like activities of the 20S proteasome are impaired in chronic EAE, while the amount of proteasome was unchanged. Proteasome failure in these animals was confirmed by the build-up of ubiquitinated proteins, mostly within astrocytes. In a cell-free system, carbonylated proteins from EAE mice with acute and chronic disease seem to be equally sensitive to proteasomal degradation. Altogether, the results support the notion that diminished activity of the 20S proteasome is a major contributor to the accumulation of carbonylated proteins in astrocytes of chronic EAE mice.

3.2 Introduction

Carbonylation refers to the non-enzymatic addition of aldehyde or ketone groups to specific amino acid residues and constitutes the major and most common oxidative alteration of proteins (Dalle-Donne *et al.*, 2003; Nystrom,

2005). Like in several CNS disorders, including Alzheimer's disease (Aksenov *et al.*, 2001), Parkinson's disease (Floor & Wetzel, 1998) and amyotrophic lateral sclerosis (Ferrante *et al.*, 1997), multiple sclerosis (MS) (Bizzozero *et al.*, 2005; Hilgart & Bizzozero, 2008) and its animal model experimental autoimmune encephalomyelitis (EAE) are also characterized by accumulation of carbonylated (oxidized) proteins (Smerjac & Bizzozero, 2008; Zheng & Bizzozero, 2010a). Carbonylation leads almost always to loss of protein function and is believed to partake in the etiology of these neurological diseases (for a review, see Bizzozero, 2009). In MOG35-55 peptide-induced EAE, the amount of the most abundant carbonylated proteins (e.g., β -actin, β -tubulin and GFAP) in cerebellar astrocytes was found to augment as disease advances from the inflammatory (acute) phase to the neurodegenerative (chronic) phase (Zheng & Bizzozero, 2010a), suggesting that this deleterious protein modification may play a role in disease progression as well.

It is clear that the amount of carbonylated protein is determined by the rates of generation and degradation of carbonyls. Proteolysis is currently considered the only physiological mechanism for elimination of carbonylated proteins, as there is no evidence for enzymatic reduction of protein-bound carbonyl groups to alcohols (Bizzozero, 2009). This and the fact that there is less oxidative stress in chronic than in acute EAE (Zheng & Bizzozero, 2010a) suggest that the accumulation of carbonylated cytoskeletal proteins in the cerebellum of chronic EAE mice may be due to impaired degradation. This phenomenon, in turn, could be the result of reduced activity of the degradation system and/or decreased

susceptibility of the oxidized proteins to proteolysis. In mammalian cells, the removal of carbonylated proteins is mostly carried out by the 20S proteasome in an ATP- and ubiquitin-independent manner (Shringarpure *et al.*, 2003; Divald & Powell, 2006). This multi-enzymatic proteolytic particle selectively recognizes and digests partially unfolded (denatured) oxidized proteins through its chymotrypsin-like activity (Ferrington *et al.*, 2005). However, the calcium-dependent cysteine protease calpain and the lysosomal cathepsins have been also implicated in the proteolytic removal of damaged proteins. For instance, oxidized neurofilaments seem to be preferentially digested by calpain *in vitro* (Troncoso *et al.*, 1995) while heavily oxidized proteins are take-up by lysosomes for partial proteolysis (Dunlop *et al.*, 2009).

In this study, we initially assessed the role of these three major degradation systems in the accumulation of carbonylated proteins in LPS-stimulated astrocytes by using well-characterized protease inhibitors. The results clearly show that only the proteasome inhibitor epoxomicin leads to a build-up of carbonylated proteins, while inhibition of lysosomal proteases and calpain do not alter protein carbonylation levels. More important, we discovered that the chymotrypsin-like activity of the 20S proteasome is impaired in the cerebellum of mice with chronic, but not acute, EAE. This observation was also consistent with the accumulation of poly-ubiquitinated proteins within cerebellar astrocytes observed in the animals with the chronic disease. Furthermore, experiments in a cell-free system showed that carbonylated cytoskeletal proteins from acute and chronic EAE are equally sensitive to proteasomal degradation. Overall, this work

provides clear evidence that supports the notion that the accumulation of carbonylated proteins in chronic EAE is likely the result of reduced proteasomal activity. To the best of our knowledge, this the first report implicating proteasome dysfunction in the pathophysiology of EAE. A preliminary account of this work has been presented in abstract form (Zheng & Bizzozero, 2010b).

3.3 Materials and Methods

3.3.1 Astrocyte culture

Rat C6 glioblastoma cells (CCL-107) were obtained from American Type Culture Collection (Manassas, VA) and were established as a monolayer culture in Dulbecco's modified Eagle's/F-12 medium supplemented with 15% horse serum, 2.5% fetal bovine serum and an antibiotic/antimycotic mixture (Invitrogen Corp., Carlsbad, CA). Cells were maintained in a humidified incubator at 37°C in an atmosphere of 95% air / 5% CO₂. To be differentiated into astrocytes, C6 cells were serum-starved for 1h and then incubated with 1mM N6-2'-O-dibutyryl cyclic-AMP (Bt2AMP; Sigma, St Louis, MO) and 0.25 mM theophylline (Sigma) for up to 72h. At this point, astrocytes were activated with 1µg/ml lipopolysaccharide (LPS; Sigma) for 24 hours. Nitrite concentration in the cell supernatants was determined spectrofluorometrically using 2,3-diaminonaphthalene (Misko *et al.*, 1993) and non-protein thiol (mostly GSH) levels in the cell homogenates were determined with 5,5'-dithiobis-(2-nitrobenzoic acid) (Bizzozero *et al.*, 2006). To identify the proteolytic system responsible for degradation of carbonylated cytoskeletal proteins, LPS-treated and untreated astrocytes were incubated in the absence or presence of the proteasome

inhibitor epoxomicin (2 μ M; Boston Biochemical, Cambridge, MA), the lysosomal inhibitor NH₄Cl (2mM, Sigma) or the calpain inhibitor calpeptin (20 μ M, Sigma). After 24h, cells were either fixed with methacarn (methanol : chloroform : acetic acid, 60 : 30 : 10 by vol) or lysed in PEN buffer (20 mM sodium phosphate, pH 7.5, 1 mM EDTA, and 0.1 mM neocuproine) containing 2 mM 4,5 dihydroxy-1,3-benzene disulfonic acid and 1 mM dithiothreitol (DTT). Protein homogenates were stored at -20°C until use. Protein concentration was assessed with the Bio-Rad DC™ protein assay (Bio-Rad Laboratories; Hercules, CA) using bovine serum albumin as standard.

3.3.2 Induction of Experimental Autoimmune Encephalomyelitis (EAE)

Housing and handling of the animals as well as the euthanasia procedure were in strict accordance with the NIH Guide for the Care and Use of Laboratory Animals, and were approved by the Institutional Animal Care and Use Committee. Eight-week-old female C57BL/6 mice were purchased from Harlan Bioproducts (Indianapolis, IN) and housed in the UNM-animal resource facility. EAE was induced by active immunization with MOG35-55 peptide (AnaSpec, San Jose, CA) as described in our previous study (Zheng & Bizzozero, 2010a). Animals were weighed and examined daily for the presence of neurological signs. At prescribed days post-immunization (DPI), EAE mice and CFA-injected controls were euthanized by decapitation. The cerebellum was removed and either fixed with methacarn (methanol : chloroform : acetic acid, 60 : 30 : 10 by vol) or homogenized in PEN buffer with antioxidants. Protein homogenates were stored and processed as described above.

3.3.3 Protease activity assays

The various proteolytic activities of the proteasome were determined in cerebellar homogenates from control and EAE mice using fluorescence assays (Rodgers *et al.*, 2003). Briefly, 50µg of protein were incubated for 2h at 25°C with 50µM of the 7-aminomethyl-4-coumarin (AMC)-labeled peptide Suc-Leu-Leu-Val-Tyr-AMC (for chymotrypsin-like activity), Boc-Leu-Arg-Arg-AMC (for trypsin-like activity) or z-Leu-Leu-Glu-AMC (for caspase-like activity) in the absence or presence of 10µM clasto-lactacystin-β-lactone (Enzo Life Sciences, Plymouth Meeting, PA) or 50µM epoxomicin (for the trypsin-like activity). The different activities of the 20S proteasome were calculated as the difference in fluorescence intensity at 460nm between the samples without and with inhibitor using an excitation wavelength of 380nm.

Total calpain activity was determined by a similar procedure using the substrate Suc-Leu-Leu-Val-Tyr-AMC in 100mM KCl, 10mM CaCl₂, 25mM HEPES buffer pH 7.5, and carrying out the incubation in the absence or presence of 10 µg calpeptin (Hassem *et al.*, 2006). To measure soluble (active) calpain activity, membrane-bound calpain was removed prior to the assay by centrifugation at 10,000 g for 25 min.

Lysosomal proteolytic activity was also measured fluorometrically by incubating cerebellar homogenates with 200µM z-Phe-Arg-AMC in 50 mM sodium acetate (pH 5.5) for 30 min at 37°C (Sitte *et al.*, 2000).

3.3.4 Western blots

Proteins (5 µg) from cells or tissue homogenates were separated by SDS–polyacrylamide gel electrophoresis on 10% gels and blotted to polyvinylidene difluoride (PVDF) membranes. Blots then were incubated overnight at 4°C with monoclonal antibodies against GFAP (1:2,000; Sigma), GAPDH (1:2,000; Chemicon, Temecula, CA) or α -subunit of 20S proteasome (1:2,000; Enzo). Membranes were rinsed three times in phosphate-buffered saline (PBS) containing 0.05% Tween-20 and incubated for 2 h with horseradish peroxidase conjugated-conjugated goat anti-mouse antibody (1:2,000; Sigma). Blots were developed by enhanced chemiluminescence (ECL) using the Western Lightning ECL™ kit from Perkin-Elmer (Boston, MA, USA).

Protein carbonyl groups were measured by western blot analysis using the OxyBlot™ protein oxidation detection kit (Intergen Co., Purchase, NY) as described earlier (Smerjac & Bizzozero, 2008). In brief, proteins (5 µg) were incubated with 2,4-dinitrophenyl-hydrazine to form the 2,4-dinitrophenyl (DNP) hydrazone derivatives. Proteins were separated by electrophoresis and blotted to PVDF membranes as above. DNP-containing proteins were detected using rabbit anti-DNP antiserum (1:500) and goat anti-rabbit IgG conjugated to horseradish peroxidase (HRP) (1:2000).

3.3.5 Quantification of carbonylation levels in specific proteins

The extent of protein carbonylation was determined using a pull-down/western blot method (Bizzozero *et al.*, 2006). Briefly, protein carbonyls were biotinylated by reaction with biotin hydrazide in the presence of

cyanoborohydride. A small aliquot of these protein homogenates was saved for western blotting and the rest was used to isolate the biotinylated proteins using streptavidin-agarose. Proteins were eluted from the beads with SDS-sample buffer and analyzed by western blotting on 10% polyacrylamide gels. Blots were probed with antibodies against individual protein species and developed by ECL as described above. Films were scanned in a Hewlett Packard Scanjet 4890 and the images were quantified using the NIH Image 1.63 imaging analysis program. Band intensities from the total and streptavidin-bound fractions were used to calculate the percentage of protein that is modified by carbonylation.

3.3.6 Immunohistochemical localization of poly-ubiquitinated proteins in cerebellum.

Accumulation of poly-ubiquitinated proteins in the cerebellum was assessed by immunohistochemistry. To this end, cerebella from control and EAE animals were fixed overnight in methacarn and then mounted in paraffin. Tissue was sectioned in the sagittal plane (6- μ m thick) and mounted on Vectabond™-treated slides (Vector Laboratories, Burlingame, CA, USA). Sections were deparafinized with xylenes and a graded alcohol series, and then rinsed with PBS for 10 min. Lesions were detected by staining with hematoxylin and eosin. The adjacent slices were collected, rinsed three times with PBS, blocked with 10% (v/v) normal goat serum and incubated overnight with the mixture of anti-polyubiquitin antibody (1:200, mouse monoclonal; Enzo) and anti-GFAP antibody (1:200, rabbit polyclonal; Dako, Carpinteria, CA). After removing the primary antibodies with PBS containing 0.1% Triton X-100, the sections were incubated for 3 h with

fluorescent conjugated secondary antibodies (Alexa Fluor® 488 and Alexa Fluor® 647, Molecular Probes, Eugene, OR, USA). Slide-mounted sections were scanned at a total magnification of 80X and images were imported into Image J software to obtain optical density of polyubiquitin in GFAP immunoreactive cells in cerebella. Briefly, the poly-ubiquitin or GFAP optical density was measured by circling the whole GFAP immunoreactive cell. Three cells per slide and three slides per animal were randomly chosen. In all cases, the background was subtracted from the average density. The final data is presented as average density of polyubiquitin or polyubiquitin divided by GFAP.

3.3.7 Statistical Analysis

Results were analyzed for statistical significance with ANOVA utilizing GraphPad Prism® program (GraphPad Software Inc., San Diego, CA).

3.4 Results

3.4.1 Differentiation of C6 cells into astrocytes and induction of oxidative stress with LPS

An in vitro study was designed to identify the major proteolytic system(s) responsible for the removal of carbonylated proteins from astrocytes under oxidative stress conditions. To this end, we first established a cell culture system in which C6 glioma cells were differentiated into astrocytes by treatment with a cyclic AMP analogue (Haghighat *et al.*, 2000). As shown in Figure 3.1, treatment of C6 cells with Bt2AMP/theophylline elevated GFAP expression already at 8 h of incubation (Figure 3.1A-B). GFAP levels in these cells continued to increase until

72 h. At this time cells displayed the morphological characteristics of astrocytes (Figure 3.1C).

Differentiated astrocytes were then incubated with LPS (1µg/ml) for 24 h to induce oxidative stress. LPS is a bacterial endotoxin and a generally accepted inducer of pro-inflammatory responses (Kalmár *et al.*, 2001). As expected, the concentration of nitrite (a marker of nitric oxide production) in the medium was significantly higher in LPS-treated astrocytes (Figure 3.2A). GSH levels in LPS-stimulated astrocytes were reduced to 83% of control values (Figure 3.2B). Surprisingly, the amount of protein carbonyls, another marker of oxidative stress, was not increased in LPS-stimulated astrocytes (Figure 3.2C). This observation suggests that either the extent of oxidative stress is not enough to induce extensive protein carbonylation or that the proteolytic machinery present in these cells is sufficient to remove oxidized proteins as they are generated.

3.4.2 Proteasome inhibition leads to accumulation of carbonylated proteins in cultured astrocytes

To identify the proteolytic system responsible for the removal of oxidized proteins, control and LPS-stimulated astrocytes were incubated for 24 h in the absence or presence of the proteasome inhibitor epoxomicin (Meng *et al.*, 1999), the lysosomal inhibitor NH₄Cl (Brown *et al.*, 1985) or the calpain inhibitor calpeptin (Tsujioka *et al.*, 1988). To achieve maximal inhibition, these drugs were used at concentrations between 20- and 200-fold higher than their respective IC₅₀. As shown in Figure 3.3, only epoxomicin causes the build-up of

carbonylated proteins in both control and LPS-stimulated cells. These findings suggest not only that the proteasome is responsible for removal of oxidized proteins *in vitro*, but also that proteasomal proteolytic activity is more important than the redox environment in determining the carbonylation status of proteins.

We next investigated whether the major oxidized proteins that accumulate in the cerebellum of mice with chronic EAE (i.e. β -actin, β -tubulin and GFAP) are also degraded by the proteasome in cultured astrocytes. Quantification of the extent of carbonylation of individual proteins was performed using a pull-down/western blot procedure. To this end, protein carbonyl moieties from LPS-treated astrocytes that had been incubated with or without epoxomicin for 24 h were first converted into biotinylated residues by reaction with biotin-hydrazide. Biotin-containing proteins were then isolated with streptavidin-agarose and analyzed by western blotting employing antibodies against each of the three polypeptides. As shown in Figure 3.4, the proportion of β -actin, β -tubulin and GFAP present in the streptavidin-bound fraction increased significantly in the epoxomicin-treated cells, indicating that these proteins are also degraded by the proteasome. It is noteworthy that the molecular weight of oxidized proteins present in the bound fraction is identical to those in the total fraction, demonstrating that they do not contain attached ubiquitin moieties (8.5 kDa per monomer). Thus, it is fair to conclude that degradation of the carbonylated forms of β -actin, β -tubulin and GFAP, and likely those of most other proteins, is carried out by the proteasome via an ubiquitin-independent mechanism.

3.4.3 Proteasomal proteolytic activity is reduced in chronic EAE

After identifying the 20S proteasome as the proteolytic system responsible for removal of oxidized proteins in cultured astrocytes, we sought to determine whether or not the proteasome proteolytic activity is impaired in chronic EAE. To this end, EAE in female C57BL/6 mice was induced by active immunization with MOG35-55 peptide as described under Materials and Methods. Symptoms were graded according to the following scale: 0, no symptoms; 1, tail weakness; 1.5, clumsy gait; 2, hind limb paresis; 2.5, partial hind limb dragging; 3, hind limb paralysis; 3.5, hind limb paralysis with fore limb paresis; 4, complete paralysis; and 5, moribund. In this well-characterized EAE model, neurological symptoms begin at 14 DPI (7 days after the boost with MOG peptide) reaching a peak at 30 DPI, and most animals remain ill (score 3.0-3.5) throughout the entire experimental period (60 DPI) (Figure 3.5A). Acute disease was defined as having clinical signs of EAE without any signs of improvement for at least three consecutive days while chronic EAE was defined arbitrarily as animals that remain in the stationary phase of the disease for 30 days (60 DPI). A complete morphological description of the cerebellar pathology in this model, including the histological and cellular distribution of carbonyls, has been presented in our previous study (Zheng & Bizzozero, 2010a).

Aliquots of cerebellar homogenates from control and EAE mice, both at the peak of the disease and in the chronic phase, were used to determine the various proteolytic activities of the 20S proteasome. The chymotrypsin-like activity, which is believed to be responsible for degrading oxidized proteins

(Ferrington *et al.*, 2005), was elevated in acute EAE and greatly reduced (~40%) in chronic EAE relative to the controls (Figure 3.5B). This finding agrees with the idea that decreased proteasomal activity is behind the accumulation of protein carbonyls as disease progresses from the inflammatory (acute) to the neurodegenerative (chronic) phase. A similar pattern was found for the proteasome caspase-like activity (Figure 3.5C). The trypsin-like activity while increased in acute EAE was surprisingly unchanged in chronic EAE (Figure 3.5D).

To establish if the changes in proteolytic activity observed during the course of EAE was a consequence of variations in proteasome concentration, we measured the relative levels of the 20S proteasome α -subunit by western blot analysis. As depicted in Figure 3.6, the amount of proteasome α -subunit in acute and chronic EAE was the same as those in the controls, suggesting that decrease activity in the chronic phase of the disease may be due to enzyme inactivation.

We also looked into the possibility that the proteolytic activity of the lysosome and/or calpain may be decreased in chronic EAE. The activity of cathepsin B, one of the major lysosomal proteases, was assayed with the z-Phe-Arg-AMC peptide at acid pH. Using these conditions, the lysosomal proteolytic activity was increased in chronic EAE as compared to control animals, while no difference was observed between acute EAE and control mice (Figure 3.7A). Neither the total (Figure 3.7C) nor the soluble (active) calpain activity (Figure 3.7B) in the cerebellum of affected animals was different from those of controls.

3.4.4 Carbonylated cytoskeletal proteins prepared from acute and chronic EAE tissues are equally sensitive to proteasomal degradation in cell-free system.

Another possibility that could explain the build-up of oxidized proteins in chronic EAE is that the carbonylated species in the chronic phase are somehow more resistant to proteolysis than those present in the acute phase. To address this issue, we incubated cerebellar homogenates from acute and chronic EAE mice with 20S proteasome in the absence or presence of the proteasome inhibitor clasto-lactacystin- β -lactone. After 2h, the proportion of carbonylated β -actin, β -tubulin and GFAP was determined using the pull-down/western blot procedure described earlier. Since the results were the same for all three proteins, only those corresponding to GFAP are presented herein (Figure 3.8). The results clearly show that the proteolytic activity present in the tissue homogenate itself is sufficient to degrade carbonylated GFAP from acute and chronic EAE samples equally well. Addition of 20S proteasome did not produce any significant increase in the extent of proteolysis. In all cases, degradation of carbonylated GFAP was prevented by addition of clasto-lactacystin- β -lactone, indicating that proteolysis of oxidized proteins in this cell-free system, like in cultured astrocytes, is indeed mediated by the 20S proteasome. The fact that degradation of oxidized GFAP in this system takes place in the absence of added ATP demonstrates once again that the mechanism does not involve ubiquitination. In sum, these data support the notion that oxidized GFAP from acute and chronic EAE are equally sensitive to degradation by the 20S proteasome.

3.4.5 Ubiquitinated proteins build-up in cerebellar astrocytes in chronic EAE

Since a significant proportion of the 20S catalytic particle is part of the 26S proteasome we reasoned that the proteolytic activity of the latter, and thus the ability to remove ubiquitinated proteins, might also be compromised in chronic EAE. This possibility was explored by immunohistochemistry using a monoclonal antibody that reacts with mono/poly-ubiquitinated proteins but not with free ubiquitin. A strong and extensive poly-ubiquitin staining, the majority of which co-localizes with GFAP, was observed the cerebellum of chronic EAE but not acute EAE mice (Figure 3.9). The intensity of poly-ubiquitinated proteins relative to that of GFAP augmented three-fold in chronic EAE compared to the age-matched control while there was no difference in this parameter between acute EAE and its control. The accumulation of ubiquitinated proteins in cerebellar astrocytes of chronic EAE mice demonstrates an impairment of proteasomal activity in this cell type. Furthermore, this finding explains why the majority of carbonylated proteins also accumulate within these cells (Zheng & Bizzozero, 2010a).

3.5 Discussion

We have previously shown that the proportion of carbonylated GFAP, β -tubulin and β -actin is notably higher in chronic EAE mice than in acute EAE animals (Zheng & Bizzozero, 2010a). Because oxidative stress is relatively low in the chronic phase, we speculated either that the degradation system responsible for removal of oxidized proteins becomes impaired as disease progresses or that the carbonylated protein species from older animals are more resistant to degradation. To investigate these two non-excluding possibilities, we first

performed an *in vitro* study to identify the specific degradation system responsible for the removal of carbonylated proteins. Using LPS-stimulated astrocytes (the cell type where the majority of carbonyls accumulate in EAE) and a number of protease inhibitors, we identified the 20S proteasome as the system involved in the proteolysis of carbonylated proteins. This conclusion agrees with studies carried out in other systems (Shringarpure *et al.*, 2003; Divald & Powell, 2006). We then discovered that there is a marked reduction in the 20S proteasome chymotrypsin-like activity in chronic EAE without significant changes in the proteasome level. Moreover, based on studies in a cell-free system (Fig. 3.8), the possibility that oxidized cerebellar proteins from chronic EAE mice are less susceptible to proteasomal degradation seems unlikely. Thus, we conclude that the accumulation of carbonylated proteins in chronic EAE is probably the result of the direct inhibition of proteasome's proteolytic activity. The fact that decreased proteasomal activity and increased protein carbonylation take place primarily in the same cell type (i.e., astrocytes) further support such relationship. It is clear, however, that only the reduction in protein carbonyl levels upon over-expression or activation of the 20S proteasome in chronic EAE animals will demonstrate this conclusion.

Mammalian cells contain several proteolytic systems including the lysosomal cathepsins, calcium-activated proteases (calpains) and the 20S/26S proteasome (Grune *et al.*, 2001). It has been shown that degradation of carbonylated proteins is carried out in an ATP- and ubiquitin-independent manner by the 20S proteasome, which selectively recognizes and digests

partially unfolded (denatured) oxidized proteins (Rivett, 1985; Pacifici *et al.*, 1993; Grune *et al.*, 1995). However, the calcium-dependent cysteine protease calpain has been also shown to preferentially degrade oxidized neurofilament over non-oxidized protein in cell-free systems (Troncoso *et al.*, 1995). Furthermore, there is some evidence that moderately or heavily oxidized proteins are taken up by lysosomes, where in some cases are incompletely degraded and accumulate in the form of lipofuscin-like, autofluorescent aggregates (Dunlop *et al.*, 2009). Our study clearly shows that degradation of carbonylated proteins in LPS-treated and untreated astrocytes is carried out by 20S proteasome as neither calpain nor lysosome inhibition led to an accumulation of the oxidized proteins in the 24h-incubation period. Furthermore, calpain and cathepsin B activities were not impaired in chronic EAE, where there is a build up of carbonylated species. The increased lysosomal cathepsin B activity in the cerebellum of chronic EAE mice is noteworthy. As suggested by Pandley *et al.*, (2007), an increase in the lysosomal degradation machinery when the proteasome system is not functioning may represent a compensatory mechanism for intracellular protein degradation.

The 20S proteasome particle is composed by two outer (alpha) and two inner (beta) rings. Three of the β subunits carry the proteolytic activity, classified as caspase-like ($\beta 1$), trypsin-like ($\beta 2$), and chymotrypsin-like ($\beta 5$), which cleaves after acidic, basic and hydrophobic amino acids, respectively (Coux *et al.*, 1996). Of these, the $\beta 5$ subunit is believed to be responsible for the degradation of oxidized (carbonylated) proteins (Ferrington *et al.*, 2005). Thus, the decrease in

20S proteasome chymotrypsin-like activity in chronic EAE mice is consistent with the accumulation of carbonylated proteins previously reported in the same animals (Zheng & Bizzozero, 2010a). Interestingly, this decrease in chymotrypsin-like activity is not due to a reduction in the number of 20S particles since β -subunit expression was unaltered in the disease. Furthermore, the various activities were not equally affected throughout the course of the disease. For instance, only chymotrypsin-like and caspase-like activities were reduced in chronic EAE while only chymotrypsin-like and trypsin-like activities were augmented in acute EAE. Based on these findings, it is fair to speculate that, as disease progresses, there is a change in the proportion of individual β -subunits within the catalytic core particle and/or that the enzyme activities are specifically inhibited. The increase in the activity associated with β 2 and β 5 subunits during the inflammatory phase of disease might be due to the β -interferon-triggered replacement of these catalytic subunits by inducible subunits $i\beta$ 1, $i\beta$ 2 and $i\beta$ 5 to form the so-called immunoproteasome, which exhibits higher chymotrypsin-like and trypsin-like activities and lower caspase-like activity (Gaczynska *et al.*, 1993). Yet this mechanism would not explain the reduction in caspase-like and chymotrypsin-like activity observed in the chronic animals. In this regard, inhibitory posttranslational modifications (e.g., oxidation) or the increased presence of endogenous inhibitors such as cross-linked proteins may explain our findings. For example, oxidative injury to the heart during ischemia-reperfusion injury has been found to induce selective rather than global inhibition of proteasomal activity (Bulteau *et al.*, 2001a). Furthermore, specific subunits of the

20S proteasome are targeted for modification by the lipid peroxidation product 4-hydroxy-2-nonenal (4-HNE) (Farout *et al.*, 2006), the glycoxidation product glyoxal (Bulbeau *et al.*, 2001b) and β -ketoaldehydes (isoketals) (Davies *et al.*, 2002). Whether similar types of modifications also take place in EAE is not known. However, using antibodies against the major reactive carbonyl species, we have not been able to detect HNE, MDA or acrolein-adducts in EAE tissue (Zheng & Bizzozero, 2010a). A more likely modification of β -subunits could be the direct carbonylation of its amino acid residues as shown for those in proteasomes of hepatocellular carcinoma HepG2 cells under oxidative stress conditions (Kessova & Cederbaum, 2005). Beside direct inactivation of the proteasome by oxidation/carbonylation, 4-HNE cross-linked proteins (Friguet *et al.*, 1994) and lipofuscin/ceroid fluorescent pigments (Sitte *et al.*, 2000) have been implicated in the inhibition of proteasome activity. An additional and still unexplored possibility might be the inactivation of proteasome activity by specific autoantibodies. Interestingly, antibodies against several proteasomal subunits have been detected in serum and CSF from MS patients (Mayo *et al.*, 2002). It will be important to know if proteasome autoantibodies occur also in animals with chronic EAE and whether they indeed cause enzyme inhibition.

While novel, the discovery that proteasome activity is decreased in chronic EAE is not entirely unexpected. Impaired proteasomal function has been reported in several chronic neurodegenerative diseases including Alzheimer's disease (Keller *et al.*, 2000) Parkinson's disease (McNaught *et al.*, 2003) and Huntington's disease (Seo *et al.*, 2004). Furthermore, preliminary studies in our

laboratory suggest that this may be also the case in MS, where accumulation of both carbonylated proteins (Bizzozero *et al.*, 2005) and ubiquitin-conjugates (Giordana *et al.*, 2002) has been already described. The pathophysiological consequences of decreased proteasomal activity in chronic EAE as well as in classical neurodegenerative disorders are unknown. The functional impact resulting from the accumulation of a number of ubiquitinated, misfolded, aggregated and oxidized proteins, along with reduced degradation of various signaling and pro-apoptotic molecules, is likely widespread and difficult to predict. Yet decreased proteasomal activity is likely pathogenic and a contributor to neurodegeneration in chronic EAE. This notion is based mostly on experiments linking proteasomal inhibition to axonal damage (Korhonen, 2004), the development of pro-inflammatory responses via up-regulation of cyclooxygenase-2 and prostaglandin E2 (Rockwell *et al.*, 2000) and apoptosis of neurons and oligodendrocytes via mitochondrial dysfunction (Goldbaum *et al.*, 2006).

Finally, it is puzzling why proteasomal inhibition and accumulation of both oxidized and ubiquitinated proteins occur mostly in astrocytes. One possibility is that the ROS and other molecules produced upon inflammatory activation of astrocytes (Keller *et al.*, 1999) are capable of damaging the 20S proteasome. Since astrocytes are more resistant than neurons and oligodendrocytes to the cytotoxic consequences of proteasomal inhibition (Tsuji *et al.*, 2005; Goldbaum *et al.*, 2006), it is also possible that as disease progresses damaged neurons and oligodendrocytes die and are removed from the tissue leaving behind astrocytes

loaded with undigested proteins. Studies in our laboratory are underway to test these possibilities.

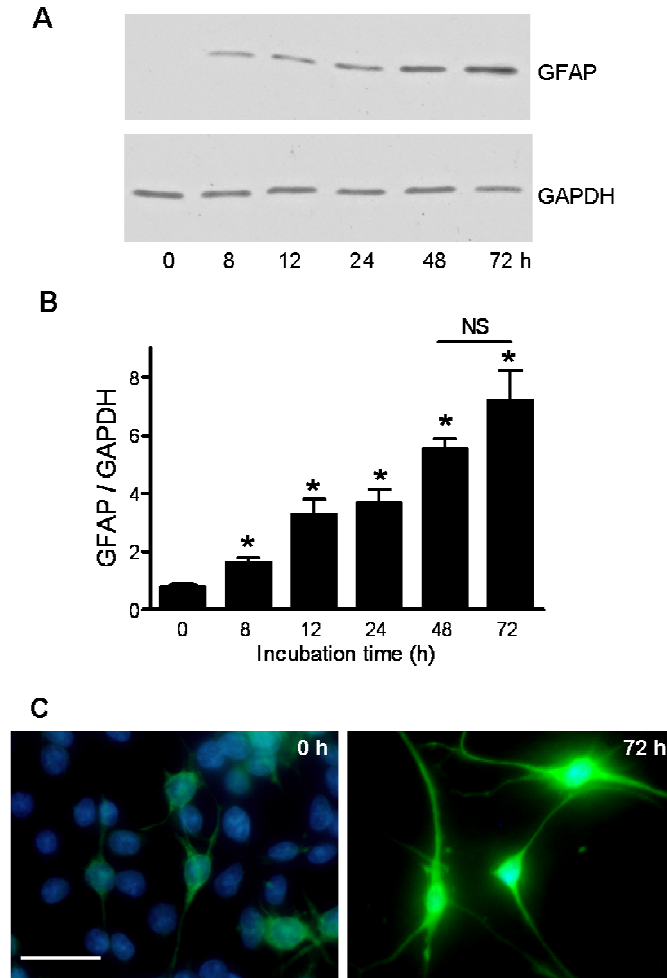


Figure 3.1 Differentiation of C6 glioma cells into astrocytes. C6 cells were incubated with Bt2AMP/theophylline for up to 72h as described in “Material and Methods”. Levels of GFAP and GAPDH were determined by western blot (panel A). Band intensities were measured by scanning densitometry and were used to calculate the GFAP/GAPDH ratio (panel B). Values represent the mean \pm SEM of 3 experiments. Asterisks denote values that are statistically different ($p < 0.05$) from non-stimulated control cells. NS, not significant. Panel C shows a double immunofluorescence picture of untreated and Bt2AMP/theophylline-treated C6 cells. GFAP and nuclear (DAPI) staining are shown in green and blue, respectively. Bar= 50 μ m. Note that at 72 h, C6 cells are not longer round and flat, but show large amount of GFAP-positive processes that are characteristics of astrocytes.

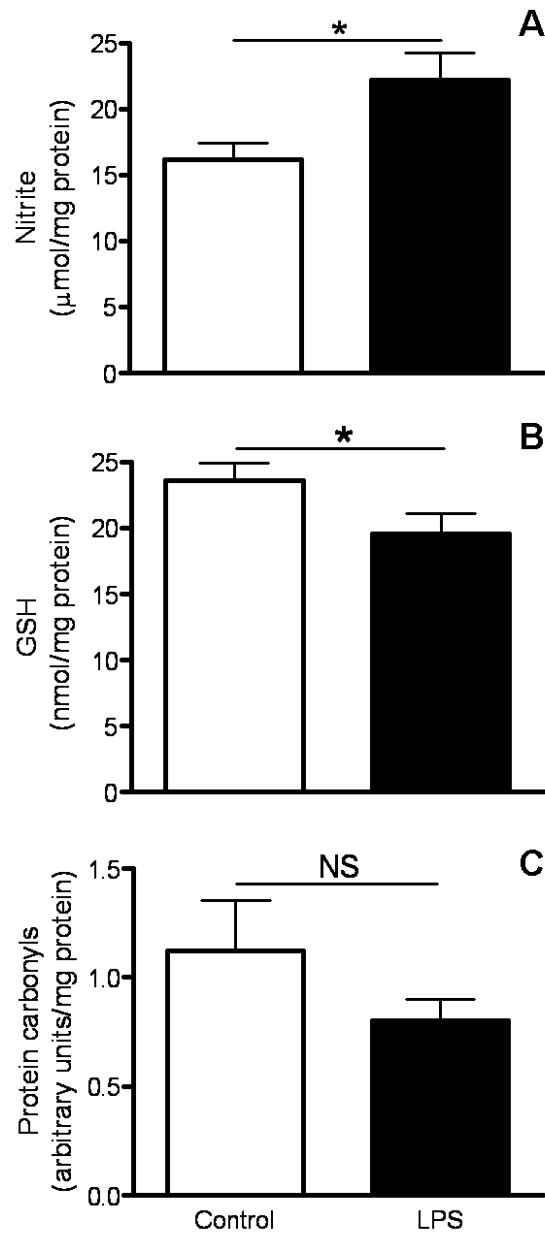


Figure 3.2 Levels of nitrosative/oxidative stress markers in control and LPS-stimulated astrocytes. Astrocytes were stimulated with 1 μg/ml of LPS. After 24h, the levels of nitrite in the medium (panel A), and those of GSH (panel B) and protein carbonyls (panel C) in the cells were determined as described under “Materials and Methods”. Values represent the mean ± SEM of 3 experiments. *p<0.05. NS, not significant.

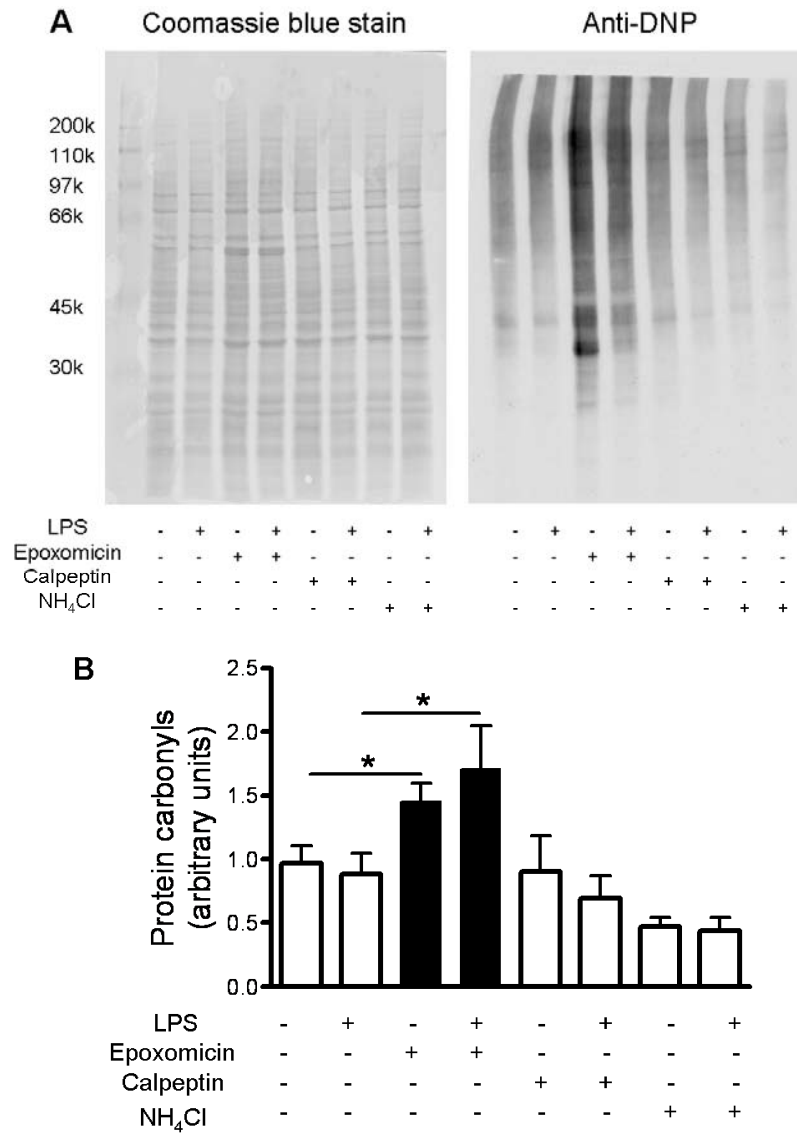


Figure 3.3 Only the proteasome inhibitor epoxomicin causes a build-up of carbonylated proteins in cultured astrocytes. Astrocytes were incubated in the presence or absence of LPS with/without a proteasome inhibitor (epoxomicin), a lysosomal inhibitor (NH₄Cl) and a calpain inhibitor (calpeptin) as described in “Materials and Methods”. After 24 h, protein carbonyl levels were determined by oxyblot analysis (Panel A). The intensity of each lane of the oxyblot was determined by scanning densitometry and divided by that of the coomassie blue stained membrane to correct for differences in gel loading (panel B). Values represent the mean ± SEM of 3 experiments. *p<0.05.

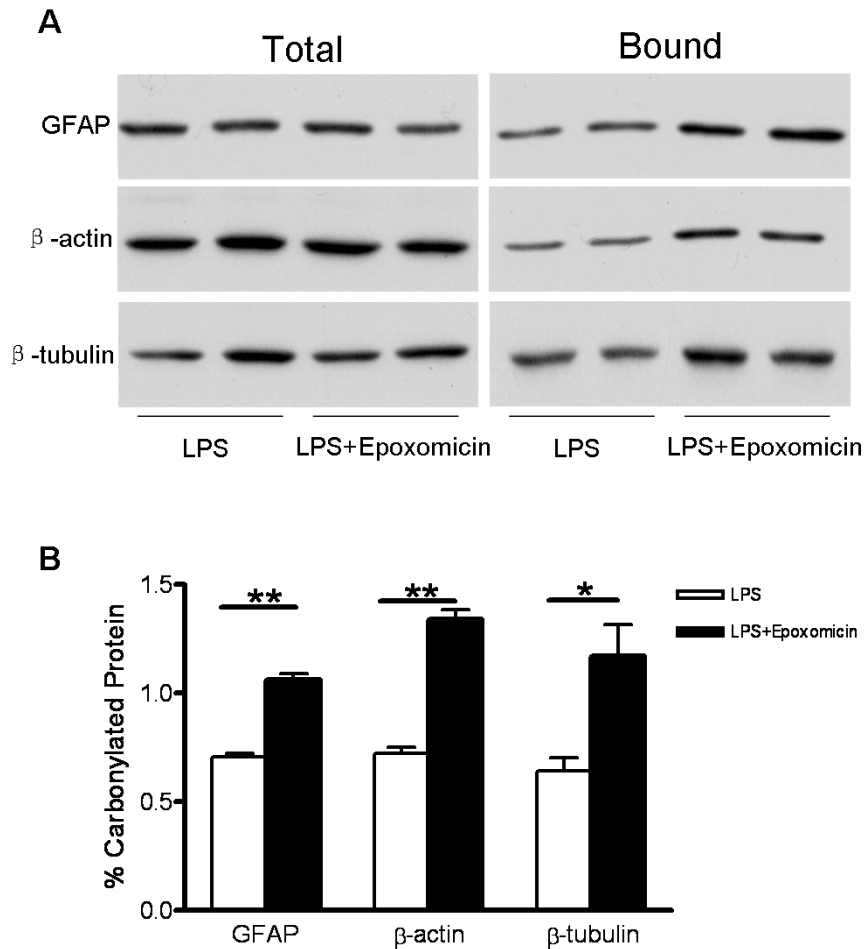


Figure 3.4 The proportion of carbonylated GFAP, β -actin and β -tubulin in LPS-stimulated astrocytes increases upon incubation with the proteasome inhibitor epoxomicin. LPS-treated astrocytes were incubated in the absence or presence of epoxomicin. After 24 hours, carbonylated proteins were converted into biotinylated proteins and were isolated using streptavidin-agarose as described in “Materials and Methods”. Aliquots of the starting material (total) and the streptavidin-purified fraction (bound) were separated on SDS-gels and transferred to PVDF membranes. Blots were probed with antibodies against β -actin, β -tubulin and GFAP, and were developed by ECL (panel A). Densitometric scans were obtained to calculate the proportion of the various carbonylated species in epoxomicin-treated and untreated activated astrocytes (Panel B). Values represent the mean \pm SEM of 3 experiments. * $p < 0.05$, ** $p < 0.01$.

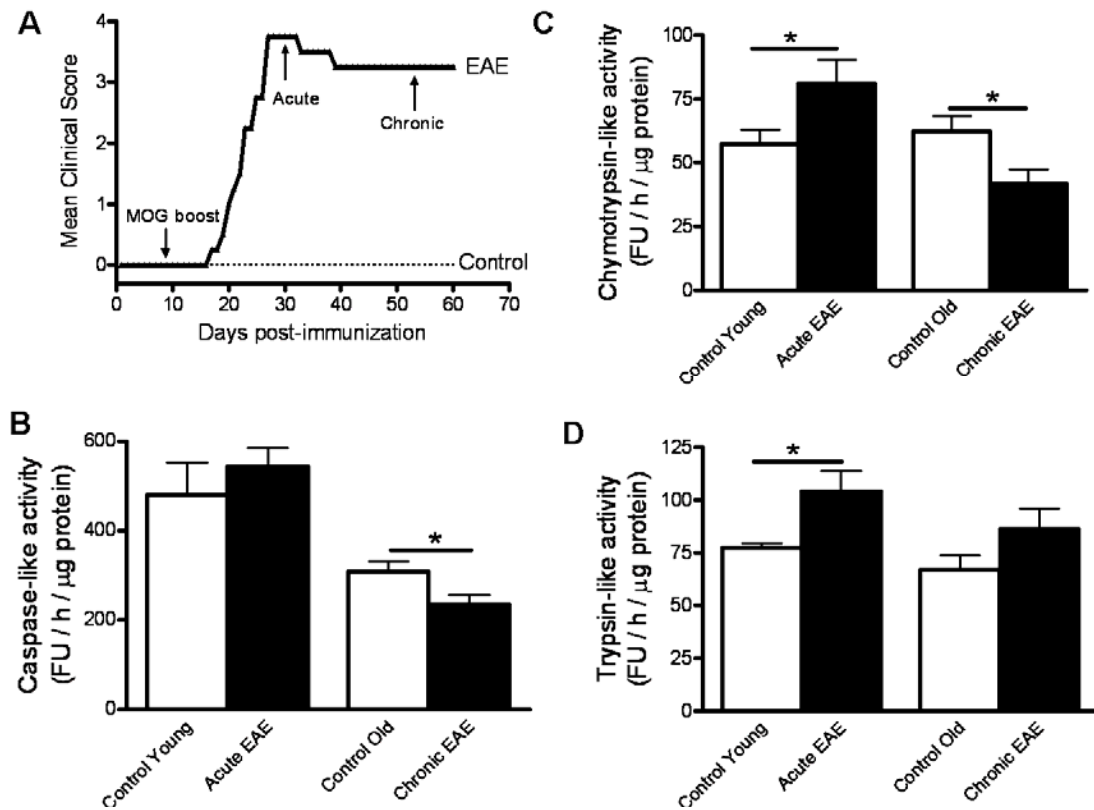


Figure 3.5 The chymotrypsin-like and caspase-like activities of the 20S proteasome are significantly reduced in chronic EAE. The disease was induced in C57BL/6 female mice by active immunization with MOG35-55 peptide as described in “Materials and Methods”. Animals were monitored daily for signs of clinical disease and scored as indicated in the text (panel A). Aliquots of cerebellum homogenates from control and EAE mice were used to determine the chymotrypsin-like (panel B), caspase-like (panel C) and trypsin-like (panel D) activity of the 20S proteasome as described in “Materials and Methods”. Values represent the mean \pm SEM of 4-10 experiments. * $p < 0.05$; FU, fluorescence units.

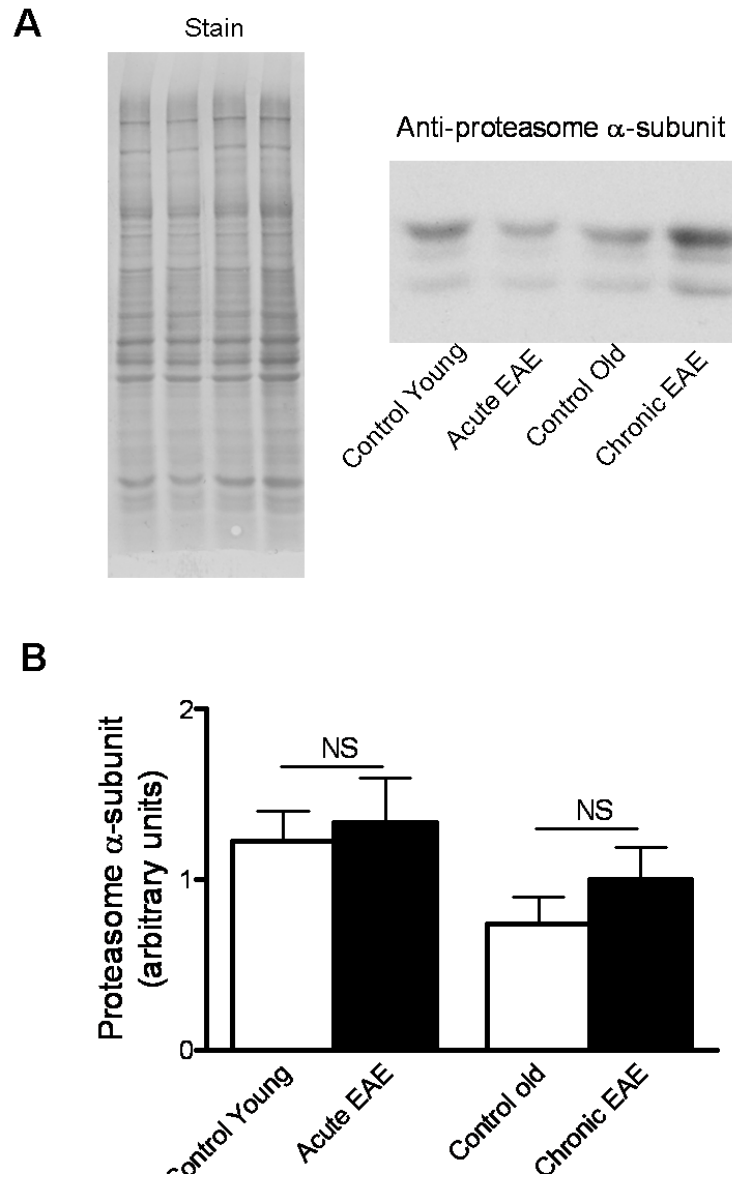


Figure 3.6 The amount of 20S proteasome is not altered in chronic EAE. Proteins from control and EAE cerebella were separated on SDS-gels and transferred to PVDF membranes. Blots were probed with antibodies against the constitutive α -subunit, and were developed by ECL (panel A). The relative levels of the proteasome were calculated by dividing the α -subunit band intensity on the western blot by that of the commassie blue stained lane. Values are the mean \pm SEM of 5-8 experiments. NS, not significant.

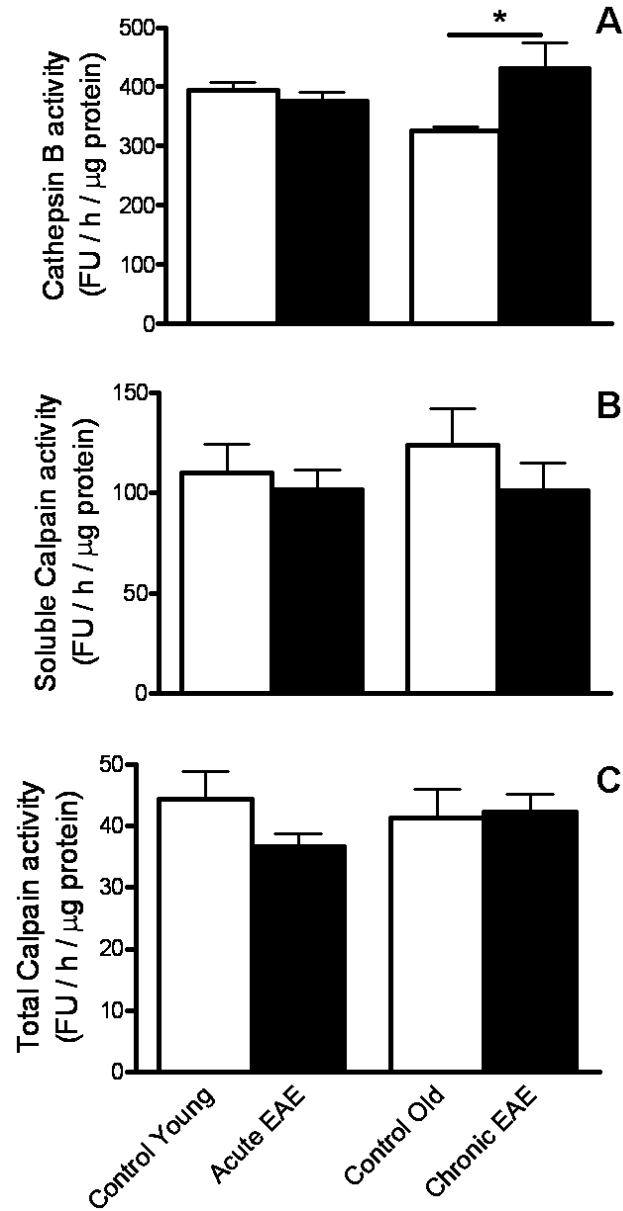


Figure 3.7 Neither cathepsin B nor calpain activity is decreased in chronic EAE. Aliquots of cerebellum homogenates from control and EAE mice were used to determine cathepsin B and total/soluble calpain activity as described in “Material and Methods”. Values are the mean \pm SEM of 4-6 experiments. * $p < 0.05$; FU, fluorescence units.

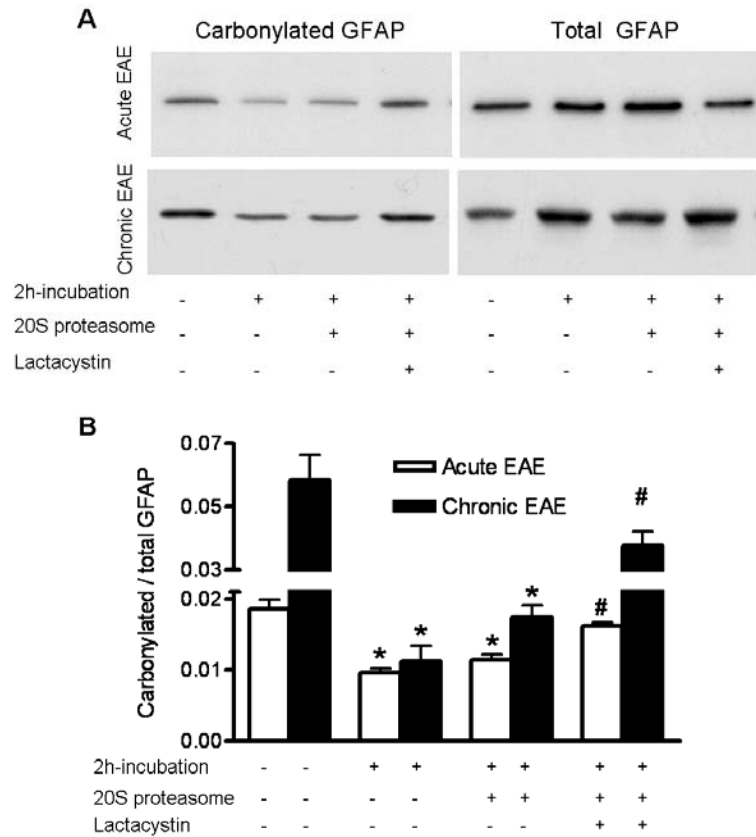


Figure 3.8 Carbonylated GFAP from acute and chronic EAE animals are sensitive to proteasomal degradation in a cell-free system. Cerebellum homogenates from acute and chronic EAE mice (200 μg protein) were incubated with 0.5 μg of 20S proteasome (Sigma) in the absence or presence of 2 μg clasto-lactacystin- β -lactone (Enzo Life Sciences). After 2 h, carbonylated proteins were isolated using the pull-down procedure described in “Materials and Methods”. A representative western blot of the total and bound fractions developed with an antibody against GFAP is shown in panel A. Densitometric scans were obtained to calculate the proportion of carbonylated GFAP in the various conditions (Panel B). The 20S chymotrypsin-like activity in the homogenates increased ~ 12 -fold upon addition of 20S proteasome and was reduced by $\sim 90\%$ in the presence of clasto-lactacystin- β -lactone. Values represent the mean \pm SEM of 4 experiments. *Significantly different ($p < 0.05$) from non-incubated condition; #Significantly different ($p < 0.005$) from the 20S proteasome-treated condition.

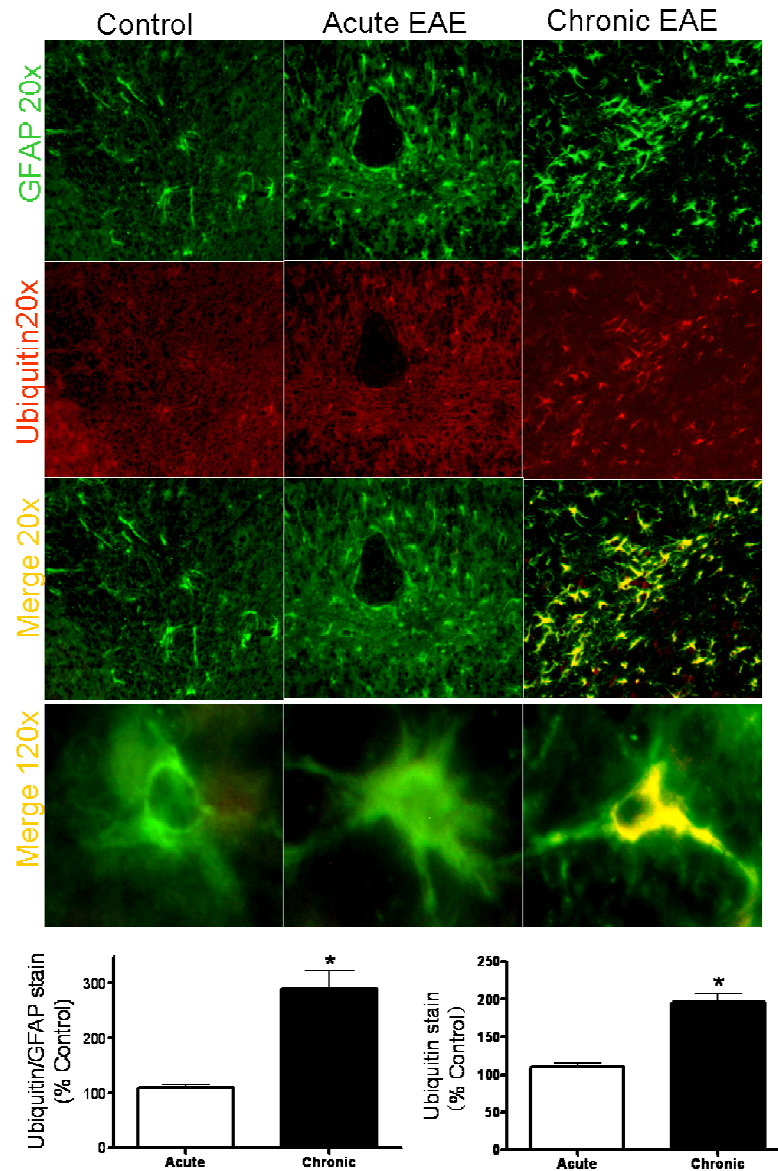


Figure 3.9 Ubiquitinated proteins build-up inside cerebellar astrocytes of mice with chronic EAE. Double immunofluorescence analysis was performed as described in “Methods and Materials”. Green channel is for GFAP while red channel is for mono/poly-ubiquitinated proteins. Immunofluorescence images show extensive poly-ubiquitin staining only in chronic EAE. The majority (~73%) of the cells containing ubiquitinated proteins are also GFAP+. Bar graphs depict the quantification of poly-ubiquitin immunoreactivity and poly-ubiquitin divided by GFAP. * $p < 0.01$

3.6 Reference

- Aksenov M.Y., Aksenova M.V., Butterfield D.A, Geddes J.W. and Markesbery W.R. (2001) Protein oxidation in the brain in Alzheimer's disease. *Neuroscience* 103, 373–383.
- Bizzozero O.A. (2009) Protein carbonylation in neurodegenerative and demyelinating CNS diseases. In "Handbook of Neurochemistry and Molecular Neurobiology" (Lajtha A, Banik N, Ray S, eds) Springer, pp. 543-562.
- Bizzozero O.A., DeJesus G., Callahan K. and Pastuszyn A. (2005) Elevated protein carbonylation in the brain white matter and gray matter of patients with multiple sclerosis. *J. Neurosci. Res.* 81, 687–695.
- Bizzozero O.A., Ziegler J.L., De Jesus G. and Bolognani F. (2006). Acute depletion of reduced glutathione causes extensive carbonylation of rat brain proteins. *J. Neurosci. Res.* 83, 656-667.
- Brown J.A., Novak E.K. and Swank R.T. (1985) Effects of ammonia on processing and secretion of precursor and mature lysosomal enzyme from macrophages of normal and pale ear mice: evidence for two distinct pathways. *J. Cell Biol.* 100, 1894-1904.
- Bulteau A.L., Lundberg K.C., Humphries K.M., Sadek H.A., Szweda P.A., Friguet B. and Szweda L.I. (2001a) Oxidative modification and inactivation of the proteasome during coronary occlusion/reperfusion. *J. Biol. Chem.* 276, 30057-30063.
- Bulteau A.L., Verbeke P., Petropoulos I., Chaffotte A.F. and Friguet B. (2001b) Proteasome inhibition in glyoxal-treated fibroblasts and resistance of glycated glucose-6-phosphate dehydrogenase to 20S proteasome degradation in vitro. *J. Biol. Chem.* 276, 45662-45668.
- Coux O., Tanaka K. and Goldberg A.L. (1996) Structure and functions of the 20S and 26S proteasomes. *Annu. Rev. Biochem.* 65, 801-847.
- Dalle-Donne I., Giustarini D., Colombo R., Rossi R. and Milzani A. (2003) Protein carbonylation in human diseases. *Trends Mol. Med.* 9, 169-176.
- Davies S.S., Amarnath V., Montine K.S., Bernoud-Hubac N., Boutaud O., Montine T.J. and Roberts L.J. (2002) Effects of reactive γ -ketoaldehydes formed by the isoprostane pathway (isoketals) and cyclooxygenase pathway (levuglandins) on proteasome function. *FASEB J.* **16**, 715–717.
- Divald A. and Powell S.R. (2006) Proteasome mediates removal of proteins oxidized during myocardial ischemia. *Free Radic. Biol. Med.* 40, 156–164.
- Dunlop R.A., Brunk U.T. and Rodgers K.J. (2009) Oxidized proteins: mechanisms of removal and consequences of accumulation. *IUBMB Life* 61, 522-527.
- Farout L., Mary J., Vinh J., Szweda L.I. and Friguet B. (2006) Inactivation of the proteasome by 4-hydroxy-2-nonenal is site specific and dependent on 20S proteasome subtypes. *Arch. Biochem. Biophys.* 453, 135-142.
- Ferrante R.J., Browne S.E., Shinobu L.A., Bowling A.C., Baik M.J., MacGarvey U., Kowall N.W., Brown R.H. and Beal M.F. (1997) Evidence of increased oxidative damage in both sporadic and familial amyotrophic lateral sclerosis. *J. Neurochem.* 69, 2064–2074.

- Ferrington D.A., Husom A.D. and Thompson L.V. (2005) Altered proteasome structure, function and oxidation in aged muscle. *FASEB J.* 19, 644-646.
- Floor E. and Wetzel M.G. (1998) Increased protein oxidation in human substantia nigra pars compacta in comparison with basal ganglia and prefrontal cortex measured with an improved dinitrophenylhydrazine assay. *J. Neurochem.* 70, 268-275.
- Friguet B., Stadman E.R. and Szweida L.I. (1994) Modification of glucose-6-phosphate dehydrogenase by 4-hydroxy-2-nonenal: Formation of cross-linked protein that inhibits the multicatalytic protease. *J. Biol. Chem.* 269, 21639–21643.
- Gaczynska M., Rock K.L. and Goldberg A.L. (1993) Gamma-interferon and expression of MHC genes regulate peptide hydrolysis by proteasomes. *Nature* 365, 264–267.
- Giordana M.T., Richiardi P., Trevisan E., Boghi A. and Palmucci L. (2002) Abnormal ubiquitination of axons in normally myelinated white matter in multiple sclerosis brain. *Neuropathol. Appl. Neurobiol.* 28, 35-41.
- Goldbaum O., Vollmer G. and Richter-Landsberg C. (2006) Proteasome inhibition by MG-132 induces apoptotic cell death and mitochondrial dysfunction in cultured rat brain oligodendrocytes but not in astrocytes. *Glia* 53, 891-901.
- Grune T., Reinheckel T., Joshi M. and Davies K.J. (1995) Proteolysis in cultured liver epithelial cells during oxidative stress. Role of the multicatalytic proteinase complex, proteasome. *J. Biol. Chem.* 270, 2344-2351.
- Grune T., Shringarpure R., Sitte N. and Davies K.J. (2001) Age-related changes in protein oxidation and proteolysis in mammalian cells. *J. Gerontol. A Biol. Sci. Med. Sci.* 56, 459-467.
- Haghighat N., McCandless D.W. and Geraminegad P. (2000) Responses in primary astrocytes and C6-glioma cells to ammonium chloride and dibutyryl cyclic-AMP. *Neurochem. Res.* 25, 277–284.
- Hassen G.W., Feliberti J., Kesner L., Stracher A. and Mokhtarian F. (2006) A novel calpain inhibitor for the treatment of acute experimental autoimmune encephalomyelitis. *J. Neuroimmunol.* 180, 135-146.
- Hilgart A.A. and Bizzozero O.A. (2008) Carbonylation of major cytoskeletal proteins in multiple sclerosis. *J. Neurochem.* 104 (Suppl.1), PTW06-03.
- Kalmár B., Kittel Á., Lemmens R., Környei Z. and Madarász E. (2001) Cultured astrocytes react to LPS with increased cyclooxygenase activity and phagocytosis. *Neurochem. Int.* 38, 453-461.
- Kessova I.G. and Cederbaum A.I. (2005) The effect of CYP2E1-dependent oxidant stress on activity of proteasomes in HepG2 cells. *J. Pharmacol. Exp. Ther.* 315, 304-312.
- Keller J.N., Hanni K.B., Gabbita S.P., Friebe V., Mattson M.P. and Kindy M.S. (1999) Oxidized lipoproteins increase reactive oxygen species formation in microglia and astrocyte cell lines. *Brain Res.* 830, 10-15.
- Keller J.N., Hanni K.B. and Marksberry W.R. (2000) Impaired proteasome function in Alzheimer's disease. *J. Neurochem.* 75, 436-439.
- Korhonen L. and Lindholm D. (2004) The ubiquitin proteasome system in synaptic and axonal degeneration. *J. Cell Biol.* 165, 27–30.

- McNaught K.S., Belizaire R., Isacson O., Jenner P. and Olanow C.W. (2003) Altered proteasomal function in sporadic Parkinson's disease. *Exp. Neurol.* 179, 38-46.
- Mayo I., Arribas J., Villoslada P., Alvarez DoForno R., Rodríguez-Vilariño S., Montalban X., De Sagarra M.R. and Castaño J.G. (2002) The proteasome is a major autoantigen in multiple sclerosis. *Brain* 125, 2658-2667.
- Meng L., Mohan R., Kwok B.H., Elofsson M., Sin N. and Crews C.M. (1999) Epoxomicin, a potent and selective proteasome inhibitor, exhibits in vivo anti-inflammatory activity. *Proc. Natl. Acad. Sci. USA* 96, 10403-10408.
- Misko T.P., Schilling R.J., Salvemini D., Moore W.M. and Currie M.G. (1993) A fluorometric assay for the measurement of nitrite in biological samples. *Anal. Biochem.* 214, 11-16.
- Nystrom T. (2005) Role of oxidative carbonylation in protein quality control and senescence. *EMBO J.* 24, 1311-1317.
- Pacifici R.E., Kono Y. and Davies K.J. (1993) Hydrophobicity as the signal for selective degradation of hydroxyl radical-modified hemoglobin by the multicatalytic proteinase complex, proteasome. *J. Biol. Chem.* 268, 15405-15411.
- Pandey U.B., Nie Z., Batlevi Y., McCray B., Ritson G.P., Nedelsky N.B., Schwartz S.L., DiProspero N., Knight M.A., Schuldiner O., Padmanabhan R., Hild M., Berry D.L., Garza D., Hubbert C.C., Yao T., Baehrecke E.H. and Taylor J.P. (2007) HDAC6 rescues neurodegeneration and provides an essential link between autophagy and the UPS. *Nature* 447, 860-864.
- Rivett A.J. (1985) Preferential degradation of the oxidatively modified form of glutamine synthetase by intracellular mammalian proteases. *J. Biol. Chem.* 260, 300-305.
- Rockwell P., Yuan H., Magnusson R. and Figueiredo-Pereira M.E. (2000) Proteasome inhibition in neuronal cells induces a proinflammatory response manifested by upregulation of cyclooxygenase-2, its accumulation as ubiquitin conjugates, and production of the prostaglandin PGE(2). *Arch. Biochem. Biophys.* 374, 325-333.
- Rodgers K.J. and Dean RT. (2003) Assessment of proteasome activity in cell lysates and tissue homogenates using peptide substrates *Int. J. Biochem. Cell Biol.* 35, 716-727.
- Seo H., Sonntag K.C. and Isacson O. (2004) Generalized brain and skin proteasome inhibition in Huntington's disease. *Ann. Neurol.* 56, 319-328.
- Shringarpure R., Grune T., Mehlhase J. and Davies K.J. (2003) Ubiquitin conjugation is not required for the degradation of oxidized proteins by proteasome. *J. Biol. Chem.* 278, 311-318.
- Sitte N., Huber M., Grune T., Ladhoff A., Doecke W., Von Zglinicki T. and Davies J.A. (2000) Proteasome inhibition by lipofuscin/ceroid during postmitotic aging of fibroblasts. *FASEB J.* 14, 1490-1498.
- Smerjac S.M. and Bizzozero O.A. (2008) Cytoskeletal protein carbonylation and degradation in experimental autoimmune encephalomyelitis. *J. Neurochem.* 105, 763-772.
- Troncoso J.C., Costello A.C., Kim J.H. and Johnson G.V. (1995) Metal-catalyzed oxidation of bovine neurofilaments in vitro. *Free Radic. Biol. Med.* 18, 891-899.

- Tsuji S., Kikuchi S., Shinpo K., Tashiro J., Kishimoto R., Yabe I., Yamagishi S., Takeuchi M. and Sasaki H. (2005) Proteasome inhibition induces selective motor neuron death in organotypic slice cultures. *J. Neurosci. Res.* 82, 443-451.
- Tsujinaka T., Kajiwara Y., Kambayashi J., Sakon M., Higuchi N., Tanaka T. and Mori T. (1988) Synthesis of a new cell penetrating calpain inhibitor (calpeptin). *Biochem. Biophys. Res. Commun.* 153, 1201-1208.
- Zheng J. and Bizzozero O.A. (2010a) Accumulation of protein carbonyls within cerebellar astrocytes in murine experimental autoimmune encephalomyelitis. *J. Neurosci. Res.* (In press).
- Zheng J. and Bizzozero O.A. (2010b) Reduced proteasomal activity contributes to accumulation of carbonylated proteins within cerebellar astrocytes in chronic EAE. *Trans. Am. Soc. Neurochem.* PTW07-07.

**4 Reduced Proteasomal Activity in the Cerebral White Matter
and Gray Matter of Patients with Multiple Sclerosis**

Jianzheng Zheng and Oscar A. Bizzozero

Department of Cell Biology and Physiology

University of New Mexico - Health Sciences Center

Albuquerque, NM 87131

(Submitted to J Neuropath Exp Neurol)

4.1 **Abstract**

We have previously shown that carbonylated (oxidized) proteins accumulate in the cerebral white matter (WM) and gray matter (GM) of patients with multiple sclerosis (MS). While oxidative stress is necessary for carbonyl generation, it is the failure of degradation systems that ultimately leads to the build-up of carbonylated proteins within tissues. In this study, we determined the activity of the 20S proteasome and other proteolytic systems in the cerebral WM and GM of 13 MS patients and 13 controls. We report that the activities of the three peptidases of the 20S proteasome (i.e. chymotrypsin-like, caspase-like and trypsin-like) in both MS-WM and MS-GM are greatly reduced without a decrease in the amount of proteasome. Furthermore, not only carbonylated proteins but also proteins containing Lys-48 poly-ubiquitin accumulate in MS tissues, indicating failure of the 26S proteasome as well. Interestingly, the amount of 20S proteasome subunits ($\beta 1$, $\beta 2$, and $\beta 5$) where the catalytic activities reside are not diminished in MS. Levels of the regulatory caps PA28 α and PA700 are also lower in MS than in controls, indicating that the activity of the more complex proteasomes may be reduced further. Finally, the activities of other proteases that might also remove oxidized proteins (calpain, cathepsin B, mitochondrial LONp) are not lessened in MS. Together, these studies suggest that direct inactivation of proteolytic centers in the 20S particle and/or the presence of specific inhibitors lead to proteasomal dysfunction in MS.

4.2 Introduction

Multiple sclerosis (MS) is a chronic inflammatory disease of the human CNS, which is characterized by perivascular inflammation, demyelination, oligodendrocyte death and axonal degeneration (1). Pathologically, the CNS in MS patients contains well-demarcated regions of myelin loss and increased astrogliosis called plaques that are surrounded by normal-appearing white matter (NAWM) (2). While most of the pathology in chronic MS is observed in the plaque, cellular and chemical abnormalities are also found in the NAWM and the normal-appearing gray matter (NAGM) as demonstrated in recent imaging (3, 4) and biochemical studies (5, 6).

Like many other chronic neurological disorders, MS is accompanied by a substantial amount of oxidative damage, which seems to play a role in disease pathogenesis (7). We have previously shown that protein carbonyls, the major oxidative modification in chronic disorders, accumulate in the NAWM and NAGM of MS patients (6) with GFAP, β -tubulin, β -actin and the neurofilaments as the major oxidized species (8). More recent studies from our laboratory have discovered that protein carbonyls are also elevated in experimental autoimmune encephalomyelitis (EAE), a widely used animal model of MS (9, 10). Carbonylation can lead to loss of protein function, the formation of insoluble aggregates and/or metabolic instability, all processes that likely result in cell damage (11). Because of their toxic nature, the concentration of carbonylated proteins within cells is normally kept very low, which is achieved through the action of efficient proteolytic systems that preferentially digest oxidized proteins

(11). This has led to the idea that while oxidative stress is clearly necessary for the induction of protein carbonyls, it is the failure of the proteolytic activities that ultimately leads to the build up of oxidized proteins within tissues.

Mammalian cells contain several major proteolytic systems including the lysosomal cathepsins, the calcium-activated calpains and the 20S/26S proteasomes, all of which could potentially remove oxidized proteins (12). However, various cell-culture studies that utilized protease inhibitors have identified the 20S proteasome as the system responsible for removal of most oxidized protein species (13,14). The 20S proteasome is a barrel-shaped structure that is made of two outer heptameric rings of α subunits and two inner heptameric rings of β subunits (15). Three of the β subunits carry the proteolytic activity, classified as caspase-like or peptidyl glutamyl-peptide hydrolytic (β 1), trypsin-like (β 2), and chymotrypsin-like (β 5), which cleave after acidic, basic and hydrophobic amino acids, respectively (16). Of these, the β 5 subunit is believed to be responsible for the degradation of oxidized (carbonylated) proteins (17). The peptidase activity of the 20S proteasome can be increased by two different types of regulatory complexes that bind to the terminal rings of this particle. These are the 11S regulator (PA28) and the 19S (PA700) regulatory complex, which form the 11S-20S proteasome and the 26S proteasome, respectively (18). A number of proteasome inhibitors, including the hsp90, PI31 and PR39, have been also described although their precise physiological role is currently unknown (19).

The objective of the present study was to determine whether the various proteolytic activities of the 20S proteasome are altered in MS. The results clearly show that the enzymatic activities of the three peptidases of the 20S proteasome are greatly reduced in both the white and gray matter of MS patients without significant decrease in the total amount of proteasome. Furthermore, the levels of the 20S proteasome β subunits where the peptidolytic activities reside are not affected in the diseased specimens. We also found that the amount of the regulatory caps PA28 α and PA700 are lower in MS than in control samples, indicating that the activity of the larger proteasomes (i.e. 26S, 11S-20S and hybrid 19S-20S-11S) may be reduced to an even larger extent. Collectively, these studies suggest that the direct inactivation of proteolytic centers in the 20S particle and/or the presence of specific inhibitors are the most likely cause for impaired proteasome function in MS and the ensuing build-up of carbonylated proteins. This notion was strengthened by the finding that the other enzymatic system that might also aid in the removal of oxidized protein, including calpain, lysosomal proteinases and the mitochondrial LON protease, are not decreased in MS.

4.3 Materials and Methods

4.3.1 Tissue Specimens

Tissue specimens were obtained from the Rocky Mountain MS Center (Englewood, CO) and from the Human Brain and Spinal Fluid Resource Center (Los Angeles, CA) and were stored at -80°C until use. A total of 26 brain specimens including 13 control and 13 MS tissues were analyzed. In all cases

the diagnosis of MS was based on clinical history, neurological examination and pathological analysis. Frozen tissue from control and pathological samples was thawed and a small piece (~50 mg) of white matter (WM) was carefully dissected so that it did not include visible plaques. Normal-looking gray matter (GM) pieces were selected from cortical areas based also on gross examination. Tissues were immediately homogenized in PEN buffer (20 mM sodium phosphate, pH 7.5, 1 mM EDTA, and 0.1 mM neocuproine) containing 2 mM 4,5 dihydroxy-1, 3-benzene disulfonic acid and 1 mM dithiothreitol (DTT) as antioxidants. Protein homogenates were stored at -20°C until use. Protein concentration was assessed with the Bio-Rad protein assay (Bio-Rad Laboratories; Hercules, CA) using bovine serum albumin as standard.

4.3.2 Protease activity assays

The various proteolytic activities of the 20S proteasome were determined in cerebral homogenates from control and MS patients using fluorescence assays (20). Briefly, 50µg of protein were incubated for 2h at 25°C with 50µM of the 7-aminomethyl-4-coumarin (AMC)-labeled peptide Suc-Leu-Leu-Val-Tyr-AMC (for chymotrypsin-like activity), Boc-Leu-Arg-Arg-AMC (for trypsin-like activity) or z-Leu-Leu-Glu-AMC (for caspase-like activity) in the absence or presence of 10µM clasto-lactacystin-β-lactone (Enzo Life Sciences, Plymouth Meeting, PA) or 50µM epoxomicin (for the trypsin-like activity). The different activities of the 20S proteasome were calculated as the difference in fluorescence intensity at 460nm between the samples without and with inhibitor using an excitation wavelength of 380nm.

Total calpain activity was determined by a similar procedure using the substrate Suc-Leu-Leu-Val-Tyr-AMC in 100mM KCl, 10mM CaCl₂, 25mM Hepes buffer pH 7.5, and carrying out the incubation in the absence or presence of 0.4 µg/µl calpeptin (21). To measure soluble (active) calpain activity, membrane-bound calpain was removed prior to the assay by centrifugation at 10,000 g for 25 min.

Lysosomal proteolytic activity was also measured fluorometrically by incubating cerebellar homogenates with 50µM z-Phe-Arg-AMC (Enzo) in 100 mM sodium acetate (pH 5.5) for 2h at 37°C (22).

4.3.3 Western blot analysis

Proteins (5 µg) from tissue homogenates were separated by SDS–polyacrylamide gel electrophoresis on 10% or 12% gels and were blotted to polyvinylidene difluoride membranes. Blots were then incubated overnight at 4°C with antibodies against Lys-48 poly-ubiquitin chain (1:2,000; Millipore Corp., Billerica, MA), 20S proteasome α-subunits (α1-3/α5-7; 1:2,000; Santa Cruz Biotechnology, Santa Cruz, CA), β1, β2 and β5 subunits (1:1,000; Enzo), PA28α (1:1,000, Enzo), 19S proteasome Rpt4 (1:1,000, Enzo); µ-calpain (1:1,000; Cell Signaling Technology, Boston, MA), cathepsin B (1:1,000; EMD Biosciences, San Diego, CA) and LONp1 protease (1:2,000; Proteintech Group Inc, Chicago, IL). Membranes were rinsed three times in phosphate-buffered saline solution containing 0.05% Tween-20 and were incubated for 2 h with horseradish peroxidase conjugated-conjugated anti-mouse antibody (1:2,000; Sigma) or anti-

rabbit antibody (1:2,000; Sigma). Blots were developed by enhanced chemiluminescence (ECL) using the Western Lightning ECL™ kit from Perkin-Elmer (Boston, MA). Films were scanned in a Hewlett Packard Scanjet 4890 and the images were quantified using the NIH Image 1.63 imaging analysis program. Band intensities were normalized by the amount of coomassie blue stain in the respective lanes.

4.3.4 Statistical Analysis

Results were analyzed for statistical significance by t-test utilizing the GraphPad Prism® program (GraphPad Software Inc., San Diego, CA).

4.4 Results

4.4.1 Proteasomal peptidase activities are decreased in MS-WM and MS-GM

The age of the patients at the time of death, gender, post-mortem interval (PMI) and the pathological diagnosis are shown in Table I. Age of controls and MS patients ranges from 34 to 80 years and from 33 to 83 years, respectively. The control group has 7 men/6 women and the MS group 4 men/9 women. PMI intervals are variable, 4h-20h for controls and 2h-25h for MS patients. Within each group (i.e. MS and controls) there was no discernible correlation between the biochemical parameters measured and either age, sex or PMI. Thus, the average values in the MS and control specimens were directly compared without segregation in subcategories.

Aliquots of cerebral homogenates from MS-GM, MS-WM and their respective controls were used to determine the various proteolytic activities of the

20S proteasome (Figure 4.1). The chymotrypsin-like activity is greatly reduced in both NAWM and NAGM of MS patients representing 56% and 38% of control values, respectively (panel A). A similar pattern was found for the caspase-like activity in MS-NAWM and MS-NAGM, which decreased by 61 % and 60 % of their respective controls (panel B). Values for the trypsin-like activity are generally more disperse but a significant decreased in both the WM and GM of diseased patients is nonetheless observed (panel C).

Since a significant proportion of the 20S catalytic particle is part of the 26S ubiquitin-dependent proteasome, we reasoned that the proteolytic activity of the latter, and thus the ability to remove ubiquitinated proteins, might also be compromised in MS. This possibility was explored by western blot analysis using an antibody that binds only poly-ubiquitin chains linked through the Lys-48 residue in ubiquitin. Lys-48 linked poly-ubiquitin chains are most commonly associated with proteins targeted for proteasomal degradation (23). As shown in Figure 4.2, several proteins containing Lys-48 poly-ubiquitin chains accumulate in the WM and GM of MS patients relative to controls. These data indicate that impairment of the 26S proteasome is also taking place in MS.

4.4.2 Levels of 20S proteasome α , β 1, β 2 and β 5 subunits are not reduced in MS tissue.

To establish if the decreased proteasomal activity observed in MS patients is due to reduction in proteasome concentration or a change in the proportion of the catalytic subunits, we measured the relative levels of the constitutive 20S

proteasome α subunit and those of each of the three protease-containing subunits (i.e. β 1, β 2 and β 5) by western blot analysis. As depicted in Figure 4.3, the amount of 20S proteasome α subunit in MS-GM is the same as those in the control group while there is a small increase in the WM of MS patients relative to the control. Furthermore, the relative amounts β 1, β 2, and β 5 subunits in the MS-WM and MS-GM are either increased or unchanged when compared to their respective controls (Figure 4.4). These data indicate that diminished proteasome peptidase activity in MS is likely due to enzyme inactivation rather than to down-regulation of enzyme proteins or reduced proteasome levels.

4.4.3 PA28 α and PA700 levels are also diminished in MS.

The 20S proteasome may associate with the PA28 and PA700 regulators, which are known to increase the proteolytic activity of the core particle (18). There are three PA28 (11S) homologues, named α , β and γ . The α and β subunits form a heteroheptamer while the γ subunit forms a homoheptamer that is confined to the cell nucleus. The PA28 β subunit is virtually absent from the brain (19) but the α subunit is present and can assemble to form a PA28 α homoheptamer that has also the capacity to activate the 20S proteasome (24). For this reason we decided to assess the levels of PA28 α in MS and controls samples. The results show a decrease of ~50% in the amount of 11S α subunit in the MS-WM and MS-GM with respect to their controls (Figure 4.5A). The relative levels of PA700 (19S) in MS and control homogenates were determined also by western blot analysis employing an antibody that recognizes the

Rpt4/S10b subunit (ATPase subunit) in this activator. The results clearly show a reduction in PA700 (19S) levels only in the MS-WM (Figure 4.5B). It is important to note that the reduced peptidolytic activities of the 20S proteasome in MS are not a consequence of decreased levels of the activators PA28 α and PA700, since under the incubation conditions used in this study (i.e. without ATP or magnesium ions and in the presence of 0.03% SDS) these caps are not attached to the catalytic particle (25). In vivo, however, these regulators may be largely bound to the 20S proteasome, suggesting that the activity of larger proteasomes (i.e. 26S, 11S-20S and hybrid 19S-20S-11S) in MS may be reduced more than that of the free 20S particle.

4.4.4 Calpain activity and expression are significantly upregulated in MS brains

The activities/levels of the three other proteolytic systems that might potentially remove oxidized proteins (calpain, lysosomal cathepsins, mitochondrial LON protease) were also determined in control and MS tissues. Calpain is normally present as a membrane-bound pro-enzyme containing an 80kDa catalytic subunit that undergoes auto-proteolytic cleavage upon calcium activation, thus releasing the 75-kDa active calpain into the cytosol (26). As shown in Fig. 6A-B, the total and the soluble (active) calpain activity are elevated in both the WM and GM of MS patients relative to their controls. Levels of total calpain-1 (μ -calpain) were determined in the brain homogenates from MS and control patients by western blotting. As depicted in Fig. 6C-D, total calpain levels in the MS-WM and MS-GM were increased by 54% and 67%, respectively.

These data indicate that the enhancement in calpain activity in MS tissues is mostly due to an increase in the amount of enzyme.

4.4.5 Lysosomal proteolytic activity is slightly increased in MS gray matter

The proteolytic activity of the lysosome was also tested in MS patients. The activity of cathepsin B, one of the major lysosomal proteases, was assayed with the z-Phe-Arg-AMC peptide at acid pH. Measured under these conditions, the lysosomal proteolytic activity in MS-WM and MS-GM increases by 40% and 38% (Figure 4.7A). Levels of the 31kDa form of cathepsin B, as determined by western blot analysis, are mostly unchanged in MS-WM and MS-GM relative to their controls (Figure 4.7 B-C).

4.4.6 Levels of Lon protease are unaltered in MS

Lon is a proteasome-like protease localized in mitochondrial matrix and responsible for the removal of oxidized proteins within this organelle (27). Therefore, it is unlikely that a deficiency in the activity of the Lon protease in MS would result in the accumulation of carbonylated cytoskeletal proteins that we have observed (8). Nonetheless, since Lon protease levels are known to decrease during aging and in several CNS disorders (28), we sought to investigate its potential role in MS. As shown in Fig. 8, western blot analysis clearly shows that the amount of this protease in both MS-WM and MS-GM are the same as that in control specimens.

4.5 Discussion

In this study we report that the peptidase activities present in the $\beta 1$, $\beta 2$ and $\beta 5$ subunits of the 20S proteasome are greatly reduced in both the WM and GM of MS patients as compared to controls. Based on the quantification of the constitutive 20S proteasome α subunit by western blotting, we conclude that changes in proteasomal activity are not due to a decline in the number of 20S proteasome particles. More importantly, altered activities are not the result of decreased levels of these subunits (Figure 4.4). Indeed, the amount of the $\beta 1$ and $\beta 2$ subunit is increased in both MS-WM and MS-GM, perhaps as a result of compensatory mechanisms. Altogether these findings suggest that the activity of these proteases in MS are inhibited, a phenomenon that we have recently also observed in the chronic phase of MOG35-55 peptide-induced EAE (29). Levels of the activators PA28 α and PA700 are also lessened in the CNS of MS patients, indicating that the catalytic efficiency of the larger proteasome particles are also affected in this disorder.

Several posttranslational modifications of the 20S subunits that are capable of reducing proteasomal activities have been discovered in oxidative stress paradigms. For example, proteasome activity can be impaired by direct carbonylation (30) or by modification with 4-hydroxy-2-nonenal (31), acrolein (32), glyoxal (33), γ -ketoaldehydes (isoketals) (34) and nitric oxide (35). Direct inactivation of the proteasome by 4-HNE cross-linked proteins (36) and lipofuscin/ceroid fluorescent pigments (22) have been also implicated in the inhibition of the 20S proteasome. An additional and still unexplored possibility

might be proteasome inactivation by specific autoantibodies. Interestingly, antibodies against several proteasome subunits have been detected in serum and CSF from MS patients (37). It will be important to know if proteasome autoantibodies are also present in the diseased brain and are indeed capable of causing enzyme inhibition. Finally, the presence of endogenous negative regulators such as hsp90, PI31 and PR39 (19) cannot be ruled out as the underlying cause for proteasomal impairment in MS. Studies are underway in this laboratory to identify potential inhibitors and the role of other regulators (e.g. PA200) using both cell extracts and purified proteasome particles from MS brain samples.

While impaired proteasomal activity has been reported in several neurodegenerative diseases, such as Alzheimer's disease (38), Parkinson's disease (39) and Huntington's disease (40), this is the first study to demonstrate proteasome dysfunction in a chronic human demyelinating disorder. Whether an identical mechanism causes proteasome dysfunction in MS and the other neurodegenerative disorders is presently unclear. Yet, it is noteworthy that in all of these diseases the failure of the peptidase activities is not related to low levels of proteasome particles or their catalytic subunits. The pathophysiological consequences of decreased proteasomal activity in chronic MS as well as in classical neurodegenerative disorders are unknown. The structural and functional impact resulting from the accumulation of a number of ubiquitinated, misfolded, aggregated and oxidized proteins, along with reduced degradation of various signaling and pro-apoptotic molecules, are likely widespread and difficult to

predict. However, decreased proteasomal activity is likely to be pathogenic and a contributor to neurodegeneration in MS. This notion is based mostly on experiments linking pharmacological inhibition of the proteasome catalytic core to axonal damage (41), the development of pro-inflammatory responses via up-regulation of cyclooxygenase-2 and prostaglandin E2 (42) and apoptosis of neurons and oligodendrocytes via mitochondrial dysfunction (43), all of which are characteristics of chronic MS.

There is general agreement that oxidized proteins are degraded by the 20S proteasome via an ATP-independent mechanism (13,14, 44-46). However, there have been some reports suggesting that other proteases may be also involved in the degradation of carbonylated polypeptides. For example, the calcium-dependent cysteine protease calpain has been found to preferentially degrade oxidized neurofilaments over the non-oxidized protein forms in cell-free systems (47) and there is some evidence that heavily oxidized proteins can be taken up by lysosomes, where in some cases are incompletely degraded and accumulate in the form of lipofuscin-like, autofluorescent aggregates (48). Furthermore, in epithelial cells some of the 4-hydroxynonenal-modified proteins are degraded in the lysosome via an ubiquitin-dependent mechanism (49). Due to these observations, we felt compelled to determine the enzymatic activities of these proteolytic systems in MS. In our study, we found that both the total and soluble calpain activities are increased in MS patients. Elevation of total calpain activity seems to be due to an increase in its translational expression. Interestingly, calpain activity and expression is not only increased MS-WM, as reported earlier

(26), but also in the MS-GM, suggesting that extensive calcium dysregulation also occurs in this CNS area. We also found that the activity of cathepsin B, the major lysosomal protease, is elevated in MS. As suggested by Pandley et al. (50), an increase in the lysosomal degradation machinery when the proteasome system is not functioning may represent a compensatory mechanism for intracellular protein degradation. Finally, the relative amount of the Lon protease, an enzyme that specifically degrades oxidized mitochondrial proteins by an ATP-stimulated mechanism (27, 28), was unaltered in MS. In sum, of the several proteolytic systems studied in post-mortem MS brains only the proteasome was found to be impaired. Proteasome failure explains the accumulation of both carbonylated proteins (6) and ubiquitin-conjugates (51; this study) in chronic MS tissue.

Table 4.1 Brain samples from control and MS patients

Sample	Age (years)	Gender	PMI (hours)	Pathological diagnosis
Control				
1	34	M	uk	Acute pancreatitis; Pneumonia
2	55	M	4	Metastatic lung cancer
3	58	M	9	Colon cancer
4	59	F	19	Lymphoma
5	68	M	10	Lung Cancer
6	71	M	14	Lymphoma
7	72	F	20	Congestive heart failure
8	73	F	12	COPD
9	74	F	12	Pancreatic cancer
10	74	F	5	Pneumonia
11	74	M	14	Metastatic lung cancer
12	75	F	15	Liver cancer
13	80	M	11	Renal cancer
Multiple Sclerosis				
1	33	F	3	Chronic/active MS; Hydrocephalus
2	36	F	4	Relapsing/remitting MS
3	37	M	5	Diffuse periventricular demyelination
4	39	F	2	Chronic/active MS
5	40	F	3	Active severe MS
6	47	F	16	Chronic/active MS
7	54	M	24	Chronic/active MS
8	57	F	25	Chronic progressive MS
9	58	F	3	Chronic MS/optic neuritis
10	61	M	3	Chronic/active MS
11	65	M	6	Chronic progressive MS
12	70	F	16	Chronic/active MS
13	83	F	3	Chronic MS

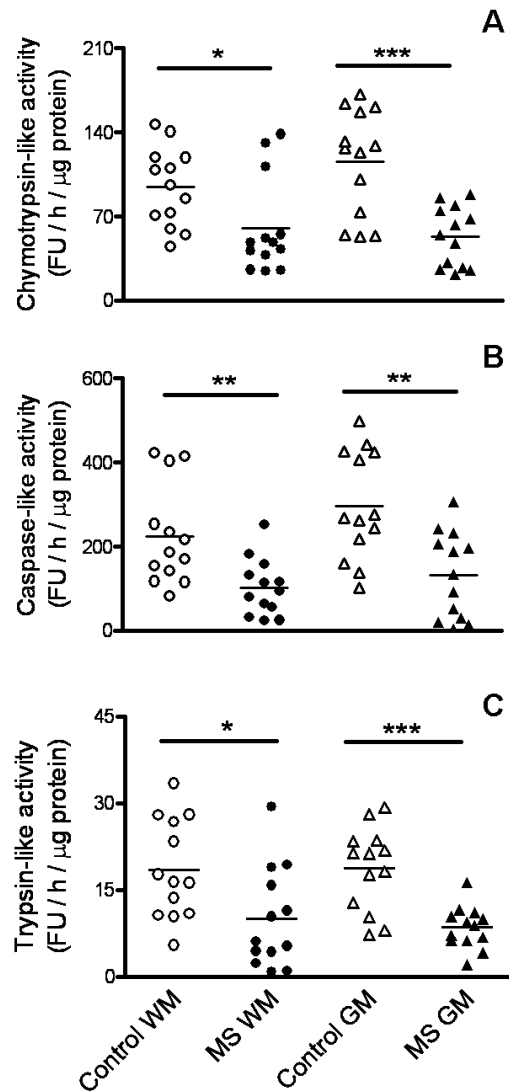


Figure 4.1 - Proteasome peptidase activities are greatly reduced in MS. Aliquots of the cerebral homogenates from control and MS patients were used to determine the chymotrypsin-like (A), caspase-like (B) and trypsin-like activity (C) of the 20S proteasome using specific fluorescent peptides as described in “Materials and Methods”. Enzyme activity values are expressed as fluorescence units (FU) / hour / μg protein. Each point represents a patient and the horizontal bar is the average. * $p < 0.05$, ** $p < 0.01$, *** $p < 0.005$. Open circles, control WM; closed circles, MS WM; open triangles, control GM; closed triangles, MS GM.

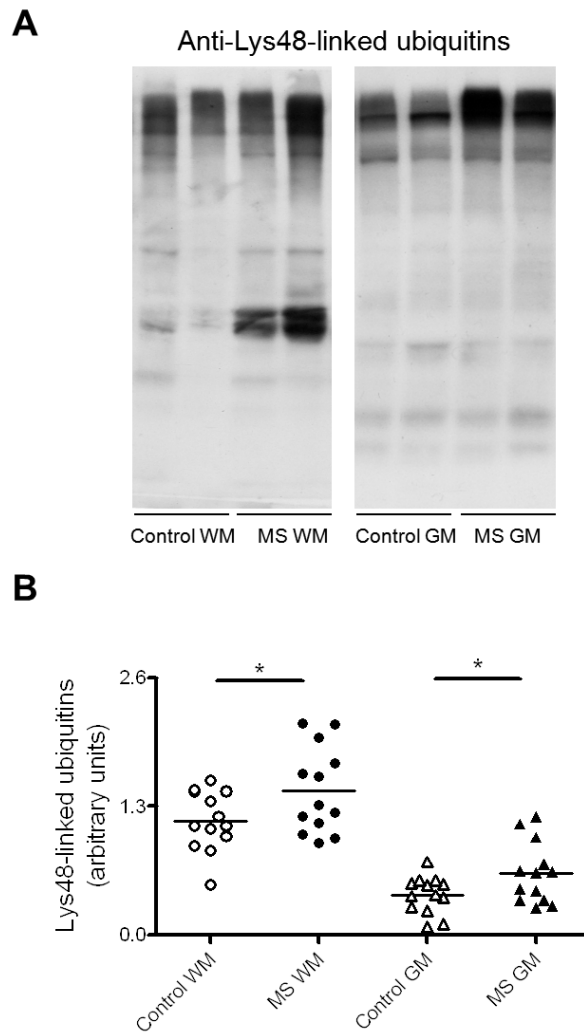


Figure 4.2 - Proteins containing Lys-48-linked poly-ubiquitin accumulate in MS-WM and MS-GM. (A) Representative immunoblots from homogenates of the brain WM and GM areas of control and MS patients developed with antibodies against the Lys-48 poly-ubiquitin. (B) The relative levels of Lys-48 ubiquitin were calculated by dividing Lys-48 ubiquitin whole lane intensity on the immunoblots by that of the corresponding coomassie blue stained lane. Each point represents a patient and the horizontal bar is the average. * $p < 0.05$. Other symbols are as in Figure 4.1.

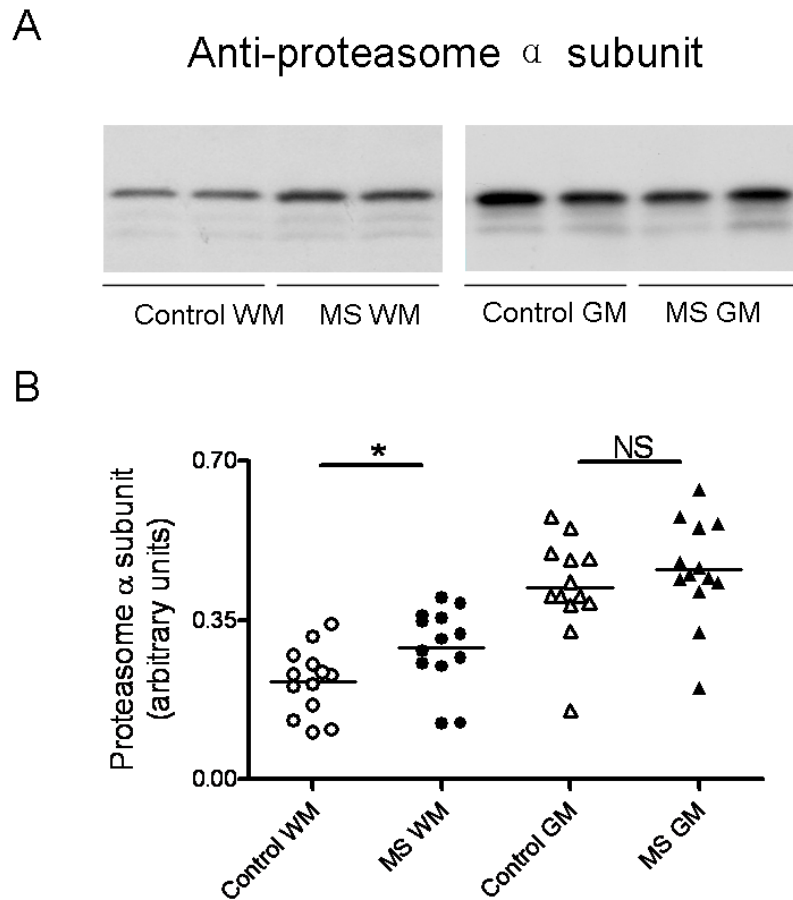


Figure 4.3 - The amount of 20S proteasome α subunits is not diminished in MS. (A) Representative immunoblots from homogenates of brain WM and GM areas of control and MS patients developed with antibodies against the constitutive α subunits of the 20S proteasome. (B) The relative levels of α subunits were calculated by dividing α subunits band intensity on the western blot by that of the corresponding coomassie blue stained lane. Each point represents a patient and the horizontal bar is the average. * $p < 0.05$. Other symbols are as in Figure 4.1.

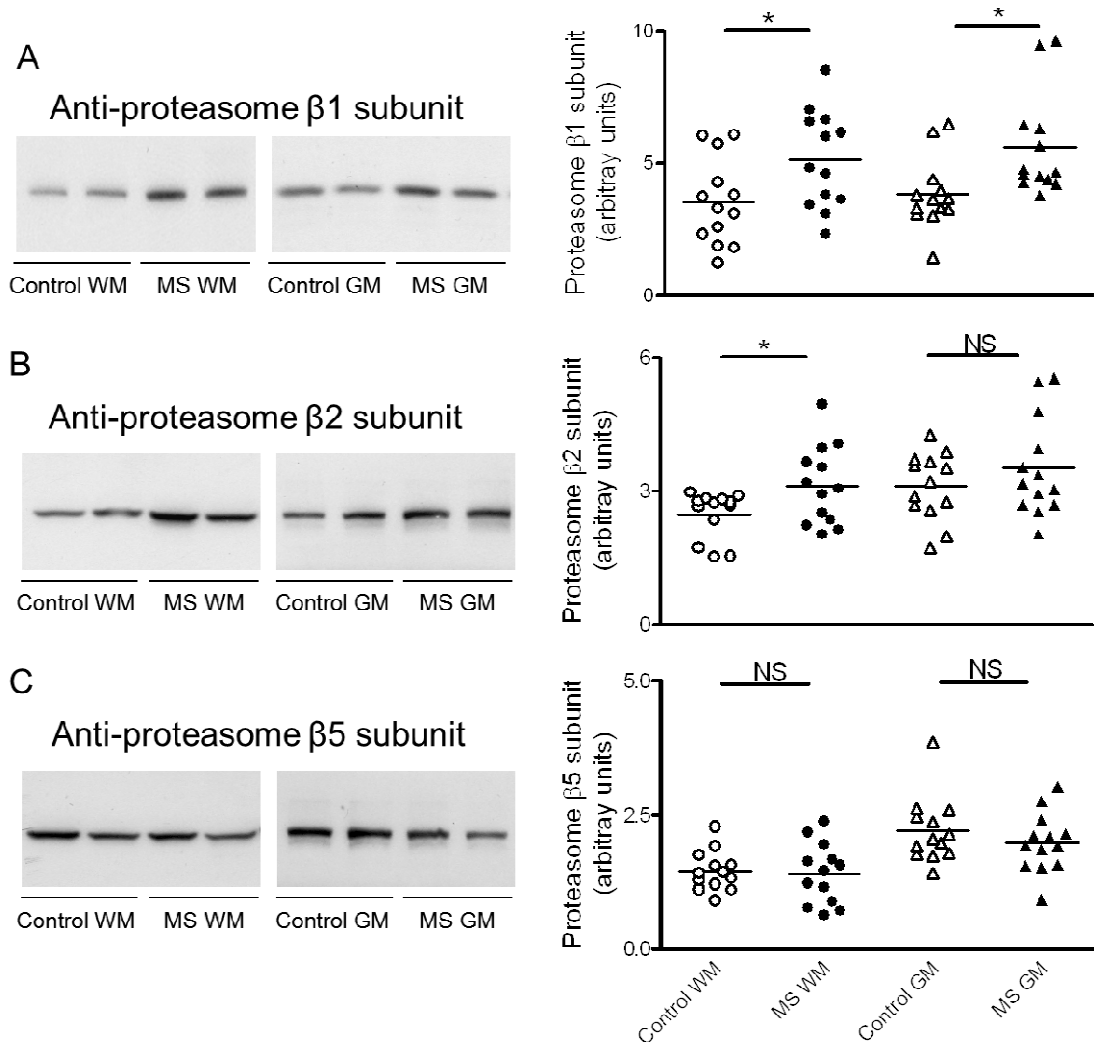


Figure 4.4 – Levels of 20S proteasome β 1, β 2 and β 5 subunits are not decreased in MS. Left three panels show representative immunoblots from homogenates of brain WM and GM areas of control and MS patients developed with antibodies against the β 1 subunit (A), β 2 subunit (B) and β 5 subunit (C) of the 20S proteasome. Right panels depict the corresponding levels of each of the β subunits, which were calculated by dividing band intensity on the western blot by that of the corresponding coomassie blue stained lane. Each point represents a patient and the horizontal bar is the average. * p <0.05. Other symbols are as in Figure 4.1.

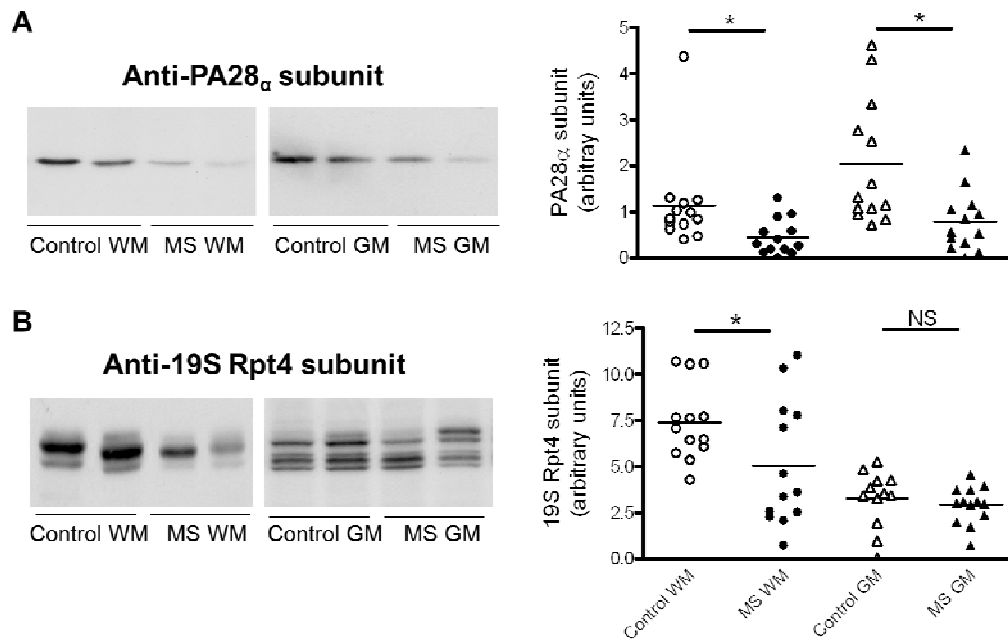


Figure 4.5 – Changes in the levels of the proteasomal regulators 11S and 19S in MS. Left two panels show representative immunoblots from homogenates of brain WM and GM areas of control and MS patients developed with antibodies against the PA28 α subunit of the 11S particle (A) and the Rpt4 subunit of the 19S particle (B). Right panels depict the corresponding levels of each of these subunits, which were calculated by dividing bands intensity on the western blot by those of the corresponding coomassie blue stained lane. Each point represents a patient and the horizontal bar is the average. * $p < 0.05$. Other symbols are as in Figure 4.1.

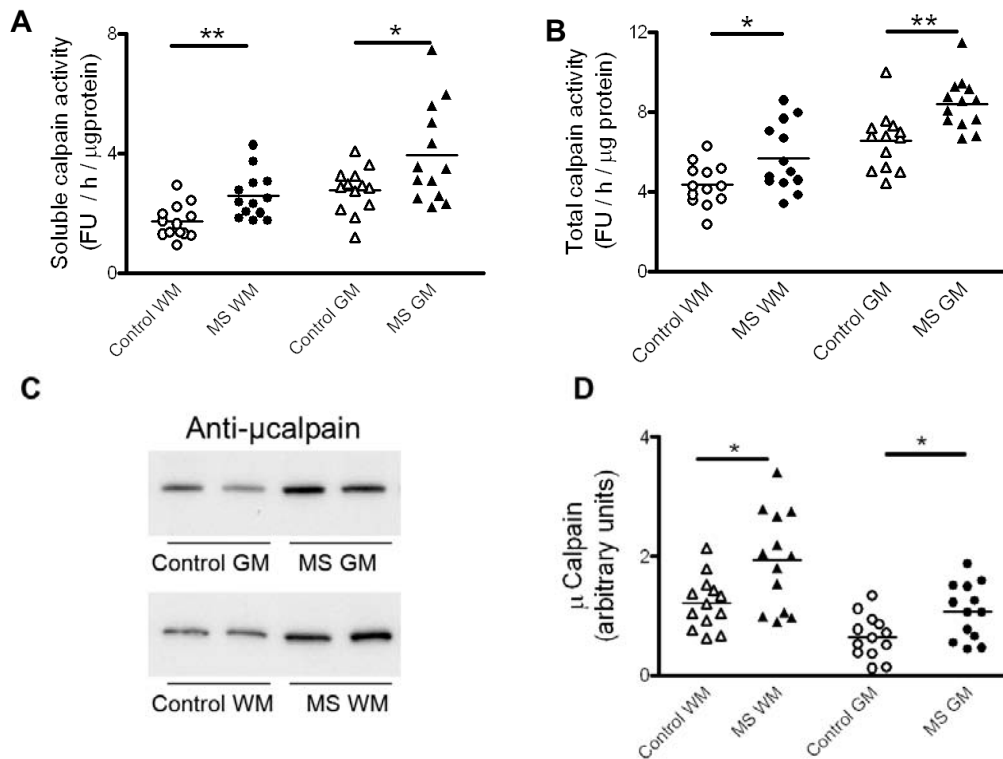


Figure 4.6 – Calpain activity and levels are increased in MS. Aliquots of the cerebral homogenates from control and MS patients were used to determine the soluble (active) (A) and total calpain activity (B) using a fluorescent peptide substrate as described in “Materials and Methods”. Enzyme activity values are expressed as fluorescence units (FU) / hour / μ g protein. (C) Representative immunoblots from homogenates of brain WM and GM areas of control and MS patients developed with antibodies against μ -calpain. (D) The relative levels of μ -calpain were calculated by dividing the band intensity on the western blot by that of the corresponding coomassie blue stained lane. Each point represents a patient and the horizontal bar is the average. * p <0.05, ** p <0.01. Other symbols are as in Figure 4.1.

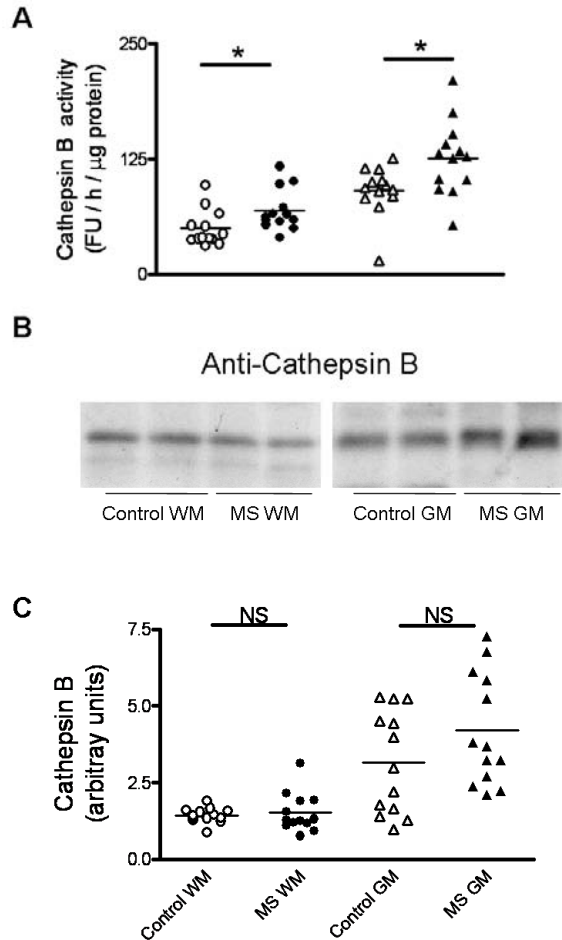


Figure 4.7 - Cathepsin B activity is increased in MS-WM and MS-GM. (A) Aliquots of the cerebral homogenates from control and MS patients were used to determine cathepsin B activity with a specific fluorescent peptide substrate at acid pH as described in "Materials and Methods". Enzyme activity values are expressed as fluorescence units (FU) / hour / μ g protein. (B) Representative immunoblots from homogenates of brain WM and GM areas of control and MS patients developed with an antibody cathepsin B. (C) The relative levels of 31kDa form of cathepsin B were calculated by dividing the band intensity on the western blot by that of the corresponding coomassie blue stained lane. Each point represents a patient and the horizontal bar is the average. * $p < 0.05$. Other symbols are as in Figure 4.1.

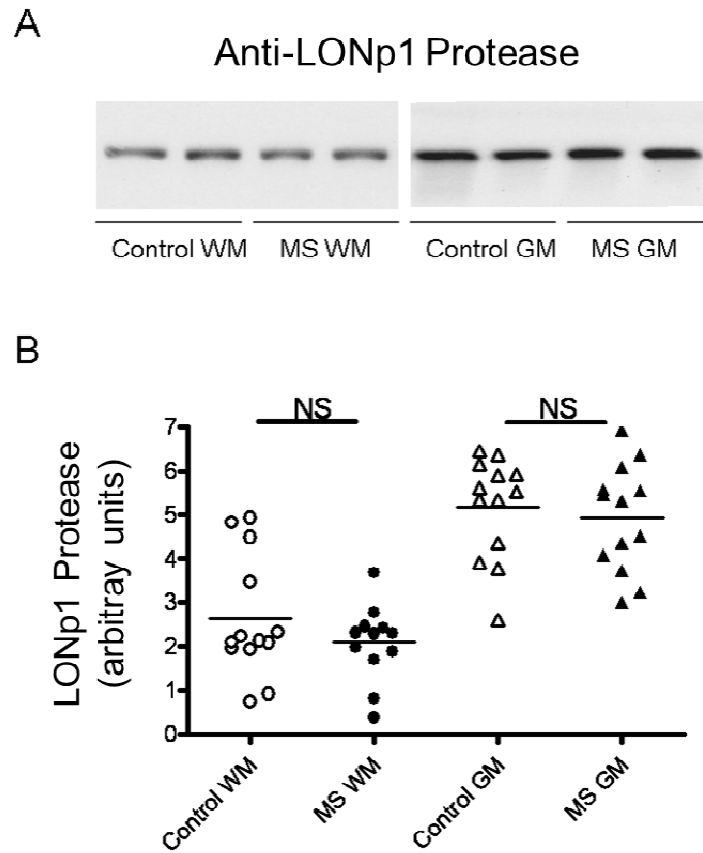


Figure 4.8 – Levels of the mitochondrial LON protease are unchanged in MS. (A) Representative immunoblots from homogenates of brain WM and GM areas of control and MS patients developed with an antibody against LONp1. (B) The relative levels of Lon protease were calculated by dividing the band intensity on the western blot by that of the corresponding coomassie blue stained lane. Each point represents a patient and the horizontal bar is the average. Other symbols are as in Figure 4.1.

4.6 References

1. Kornek B, Lassmann H. Axonal pathology in multiple sclerosis: a historical note. *Brain Pathol* 1999; 9: 651–656.
2. Lucchinetti CF, Bruck W, Rodriguez M, et al. Distinct patterns of multiple sclerosis pathology indicate heterogeneity in pathogenesis. *Brain Pathol* 1996; 6: 259-274.
3. Sharma R, Narayana PA, Wolinsky JS. Gray matter abnormalities in multiple sclerosis: proton magnetic resonance spectroscopic imaging. *Mult Scler* 2001; 7: 221-226.
4. Husted CA, Goodin DS, Hugg JW, et al. Biochemical alterations in multiple sclerosis lesions and normal-appearing white matter detected by in vivo 31P and 1H spectroscopic imaging. *Ann Neurol* 1994; 36: 157-165.
5. Bizzozero OA, DeJesus G, Bixler HA, et al. Evidence of nitrosative damage in the brain white matter of patients with multiple sclerosis. *Neurochem Res* 2005; 30: 139-149.
6. Bizzozero OA, DeJesus G, Callahan K, et al. Elevated protein carbonylation in the brain white matter and gray matter of patients with multiple sclerosis. *J Neurosci Res* 2005; 81: 687–695.
7. Smith K. Demyelination: the role of reactive oxygen and nitrogen species. *Brain Pathol* 1999; 9: 69-92.
8. Hilgart AA, Bizzozero OA. Carbonylation of major cytoskeletal proteins in multiple sclerosis. *J Neurochem* 2008; 104 (Suppl.1): PTW06-03.
9. Smerjac SM, Bizzozero OA. Cytoskeletal protein carbonylation and degradation in experimental autoimmune encephalomyelitis. *J Neurochem* 2008; 105: 763-772.
10. Zheng J, Bizzozero OA. Accumulation of protein carbonyls within cerebellar astrocytes in murine experimental autoimmune encephalomyelitis. *J Neurosci Res* 2010; (In press).
11. Bizzozero OA. (2009) Protein carbonylation in neurodegenerative and demyelinating CNS diseases. In “Handbook of Neurochemistry and Molecular Neurobiology” (Lajtha A, Banik N, Ray S, eds) Springer, pp. 543-562.
12. Grune T, Shringarpure R, Sitte N, et al. Age-related changes in protein oxidation and proteolysis in mammalian cells. *J Gerontol A Biol Sci Med Sci* 2001; 56: 459-467.
13. Shringarpure R, Grune T, Mehlhase J, et al. Ubiquitin conjugation is not required for the degradation of oxidized proteins by proteasome. *J Biol Chem* 2003; 278: 311–318.
14. Divald A, Powell SR. Proteasome mediates removal of proteins oxidized during myocardial ischemia. *Free Radic Biol Med* 2006; 40:156–164.
15. Murata S, Yashiroda H, Tanaka K. Molecular mechanism of proteasome assembly. *Nat Rev Mol Cell Biol* 2009; 10: 104-115.
16. Coux O, Tanaka K, Goldberg AL. Structure and functions of the 20S and 26S proteasomes. *Annu Rev Biochem* 1996; 65: 801-847.
17. Ferrington DA, Husom AD, Thompson LV. Altered proteasome structure, function and oxidation in aged muscle. *FASEB J* 2005; 19: 644-646.

18. DeMartino GN, Slaughter CA. The proteasome, a novel protease regulated by multiple mechanisms. *J Biol Chem* 1999; 274: 22123-22136.
19. Rechsteimer M, Hill CP. Mobilizing the proteolytic machine: cell biological roles of proteasome activators and inhibitors. *Trends Cell Biol* 2005; 15: 27-33.
20. Rodgers KJ, Dean RT. Assessment of proteasome activity in cell lysates and tissue homogenates using peptide substrates. *Int J Biochem Cell Biol* 2003; 35: 716-727.
21. Hassen GW, Feliberti J, Kesner L, et al. A novel calpain inhibitor for the treatment of acute experimental autoimmune encephalomyelitis. *J Neuroimmunol* 2006; 180: 135-146.
22. Sitte N, Huber M, Grune T, et al. Proteasome inhibition by lipofuscin/ceroid during postmitotic aging of fibroblasts. *FASEB J* 2000; 14: 1490-1498.
23. Glickman MH, Ciechanover A. The ubiquitin-proteasome proteolytic pathway: destruction for the sake of construction. *Physiol Rev* 2002; 82: 373-428.
24. Realini C, Jensen CC, Zhang Z, et al. Characterization of recombinant REGalpha, REGbeta, and REGgamma proteasome activators. *J Biol Chem* 1997; 272: 25483-25492.
25. Rivett AJ, Bose S, Pemberton AJ, et al. Assays of proteasome activity in relation to aging. *Exp Gerontol* 2002; 37: 1217-1222.
26. Shields DC, Schaecher KE, Saido TC, et al. A putative mechanism of demyelination in multiple sclerosis by a proteolytic enzyme, calpain. *Proc Natl Acad Sci USA* 1999; 96: 11486-11491.
27. Bota DA, Davies KJ. Lon protease preferentially degrades oxidized mitochondrial aconitase by an ATP-stimulated mechanism. *Nat Cell Biol* 2002; 4: 674-680.
28. Ugarte N, Petropoulos I, Friguet B. Oxidized mitochondrial protein degradation and repair in aging and oxidative stress. *Antiox Redox Signal* 2010; 13: 539-549.
29. Zheng J, Bizzozero OA. Reduced proteasomal activity contributes to accumulation of carbonylated proteins within cerebellar astrocytes in chronic EAE. *Trans Am Soc Neurochem* 2010; PTW07-07.
30. Kessova IG, Cederbaum AI. The effect of CYP2E1-dependent oxidant stress on activity of proteasomes in HepG2 cells. *J Pharmacol Exp Ther* 2005; 315: 304-312.
31. Farout L, Mary J, Vinh J, et al. Inactivation of the proteasome by 4-hydroxy-2-nonenal is site specific and dependent on 20S proteasome subtypes. *Arch Biochem Biophys* 2006; 453: 135-142.
32. Shamoto-Nagai M, Maruyama W, Kato Y, et al. An inhibitor of mitochondrial complex I, rotenone, inactivates proteasome by oxidative modification and induces aggregation of oxidized proteins in SH-SY5Y cells. *J Neurosci Res* 2003; 74: 589-597.
33. Bulteau AL, Verbeke P, Petropoulos I, et al. Proteasome inhibition in glyoxal-treated fibroblasts and resistance of glycated glucose-6-phosphate dehydrogenase to 20S proteasome degradation in vitro. *J Biol Chem* 2001; 276: 45662-45668.
34. Davies SS, Amarnath V, Montine KS, et al. Effects of reactive γ -ketoaldehydes formed by the isoprostane pathway (isoketals) and cyclooxygenase pathway (levuglandins) on proteasome function. *FASEB J* 2002; 16: 715-717.

35. Glockzin S, von Knethen A, Scheffner M, et al. Activation of the cell death program by nitric oxide involves inhibition of the proteasome. *J Biol Chem* 1999; 274: 19581–19586.
36. Friguet B, Stadman ER, Szweda LI. Modification of glucose-6-phosphate dehydrogenase by 4-hydroxy-2-nonenal: Formation of cross-linked protein that inhibits the multicatalytic protease. *J Biol Chem* 1994; 269: 21639–21643.
37. Mayo I, Arribas J, Villoslada P, et al. The proteasome is a major autoantigen in multiple sclerosis. *Brain* 2002; 125: 2658-2667.
38. Keller JN, Hanni KB, Marksberry WR. Impaired proteasome function in Alzheimer's disease. *J Neurochem* 2000; 75: 436-439.
39. McNaught KS, Belizaire R, Isacson O, et al. Altered proteasomal function in sporadic Parkinson's disease. *Exp Neurol* 2003; 179: 38-46.
40. Seo H, Sonntag KC, Isacson O. Generalized brain and skin proteasome inhibition in Huntington's disease. *Ann Neurol* 2004; 56: 319-328.
41. Korhonen L, Lindholm D. The ubiquitin proteasome system in synaptic and axonal degeneration. *J Cell Biol* 2004; 165: 27–30.
42. Rockwell P, Yuan H, Magnusson R, et al. Proteasome inhibition in neuronal cells induces a proinflammatory response manifested by upregulation of cyclooxygenase-2, its accumulation as ubiquitin conjugates, and production of the prostaglandin PGE(2). *Arch Biochem Biophys* 2000; 374: 325-333.
43. Goldbaum O, Vollmer G, Richter-Landsberg C. Proteasome inhibition by MG-132 induces apoptotic cell death and mitochondrial dysfunction in cultured rat brain oligodendrocytes but not in astrocytes. *Glia* 2006; 53: 891-901.
44. Grune T, Reinheckel T, Joshi M, et al. Proteolysis in cultured liver epithelial cells during oxidative stress. Role of the multicatalytic proteinase complex, proteasome. *J Biol Chem* 1995; 270: 2344-2351.
45. Rivett AJ. Preferential degradation of the oxidatively modified form of glutamine synthetase by intracellular mammalian proteases. *J Biol Chem* 1985; 260: 300-305.
46. Pacifici RE, Kono Y, Davies KJ. Hydrophobicity as the signal for selective degradation of hydroxyl radical-modified hemoglobin by the multicatalytic proteinase complex, proteasome. *J Biol Chem* 1993; 268: 15405-15411.
47. Troncoso JC, Costello AC, Kim JH, et al. Metal-catalyzed oxidation of bovine neurofilaments in vitro. *Free Radic Biol Med* 1995; 18: 891-899.
48. Dunlop RA, Brunk UT, Rodgers KJ. Oxidized proteins: mechanisms of removal and consequences of accumulation. *IUBMB Life* 2009; 61, 522-527.
49. Marques C, Pereira P, Taylor A, et al. Ubiquitin-dependent lysosomal degradation of the HNE-modified proteins in lens epithelial cells. *FASEB J* 2004; 18: 1424-1426.
50. Pandey UB, Nie Z, Batlevi Y, et al. HDAC6 rescues neurodegeneration and provides an essential link between autophagy and the UPS. *Nature* 2007; 447: 860-864.
51. Giordana MT, Richiardi P, Trevisan E, et al. Abnormal ubiquitination of axons in normally myelinated white matter in multiple sclerosis brain. *Neuropathol Appl Neurobiol* 2002; 28: 35-41.

5 General Discussion

5.1 Major Conclusions

Multiple sclerosis (MS) is an inflammatory demyelinating disease of the human CNS (Trapp and Syts, 2009) and experimental autoimmune encephalomyelitis (EAE) is a classical animal model recapitulating a number of clinical and pathological features of MS (Gold *et al.*, 2000). A substantial amount of data has shown that oxidative stress plays a major role in the pathogenesis of both MS and EAE. One of the most significant consequences of severe oxidative stress is protein carbonylation (Bizzozero, 2009). This laboratory has recently shown that protein carbonyls accumulate in the brain of MS patients (Bizzozero *et al.*, 2005) and in the spinal cord of rats with acute EAE (Smerjac and Bizzozero, 2008). However, our knowledge of protein carbonylation in inflammatory demyelinating disorders is still limited. The objectives of this thesis were (1) to identify the target cells and oxidized proteins in the cerebellum of EAE animals, and (2) to uncover the mechanism(s) underlying the accumulation of carbonylated proteins in the chronic phase of EAE and in MS patients.

First, I characterized the occurrence of protein carbonylation in the acute (inflammatory) and the chronic (neurodegenerative) phase of EAE. Double immunofluorescence microscopy of affected cerebella showed that most of the carbonyl staining is occurring in white matter astrocytes, and to a lesser extent in microglia/macrophages, both in the acute and chronic phase. By 2D-oxyblot and mass spectrometry, β -actin, β -tubulin, GFAP and HSC-71 were identified as the

major targets of carbonylation throughout the disease (Chapter 2). An increase in the proportion of carbonylated cytoskeletal proteins was then observed in cerebellar astrocytes during the chronic phase of EAE (Table 5.1). Astrocytes are very important in MS and EAE since they aid in degeneration and demyelination, by promoting inflammation, damage of oligodendrocytes and axons, and glial scarring.

Second, I explored the mechanism(s) underlying the accumulation of protein carbonyls in chronic EAE. Since the amount of protein carbonyls is determined by the rate of generation and degradation and since there is less oxidative stress in the chronic relative to the acute phase of EAE (Table 5.1), I proposed that the accumulation of carbonylated cytoskeletal proteins in chronic EAE might be due to a decline in their catabolism. This could be caused either by a defective proteolytic system or by reduced susceptibility of carbonylated proteins to degradation. This hypothesis was tested by identifying the proteolytic system responsible for removal of carbonylated proteins in LPS-stimulated astrocytes. The results clearly showed that only the proteasome inhibitor epoxomicin causes a build-up of carbonylated proteins. More importantly, we discovered that the proteasomal chymotryptic-like activity, which is responsible for the removal of oxidized proteins, is impaired in the cerebellum of mice with chronic EAE while the activities of the other two proteolytic systems (calpain and lysosomal cathepsin B) remain the same or are increased. Furthermore, experiments in a cell-free system showed that carbonylated cytoskeletal proteins from acute and chronic EAE are equally susceptible to proteasomal degradation.

Altogether, these data indicate that diminished proteasomal activity may contribute the accumulation of carbonylated cytoskeletal proteins in chronic EAE (see Chapter 3).

Table 5.1 Summary of protein carbonyl levels in acute and chronic EAE

	Acute	Chronic
Oxidative stress	Yes: ↓GSH (~60% of control)	Yes: ↓ GSH (~83% of control)
Carbonylated GFAP/total GFAP	No change	↑(4-5 folds)
Carbonylated β-Actin/total β-actin	No change	↑(2-3 folds)
Carbonylated β-Tubulin/total β-Tubulin	No change	↑(1-2 folds)

Third, based on the finding of reduced proteasomal activities in chronic EAE, I asked whether the function of the 20S proteasome is also impaired in MS. To this end, I measured the various proteasomal activities and the capacity to digest ubiquitinated proteins in 13 control and 13 MS brains. Similar to what we found in chronic EAE, the three peptidolytic activities of 20S proteasome are reduced in the white matter and gray matter of MS patients. Accumulation of proteins containing Lys-48 polyubiquitin also demonstrates failure of the 26S proteasome. In addition, I assessed the content of the alpha, the three beta (catalytic) subunits and the two major activators (19S and PA28) in MS patients. Interestingly, the amount of proteasome and that of the catalytic subunits are not lessened in MS, suggesting inactivation of 20S proteasome. While the amount of

19S is decreased only in MS white matter, the content of PA28 is reduced in both white matter and gray matter of MS. Moreover, under the conditions of the cell-free assay used in this study, the 19S and PA28 caps are unlikely to be attached to the 20S core particle (Rivett, 2002). Therefore, the reduced level of these activators is not likely responsible for the impairment of proteasomal activity. The possible mechanisms underlying the diminished proteasomal function will be discussed later in this chapter.

The findings presented in this thesis are important not only for understanding why PCOs accumulate in the CNS of EAE animals and MS patients, but also for gaining better insights into the pathophysiology of these disorders. In addition, my findings provide the basis for exploring the mechanisms underlying proteasomal impairment in inflammatory demyelinating disorders. It is tempting to speculate that activating the proteasome or preventing proteasomal dysfunction might be of benefit for MS patients.

5.2 The proteasome may play an important role in the pathophysiology of EAE/MS.

The role of the proteasome system in the pathophysiology of EAE/MS is not completely understood. The 20S proteasome is responsible for the degradation of oxidized protein while the ubiquitin proteasome system is involved in the degradation of cellular proteins including many signal molecules (Shringarpure *et al.*, 2003) and myelin/axonal proteins (Ehlers, 2004; Korhonen and Lindholm, 2004). Therefore, proteasome impairment is likely to cause the

accumulation of oxidized/misfolded proteins and proapoptotic factors that could lead to a series of deleterious events including apoptosis.

Findings in cell systems and in several animal models have demonstrated that disturbances of proteasome activity cause oligodendrocyte/neuron death, neurodegeneration and axonal damage, which interestingly are the major histopathological features of chronic MS/EAE (Kurnellas *et al.*, 2007). For example, proteasome inhibition induces mitochondrial and endoplasmic reticulum dysfunction and apoptotic cell death in cultured oligodendrocytes and neurons (Ustundag *et al.*, 2007; Goldbaum *et al.*, 2006). In addition, inhibition of proteasome activity may play a causal role in mediating the neuropathology in Alzheimer's disease (Ding, 2003). Also, the accumulation of ubiquitinated proteins resulting from proteasome inhibition in neuronal cells were shown to trigger a proinflammatory response characterized by upregulation of COX-2 and production of prostaglandin PGE₂, which in turn contributes to neurodegeneration (Rockwell *et al.*, 2000). Furthermore, it has been shown that both protein trafficking and neuronal connectivity become dysfunctional by protein aggregates. This is caused by decreased proteasomal activity in the neuronal cell body which specifically triggers increased proteasomal activity in the axon, leading to its damage (Korhonen and Lindholm, 2004). Finally, proteasome activity is required for activation of NFκB (Hershko and Ciechanover, 1992), a transcription factor with neuroprotective properties *in vitro* and *in vivo* (Mattson and Furukawa, 1998). Therefore, a fully functional proteasome (both 20S and 26S) may play an important role as a protective barrier, preventing

sudden elevations in oxidative damage, preserving cellular homeostasis, and preventing the activation of apoptotic cascades (Ding, 2006).

In acute EAE, where extensive inflammation leads to severe oxidative stress, cells have normal or even increased proteasomal activity. Because of this elevated degradation capacity, the amount of carbonylated cytoskeletal proteins including β -actin, β -tubulin and GFAP were unaltered. The augmented proteasomal activity is most likely the result of proteasome plasticity and/or the overexpression of heat shock proteins. Proteasome plasticity means that the expression and composition of individual 20S subunits can be altered in response to environmental and genetic stimuli (James *et al.*, 2006). For example, proteasome expression in neural cells is dramatically altered in response to oxidative stress while inflammatory stimuli could alter both proteasome expression and proteasome composition (from constitutive proteasome to immuno-proteasome) (Keller *et al.*, 2002).

As one transitions from the acute to the chronic phase and once the amount of oxidized substrates reaches a point where proteasome can no longer digest them, cells lose the homeostasis. In this situation, the capacity of the proteasome to protect against stress may become compromised as well. Moreover, a rise in oxidative stress and activation of apoptotic pathways likely cause a feed-forward cycle that results in additional proteasome inhibition, greater accumulation of damaged proteins and further activation of death cascades (Ding, 2006). Therefore, proteasome inhibition in the chronic disease

may be a trigger for initiation of these deleterious events. In other words, the time required for the onset of neuropathology and neurodegeneration may depend on how much the proteasome can preserve its function. After that, loss of proteasome function will lead to the development of neurodegeneration.

It is well known that binding of PA28 with the 20S core containing the inducible β subunits aids in the generation of immunogenic peptides (Kloetzel, 2001). Thus, the lower amount of PA28 in MS may have a negative impact on immune function as well. However, it is also possible that the lower content of regulatory proteins in MS may be an adaptive response to the increased demand for degrading oxidized proteins. As suggested by Ferrington (2005), low levels of regulatory proteins guarantees that a population of 20S remains free and available to degrade oxidized proteins (Ferrington *et al.*, 2005).

In the future, we will need to answer several questions. In this study we have shown that there is an increase of chymotrypsin-like proteasome activity in acute EAE, pathologically characterized by inflammation, and a decline in chronic EAE, pathologically characterized by demyelination. Knowing when during the course of EAE the proteasomal activity becomes compromised will be important (1) for understanding the role of proteasome demise in this disease, and (2) for identifying the time point for future pharmacological intervention directed towards activating the proteasome. Furthermore, since the goal of this study was to explore the mechanism underlying the accumulation of carbonylated cytoskeletal proteins within cerebellar astrocytes in chronic EAE, I measured the

accumulation of poly-ubiquitinated proteins only in these cells. However, exposure to environmental stressors (e.g., free radicals) and protective mechanisms (e.g., heat shock proteins, antioxidants) that are unique to each cell type can influence the extent and specificity of the effect (Kappahn *et al.*, 2007). Therefore, it will be important to know whether proteasome impairment is happening in other cell types, particularly in neurons and oligodendrocytes. It is quite possible that as disease progresses damaged neurons and oligodendrocytes die and are removed from the tissue by autophagy; leaving behind astrocytes loaded with undigested proteins. Moreover, my study did not investigate proteasomes in different cellular compartments. As a result, possible disease-associated changes in subcellular localization of this particle were not detected. Altering the subcellular content of proteasomes could impact on specific functions, such as cell cycle regulation, control of signal transduction and gene expression, the degradation of oxidized/misfolded proteins, and antigen presentation and DNA repair (Martinez-Vicente *et al.*, 2005). In addition, studies have reported that the 26S proteasome may be more vulnerable to inactivation as compared to the 20S proteasome (Das *et al.*, 2005), raising the possibility that 26S proteasome function may be compromised prior to the 20S proteasome in neurodegenerative disorders.

5.3 Future directions

5.3.1 Carbonylation may affect the major properties of cytoskeletal proteins like GFAP.

As discussed in Chapter 2, the amount of oxidized cytoskeletal proteins including β -actin, β -tubulin and GFAP in cerebellum were elevated in chronic EAE. Since protein carbonylation is known to affect cytoskeleton stability, it is fair to suggest that the observed changes have physiological consequences. As mentioned before, carbonylation of tubulin leads to disassembly and instability microtubules, and actin filament are easily depolymerized upon carbonylation (Banan *et al.*, 2001). Yet, the effect of carbonylation on GFAP solubility, stability and polymerization has never been investigated. I therefore studied if GFAP oxidation may affect its properties. To this end, I prepared carbonylated GFAP by culturing astrocytes in the presence of the glutathione depletor DEM and then tested the solubility of oxidized GFAP at various concentrations of salt. This technique has been used to evaluate the stability of intermediate-filament-associated protein interactions (Hsiao *et al.*, 2005). As shown in Appendix B, the proportion of carbonylated GFAP in cultured astrocytes was significantly elevated after incubation with DEM. The cell lysates from control and DEM-treated astrocytes were then incubated with increasing concentrations of potassium chloride, starting at 150mM which is close to the ionic strength in physiological medium. Interestingly, after 2 hours of incubation with 150mM KCl, the ratio of GFAP monomer to polymer is greatly elevated in the cell lysates from DEM-treated astrocytes relative to the control (Figure 5.1). These data indicate that

DEM-induced oxidation decreased the stability of GFAP under physiological ionic strength. Higher concentration of KCl (500mM and 1M) disassembles most of GFAP polymers into monomers even in the control cells (Figure 5.1). Similar pattern was observed for β -actin and β -tubulin (see appendix C).

While these results are exciting and they seem to support the stated hypothesis, more detailed studies are needed before we can definitively conclude that carbonylation decreases the stability of GFAP. Particularly, because the monomer-polymer equilibrium is affected by a number of additional factors (William *et al.*, 1987). Further studies on GFAP properties in cell-free system upon direct carbonylation should be performed to clarify the relationship of carbonylation and GFAP properties.

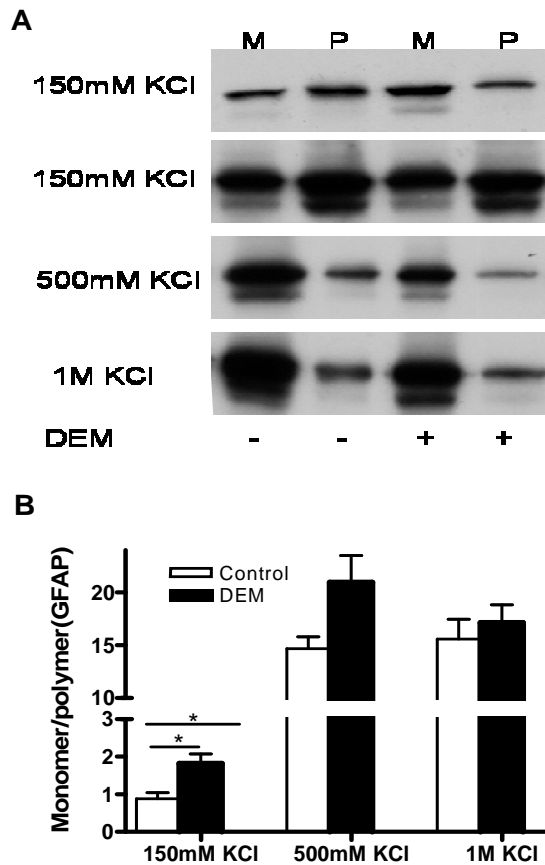


Figure 5.1 The solubility of GFAP in DEM-treated astrocytes augmented upon incubation of KCl. The cell homogenates from control and DEM treated astrocytes were incubated with different concentration of KCl in the presence of 0.5% v/v Triton X-100. After 2 hours, supernatant (monomer, M) and pellet (polymer, P) were separated by 16,000 g of centrifugation. The same volume of supernatant and pellet was loaded and probed with antibodies against GFAP. Densitometric scans were obtained to calculate the ratio of monomer to polymer in GFAP under various conditions (Panel B). Panel A is the representative blot. The data from the condition of 150mM KCl are based on the film with the shorter exposure time, shown in the upper row. Values represent the mean \pm SEM of 3 experiments. * $p < 0.05$.

5.3.2 Possible mechanisms underlying proteasome impairment in chronic EAE and MS.

Decreased proteasomal activity has been reported in several neurodegenerative disorders including Alzheimer's disease, Parkinson disease, amyotrophic lateral sclerosis, and Huntington's disease (Ciechanover and Brundin, 2003). Thus, a loss of proteasome function may be a general phenomenon of neurodegenerative disorders. A missing aspect from all of these studies is a mechanistic understanding of the cause(s) for diminished proteasome function.

One potential explanation for the reduced proteasome function in EAE/MS might be a decreased expression of the catalytic core particle. However, based on the quantification of the 20S proteasome α and β subunits in MS by western blot, I concluded that changes in proteasome unit numbers may not explain the observed decrease in proteasome activity. Therefore, I proposed several mechanisms underlying proteasomal impairment in MS/EAE: (1) inadequate content of endogenous proteasomal activators, (2) enhanced concentration of endogenous proteasomal inhibitors, (3) increased immunoproteasome levels, (4) impaired proteasomal assembly, (5) post-translational modification including phosphorylation and oxidative damage, and (6) changes in proteasomal stability and structural conformation (Figure 5.2).

The best known activator of 20S proteasome is PA700 (19S), which stimulates the degradation of protein substrates in an ATP- and ubiquitin-dependent manner. Two other activators, PA28 (11S) and PA200, do not

recognize ubiquitinated proteins or use ATP (Rechsteiner and Hill, 2005). PA200 is nuclear and involved in DNA repair. The role of this protein on activating proteasome is still controversial since it is also reported that yeast protein Blm3p, homologous to mammalian PA200, does not stimulate proteasome activity *in vitro* (Fehlker *et al.*, 2003). While reduced PA700 levels are observed in white matter of MS relative to the control, it is also possible that PA 700 may contain defects (e.g. oxidative modifications) that prevent its binding to and activation of the 20S particle. Thus, it is likely that decreased assembly of the 26S proteasome could result in delayed degradation of ubiquitin-conjugated proteins. With regard to the other cap, it is well known that PA28 in the cytoplasm forms a hybrid proteasome that functions in class I antigen presentation (see Chapter 1). However, in the absence of inflammation, elevated levels of PA28 may generate more hybrid proteasomes, thereby enhancing the total proteolytic activity (Tanahashi *et al.*, 2000). A possible mechanism underlying proteasomal activation by 11S is that the activator binding induces opening of the entrance and exit gate of the proteasome and that a central channel formed through the center of the activator aligns with the open entrance gate of the proteasome. As a consequence, peptide substrates can easily diffuse through the central channel of the activator and into the proteasomal interior (Rechsteiner and Hill, 2005). I found a low 11S expression in MS patients relative to the control, suggesting that down-regulation of this cap might partially contribute to proteasomal impairment. However, under the assay conditions employed herein, the 11S or 19S complexes are likely to be detached from the 20S particle. Hence, additional

mechanisms are probably responsible for the loss of proteasomal function in EAE and MS.

Several proteins including hsp90, PI31, and PR39 have been identified as negative regulators of proteasomal activity. The chaperone protein hsp90 inhibits hydrolysis of fluorogenic peptides by the 20S proteasome approximately two-fold and the inhibition is abrogated by low levels of PA28 (Lu *et al.*, 2001). Two other proline-rich proteins, PI31 and PR39, inhibit the chymotrypsin-like and caspase-like active sites of the proteasome more than the trypsin-like site (Zaiss *et al.*, 1999), which interestingly is a pattern of inhibition similar to what I found in chronic EAE. PI31 is a competitive inhibitor of PA28 activation while PR39 is a noncompetitive reversible inhibitor of all proteasome complexes (Rechsteiner and Hill, 2005). It has been suggested that PR39 binds to the $\alpha 7$ subunit, preventing proteasome complexes from switching between open and closed conformations (Gaczynska *et al.*, 2003). PI31 has been shown to have a 50-fold higher affinity for the 20S proteasome than that of PA28; however, inhibition of proteasome complexes is less than 50%, even at extremely high levels of PI31 (McCutchen-Maloney *et al.*, 2000). Consequently, the decrease of >50% in proteasomal activities that I measured in the MS specimens cannot be accounted by an increase in PI31. Furthermore, I have obtained preliminary data suggesting that amount of PI31 is actually decreased in MS. The role of other proteasome inhibitors such as 4-HNE cross-linked proteins (Friguet *et al.*, 2006) and lipofuscin/ceroid fluorescent pigments (Sitte *et al.*, 2000), will also need to be investigated in these disorders.

Under conditions of acute immune or stress response, 20S proteasome core subunits $\beta 1$, $\beta 2$, $\beta 5$ are substituted by the interferon- γ inducible subunits $\beta 1i$, $\beta 2i$, $\beta 5i$. The resulting immuno-proteasome has lower chymotrypsin-like and caspase-like activities than the regular 20S subunit (Ferrington *et al.*, 2005). Therefore, an elevation in immuno-proteasome levels could be another possibility for the decreased hydrolysis of fluorogenic peptides in MS tissue. In fact, inflammatory cytokine TNF- α and nitric oxide (NO) have been detected in several inflammatory diseases including MS (Farias *et al.*, 2007), and cultured cells respond to TNF- α and NO by up-regulating expression of the inducible β subunits (Husom *et al.*, 2004).

The present studies did not allow me to determine if the diminished peptidolytic activity in EAE/MS is due to failure of the various subunits to assemble into a functional complex. However, in the case of EAE this is unlikely, since peptide hydrolysis occurs only within the functional catalytic core (i.e. free subunits are inactive) (Kapphahn, 2007) and the trypsin-like activity is not altered. At this time, I cannot rule out the possibility of impaired proteasomal assembly in MS since all of the three peptidolytic activities are reduced to a similar extent. Proteasomal assembly involves the following two events: (a) organization of α -subunits in seven-member rings under the supervision and assistance of proteasome assembling chaperones 1, 2 and 3 (PAC1-3), and (b) association of precursor β -subunits with UMP1/POMP accessory protein that in conjunction to the α -subunits rings gives rise to 20S proteasomes (Chondrogianni and Gonos, 2008). In addition, proteasomal ATPase-associated factor 1 (PAAF1) that

interacts with proteasomal ATPases, has been shown to act as negative regulator of the proteasome activities by affecting the assembly/disassembly of the 26S complex (Chondrogianni and Gonos, 2008). It is clear that more studies on the assembly/disassembly of 20S proteasome, 26S complex, PA28-20S complex and hybrid proteasome need to be performed in the future.

Some post-translational modifications of the 20S subunits have been identified that affect proteasome activities (Fig. 5.2; Post-translational modifications). Specific subunits of the 20S proteasome are targeted for modification by the lipid peroxidation product 4-hydroxy-2-nonenal (4-HNE) and the modified proteasomes exhibit a decline in peptidase activities (Reinheckel *et al.*, 2000; Bulteau *et al.*, 2001; Farout, 2006). In addition to lipid peroxidation, proteasome activity can be impaired by the glycoxidation product glyoxal (Bulteau *et al.*, 2001b), γ -ketoaldehydes (isoketals) (Davies *et al.*, 2002), direct carbonylation (Kessova and Cederbaum, 2005), nitric oxide and nitrosylated glutathione (Glockzin *et al.*, 1999), which are all increased during oxidative stress (Keller *et al.*, 1998).

In addition, the serum and CSF of patients with multiple sclerosis contain autoantibodies against the proteasome (Mayo *et al.*, 2002). Therefore, it is possible that the reaction of autoantibodies and proteasome antigen could reduce its activity.

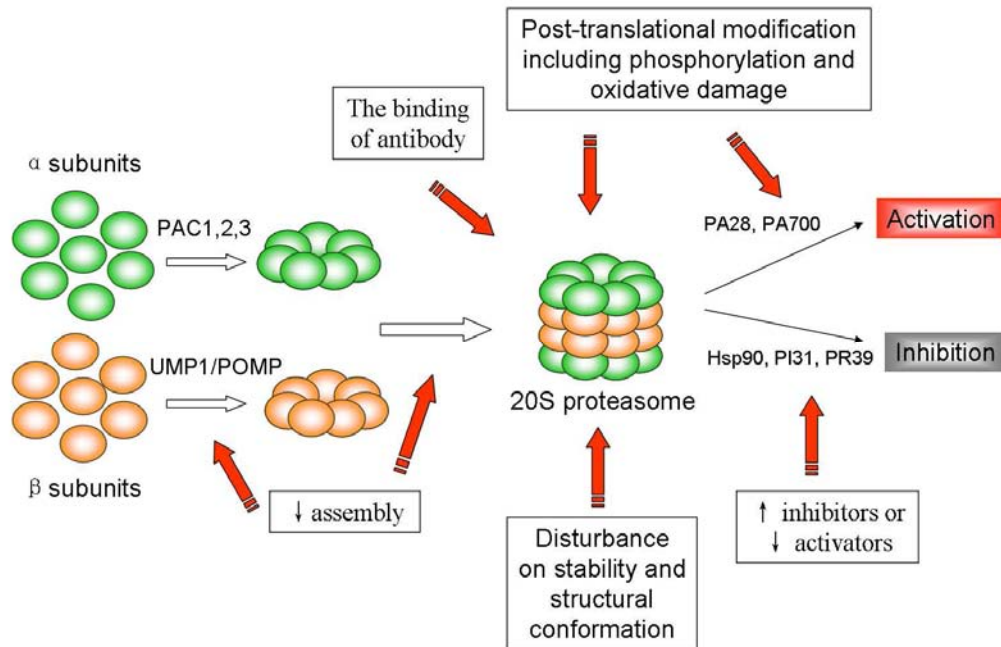


Figure 5.2 Possible mechanisms underlying proteasomal impairment. In conclusion, the understanding of proteasomal impairment in MS/EAE is a major but worthwhile undertaking. Since the proteasome is considered to be a therapeutic target, the knowledge of the precise molecular mechanisms underlying the alteration of proteasome functions will help to design more specific and probably more effective compounds that modulate its activity.

5.4 Scientific Impact

This is the first study showing an initial increase and then decline in the proteasomal peptidolytic activities during the course of EAE. The proteasomal impairment is also observed in MS patients. While the current studies raise a number of questions, the finding that proteasomes are inhibited in chronic EAE/MS will aid our understanding of the pathophysiology of EAE/MS, and may provide the foundation for future studies aimed at developing new approaches to treat MS.

Appendix A

Traditional reactive carbonyl scavengers do not prevent the carbonylation of brain proteins induced by acute glutathione depletion

Jianzheng Zheng and Oscar A. Bizzozero

Department of Cell Biology and Physiology

University of New Mexico School of Medicine

Albuquerque, NM 87131

Published in Free Radic Res (2010) 44, 258-66.

Abstract

We have investigated the effect of reactive carbonyl species (RCS)-trapping agents on the formation of protein carbonyls during depletion of brain glutathione (GSH). To this end, rat brain slices were incubated with the GSH-depletor diethyl maleate in the absence or presence of chemically different RCS scavengers (hydralazine, methoxylamine, aminoguanidine, pyridoxamine, carnosine, taurine and z-histidine hydrazide). Despite their strong reactivity towards the most common RCS, none of the scavengers tested, with the exception of hydralazine, prevented protein carbonylation. These findings suggest that the majority of protein-associated carbonyl groups in this oxidative stress paradigm do not derive from stable lipid peroxidation products like malondialdehyde (MDA), acrolein and 4-hydroxynonenal (4-HNE). This conclusion was confirmed by the observation that the amount of MDA-, acrolein- and 4-HNE-protein adducts does not increase upon GSH depletion. Additional studies revealed that the efficacy of hydralazine at preventing carbonylation was due to its ability to reduce oxidative stress, most likely by inhibiting mitochondrial production of superoxide and/or by scavenging lipid free radicals.

Introduction

Carbonylation constitutes the major and most common oxidative modification of proteins [1]. Protein carbonyls (PCOs) have been shown to affect the function and/or metabolic stability of the modified proteins [2], and thus they are likely to play an important role in the pathophysiology of disorders with

considerable oxidative stress. Carbonylation of brain proteins has been implicated in the etiology and/or progression of several neurodegenerative disorders including Alzheimer's disease [3], Parkinson's disease [4], amyotrophic lateral sclerosis [5] and multiple sclerosis [6].

Carbonyl groups are introduced into proteins by two distinct mechanisms: oxidative (direct) and non-oxidative (indirect). Oxidative mechanisms, which are metal ion-catalyzed, involve the direct reaction of certain reactive oxygen species (e.g. hydrogen peroxide, lipid hydroperoxides, etc) with protein side-chains. Common amino acid targets of direct oxidative processes leading to carbonylation are Thr, Lys, Arg, and Pro. Threonine side-chains are oxidized to α -amino- β -ketobutyric acid while oxidative deamination of Lys, Arg and Pro generates α -aminoadipic semialdehyde and glutamic semialdehyde [7]. Non-oxidative carbonylation of proteins involves the reaction of the nucleophilic centers in Cys, His or Lys residues with reactive carbonyl species (RCS). RCS are carbonyl-containing molecules derived from the oxidation of lipids (e.g. 4-hydroxynonenal (4-HNE), malondialdehyde (MDA), acrolein) and carbohydrates (e.g. glyoxal, methylglyoxal) [7].

To understand the process underlying the formation and accumulation of PCOs during oxidative stress, we recently utilized a brain slices system where carbonyls are induced by acute depletion of cellular glutathione (GSH) with diethyl maleate (DEM) or with 1,2-bis(2-chloroethyl)-1-nitrosourea [8]. We found that under these conditions there is an increased mitochondrial production of reactive oxygen species (ROS), which leads to extensive lipid peroxidation (LPO)

and protein carbonylation by a metal ion-catalyzed process likely involving the formation of hydroxyl radical. More recently we demonstrated that LPO is required for the carbonylation of cytoskeletal and membrane proteins [9]. Furthermore, evidence was presented suggesting that the mechanism underlying LPO-mediated protein carbonylation is the direct oxidation of amino acid side-chains by lipid hydroperoxides (or their immediate decomposition products lipid peroxy and lipid alkoxy radicals) rather than the attachment of RCS like 4-HNE and MDA.

The present study was designed to determine if carbonylation of brain proteins that takes place during acute GSH depletion indeed occurs by an oxidative mechanism. To achieve this objective we have (1) investigated the possible presence of protein-bound lipid aldehydes using antibodies against MDA, 4-HNE and acrolein, and (2) tested the efficacy of several RCS-trapping agents (hydralazine, methoxylamine, aminoguanidine, pyridoxamine, carnosine, taurine and histidine hydrazide) at preventing protein carbonylation in rat brain slices incubated with DEM. The results show that GSH depletion does not generate protein carbonyls by the indirect (non-oxidative) mechanism. This was confirmed by the finding that none of the RCS scavengers tested, with the exception of hydralazine, prevented protein carbonylation. Additional studies revealed that the efficacy of hydralazine is mostly due to its antioxidant properties. A preliminary account of these results has been presented in abstract form [10].

Materials and Methods

Chemicals

Aminoguanidine, apocynin, L-carnosine, clorgyline, deprenyl, DEM, hydralazine, hydroxylamine, methoxylamine and taurine were purchased from Sigma-Aldrich (St. Louis, MO). Pyridoxamine was from Fluka (Ronkonkoma, NY). z-Histidine hydrazide was from Peninsula Laboratories (San Carlos, CA). 15-Hydroperoxy-5,8,11,13-eicoanotetraenoic acid (15-HpETE) was obtained from Cayman Chemicals (Ann Arbor, MI). Anti-4-HNE (AB46544), anti-MDA (AB27642) and anti-acrolein (AB37110) rabbit polyclonal antibodies were from Abcam (Cambridge, MA). All other reagents were of the highest purity available.

Incubation of rat brain slices

Forty-day old Sprague-Dawley male rats were used throughout. Housing and handling of the animals as well as the euthanasia procedure were in strict accordance with the NIH Guide for the Care and Use of Laboratory Animals, and were approved by the Institutional Animal Care and Use Committee. Animals were killed by decapitation, and the brains were rapidly removed and sliced in two directions at right angle in sections 400 μ m-thick using surgical grade, carbon steel razor blades. Slices corresponding to ~80 mg of tissue were transferred to flasks containing 3 ml of Hank's balanced salt solution supplemented with 10 mM D-glucose, and were incubated at 37°C under 95% O₂/5% CO₂. Drugs were added at the beginning of the incubation period as indicated in the figure legends. After 2h, aliquots were taken from the supernatant for H₂O₂ determination using

the Fe/xylene orange (FOX) assay [11]. Tissue sections were then collected by low-speed centrifugation and rinsed twice with 2 ml of ice-cold saline solution. Slices were homogenized by sonication in PEN buffer (10 mM sodium phosphate pH 7.0, 1 mM EDTA and 0.1 mM neocuproine) containing 1mM 4,5-dihydroxy-1,3-benzene sulfonate and 0.5mM dithiothreitol to prevent further protein oxidation. Homogenates were kept at -20°C until use. Protein concentration was assessed with the Bio-Rad DCT protein assay using bovine serum albumin (BSA) as standard.

Determination of non-protein thiols (NPSHs)

NPSHs, which are made mostly of GSH and small amounts of cysteine and homocysteine, were determined spectrophotometrically with 5,5'-dithiobis(2-nitrobenzoic) acid [12].

Measurement of lipid peroxidation

Lipid peroxidation was assessed by measuring the amount of thiobarbituric acid reactive substances (TBARS) in the tissue homogenates as described previously [13].

Measurement of protein carbonylation by western blotting

Protein carbonyl groups were measured by western blot analysis using the OxyBlot™ protein oxidation detection kit (Intergen Co., Purchase, NY) as we described earlier [9]. In brief, proteins (5 µg) were incubated with 2,4-dinitrophenyl-hydrazine to form the 2,4-dinitrophenyl (DNP) hydrazone

derivatives. Proteins were separated by sodium dodecyl sulfate-polyacrylamide gel electrophoresis (SDS-PAGE) and blotted to polyvinylidene difluoride (PVDF) membranes. DNP-containing proteins were then immunostained using rabbit anti-DNP antiserum (1:500) and goat anti-rabbit IgG conjugated to horseradish peroxidase (HRP) (1:2000). Blots were developed by enhanced chemiluminescence (ECL) using the Western Lightning ECL™ kit from Perkin-Elmer (Boston, MA). The developed films were scanned in a Hewlett Packard Scanjet 4890 and the images quantified using the NIH image analysis program version 1.63.

Reaction of oxidized brain proteins with carbonyl scavengers

Proteins from DEM-treated brain slices were precipitated with 1% sulfosalicylic acid and suspended 20mM sodium phosphate buffer pH 7.5 containing 2mM EDTA. Aliquots (50µg of protein) were incubated at 20°C in the absence or presence of various carbonyl scavengers. After 2h, proteins were derivatized with DNPH and analyzed by western blotting as described above.

Assessment of MDA-, 4-HNE- and acrolein-protein adducts by western blotting

Proteins from control and GSH-depleted brain slices were separated by SDS-PAGE and blotted against PVDF membranes. RCS-protein adducts were detected using polyclonal rabbit antibodies against MDA (1:1000), 4-HNE (1:1000) and acrolein (1:2000) and HRP-conjugated goat anti-rabbit IgG (1:2000). Blots were developed by ECL as described above.

Additional assays

The effect of hydralazine (50 μ M-50mM) on the rate of pyrogallol autoxidation was carried out as described by Semsei *et al.*, [14]. The effectiveness of RCS-scavengers at removing MDA was assessed by titrating the unreacted dialdehyde with thiobarbituric acid [13]. The efficacy of RCS-trapping drugs at scavenging 4-HNE was measured by titrating the unreacted unsaturated alkenal with N-methyl-2-phenylindole in the presence methanesulfonic acid [6]. The ability of RCS-trapping agents at scavenging acrolein was determined with treating unreacted acrolein with cysteine ethyl ester and then titrating the excess thiols with 5,5'-dithiobis(2-nitrobenzoic) acid.

Statistical Analysis

Results were analyzed for statistical significance with Student's unpaired *t* test utilizing the GraphPad Prism® (version 4) program (GraphPad Software Inc., San Diego, CA).

Results

DEM-induced protein carbonylation in brain slices

DEM is an α,β -unsaturated dicarboxylic acid that conjugates to GSH via a reaction catalyzed by glutathione-S-transferase [15]. Incubation of brain slices with 10mM DEM for 2 h diminishes NPSHs by 85% and increased TBARS and PCO levels by 70% and 100%, respectively [8]. As described in our previous study [9], the majority of the carbonylated proteins from both control and DEM-

treated slices have molecular weights between 40K and 120K. Among these species are the major cytoskeleton proteins including α/β -tubulin, β -actin, the neuronal intermediate filament proteins and glial fibrillary acidic protein.

Effect of carbonyl scavengers on DEM-induced protein carbonylation in brain slices

The detailed chemical structure of the carbonyl trapping agents used in this study is shown in Fig. A.1. These agents include three hydrazines (hydralazine [16], aminoguanidine [17] and z-histidine hydrazide [18]) and four primary amines (methoxylamine [19], pyridoxamine [20], carnosine [21] and taurine [22]). We chose several, chemically different RCS scavengers because their reactivity toward various RCS differs considerably [23]. In cell-free systems we found that only the three hydrazines, and to a lesser extent carnosine, effectively trap MDA (Fig.A.2A), while all the scavengers showed high reactivity towards 4-HNE (Fig. 2B). Except for aminoguanidine, most drugs also adducted the highly reactive acrolein (Fig. A.2C). It is important to note that these scavengers were also able to prevent the formation protein-RCS adducts in tissue slices incubated with MDA or 4-HNE, indicating that they are cell-permeable (data not shown). We then tested the ability of these RCS scavengers to prevent the appearance of protein carbonyls in brain sections incubated with DEM. As shown in Fig. A.3, none of the carbonyl scavengers prevented DEM-induced glutathione depletion and, among the seven drugs tested, only hydralazine (50 μ -500 μ M) inhibited the formation of protein carbonyls. Aminoguanidine shows an effect only at concentrations ≥ 1 mM [9]. The observation that just hydralazine prevents PCO

formation was surprising, and suggests that either protein carbonylation takes place through an indirect mechanism and that only hydralazine effectively traps RCS in intact cells, or that the efficacy of this drug is due to some property that is unrelated to RCS adduction.

To distinguish between the above possibilities, we determined by western blot analysis whether or not RCS-protein adducts are formed in GSH-depleted brain slices. As depicted in Fig. A.4, antibodies against MDA, acrolein and 4-HNE labeled a number of distinct bands, and the intensity of neither the whole lane nor the individual modified proteins was changed in DEM-treated sections. This indicates that MDA-protein, ACR-protein and 4-HNE-protein adducts are not formed to any appreciable degree in this model of oxidative stress and that the effect of hydralazine on protein carbonylation is not due to its ability to remove RCS.

The possibility that hydralazine reacts directly with protein carbonyls was examined by incubating carbonylated proteins derived from DEM-treated brain slices with hydralazine (0.1-1mM). Only 1mM hydralazine efficiently reduced the amount of protein bound carbonyls, suggesting that the effectiveness of 50 μ M hydralazine at preventing protein carbonylation in intact cells is unlikely caused by a direct reaction between the drug and protein-bound carbonyl groups (Fig. A.5A). Interestingly, 100 μ M hydralazine was found to partially inhibit the 15-HpETE-induced oxidation of proteins (Fig. A.5B), and this could be due to scavenging of alkoxyl and peroxy radicals produced during the metal ion-catalyzed decomposition of the lipid hydroperoxide and/or to the sequestration of

iron and copper ions. In any case, the concentration of hydralazine needed to cause this effect in a cell-free system is still higher than that required to suppress PCO formation in GSH-depleted brain sections (see below).

Antioxidant properties of hydralazine

Because hydralazine is known to have antioxidant properties in several oxidative stress settings [24] and based on the observation that it also lowers the levels of TBARS in GSH-depleted brain sections (data not shown), we hypothesized that this drug may just be reducing oxidative stress and indirectly carbonyl formation. To address this issue, we determined hydrogen peroxide and PCO levels in DEM-treated brain slices incubated with different concentrations of hydralazine. As shown in Fig. A.6, both H_2O_2 levels and the amount of protein carbonyls diminished with increasing concentrations of hydralazine (0.5-500 μ M), indicating that the inhibitor is acting mostly as an antioxidant.

A series of additional studies were conducted to ascertain the mechanism underlying the antioxidant properties of hydralazine. We first investigated the possibility that hydralazine could be scavenging peroxides (H_2O_2 , lipid hydroperoxides) or superoxide radicals. Fig. A.7A shows that hydralazine does not react with either H_2O_2 or 15-HpETE even at high concentrations (0.5mM). The ability of hydralazine to scavenge superoxide was tested with pyrogallol. In the pyrogallol system, superoxide radicals are formed from molecular oxygen and the detecting system is the pyrogallol itself. Hydralazine reduced superoxide levels only at a concentration \geq 5mM, which is 1000-times higher than that

required to abolish H₂O₂ production (Fig. A.7B). Thus, the most likely mechanism underlying the antioxidant effects of hydralazine is the inhibition of processes responsible of ROS production.

In a previous study we showed that most of the superoxide generated during GSH depletion comes from mitochondria (inhibited by carbonyl cyanide 3-chlorophenylhydrazone) and to a lesser extent from cytochrome P-450 (inhibited with proadifen), but not from xanthine oxidase (unaltered by oxypurinol) [8]. However, other possible sources of superoxide that are targeted by hydralazine, like NADPH oxidase (24) and monoamine oxidase (MAO) [25], were not investigated in that study. To address this issue, brain slices were incubated with DEM in the presence or absence of apocynin (NADPH oxidase inhibitor [26]), clorgyline (MAO-A inhibitor, [25]), deprenyl (MAO-B inhibitor [25]) or hydroxylamine (MAO-A/B inhibitor [27]). As shown in Fig. A.8, protein carbonylation was not decreased by any of these drugs, indicating that these enzymes are not involved in the generation of superoxide during GSH depletion. In sum, the above results are in agreement with previous findings suggesting that hydralazine reduces superoxide production from mitochondria [28, 29]. At this time, however, we cannot rule out the possibility that hydralazine acts also by scavenging of lipid alkoxyl and peroxy radicals, mainly because the concentration of these radicals and hydralazine in the cell membranes may be quite different than those used in our cell-free experiment (Fig. A.5B).

Discussion

In this study, we present evidence that RCS-trapping drugs do not prevent the carbonylation of brain proteins during depletion of the antioxidant glutathione. Commonly used RCS-scavengers like aminoguanidine, pyridoxamine, methoxylamine, carnosine, taurine and z-histidine hydrazide were unable to reduce the appearance of protein carbonyls during DEM-induced oxidative stress. Only hydralazine prevented PCO accumulation at relatively low concentrations, but the effect is due to its antioxidant properties rather than to its ability to trap RCS or to react with PCOs directly. This suggests that the majority of protein-associated carbonyl groups in this oxidative stress paradigm do not derive from stable LPO products like MDA, acrolein and 4-HNE. This conclusion was confirmed by the observation that the amount of MDA-, acrolein- and 4-HNE-protein adducts does not increase in GSH-depleted sections. Thus, this system is best suited to test the effect of antioxidants on protein carbonylation rather than to explore the efficacy of new RCS-trapping agents.

Oxidation of polyunsaturated fatty acids gives rise to three major products, all of which are known to introduce carbonyl groups into proteins. These compounds include (I) dialdehydes (e.g. MDA), which react with lysine residues to form carbonyl derivatives; (II) α,β -unsaturated aldehydes (e.g. 4-HNE, 4-hydroxy-2-hexenal, acrolein), which undergo a Michael addition reaction with the ϵ -amino group of lysine residues, the thiol group of cysteine residues and the imidazole group of histidine residues; and (III) lipid hydroperoxides, which can

undergo metal ion-catalyzed decomposition to produce alkoxy and peroxy radicals that can react directly with amino acid residues. Previous work from our laboratory suggested that lipid hydroperoxide-mediated oxidation is the major mechanism by which brain proteins (particularly cytoskeletal and membrane proteins) are carbonylated during acute GSH depletion [9]. In the present study we have strengthened this conclusion by the finding that none of the classical RCS scavengers prevent the carbonylation of proteins but more importantly by the absence of MDA-, 4-HNE- and ACR-protein adducts as measured on western blots. Lipid hydroperoxide-induced protein carbonylation was initially proposed by Refsgaard *et al.*, [30], who discovered that metal-catalyzed oxidation of proteins is greatly enhanced by addition of polyunsaturated fatty acids. These investigators speculated that alkoxy radicals, derived from metal-catalyzed heterolytic cleavage of lipid hydroperoxides, are responsible for the introduction of carbonyls into proteins by a mechanism that might involve site-specific interaction with lysine residues. Lipid-derived alkoxy radicals were found to be involved also in the oxidation of retinal proteins in diabetes [31], suggesting that this mechanism is more common than previously thought.

Accumulation of PCOs has been implicated in the etiology and/or progression of several neurodegenerative disorders such as Alzheimer's disease [3], Parkinson's disease [4], and amyotrophic lateral sclerosis [5]. Our recent discovery that carbonylation of CNS proteins is augmented in multiple sclerosis [6, 32] and its animal model experimental allergic encephalomyelitis [33], suggests that this type of protein modification may play a critical

pathophysiological role in inflammatory demyelinating diseases as well. Therefore, approaches to reduce the extent of protein carbonylation may be beneficial for treating these disorders. In recent years carbonyl trapping has received considerable attention as a specific treatment for conditions with severe carbonyl stress. Carbonyl trapping agents like those tested in this study react with RCS at a faster rate than do cell macromolecules, thereby ensuring the safe excretion of drug-carbonyl conjugates. However, this approach is effective only if protein carbonylation takes place by an indirect mechanism, which does not seem to be the case during acute depletion of glutathione. Furthermore, α -amino adipic semialdehyde and glutamic semialdehyde, which result from direct oxidation of lysine, arginine and proline residues, are the major carbonylated amino acids in CNS proteins during aging and in neurodegenerative disorders [34, 35]. Thus, in most cases, prevention of protein carbonylation will have to be achieved with agents that reduce oxidative stress, limit LPO and/or interfere with the direct oxidation of amino acids. The antihypertensive hydralazine seems to possess all of these properties since it reduced oxidative stress in intact cells (Fig. 6) and interfered with lipid hydroperoxide-induced protein carbonylation in a cell-free system (Fig. 5B), and there is also evidence that it strongly inhibits LPO [36]. Preliminary studies in our laboratory have shown that administration of hydralazine reduces CNS damage and decrease neurological symptoms of rats with acute experimental autoimmune encephalomyelitis, suggesting that this drug could be potentially useful for treating neuroinflammatory disorders.

The antioxidant properties of hydralazine have been reported in several studies and have been attributed to: (1) inhibition of ROS-generating enzymes such as NADPH oxidase [24], monoamine oxidase [25] and xanthine oxidase [37], (2) scavenging of superoxide and peroxynitrite [29], and (3) decreased mitochondrial superoxide production [28, 29]. In this study we ruled out the participation of NADPH oxidase and monoamine oxidases in the generation of ROS during GSH depletion, and that of xanthine oxidase was excluded in our previous study [8]. In addition, we have eliminated the possibility of a direct reaction of superoxide, hydrogen peroxide and lipid hydroperoxides with hydralazine. The possibility that hydralazine reduces protein carbonylation by scavenging peroxynitrite is also unlikely since this oxidant is not produced in this oxidative stress paradigm as demonstrated by the lack of nitrotyrosine [9]. Furthermore, addition of two peroxynitrite-scavengers (uric acid and dimethylthiourea) [8] and a nitric oxide synthetase inhibitor aminoguanidine (this study) has not effect on protein oxidation in this system. All of these findings, along with recent observations that hydralazine does not inhibit cytochrome P-450 [38], point out to mitochondria as the most likely target of hydralazine in the DEM-treated brain sections. There is some evidence that hydralazine reduces the mitochondrial production of superoxide and consequently hydrogen peroxide [28, 29], and we are currently investigating the molecular mechanism underlying this effect.

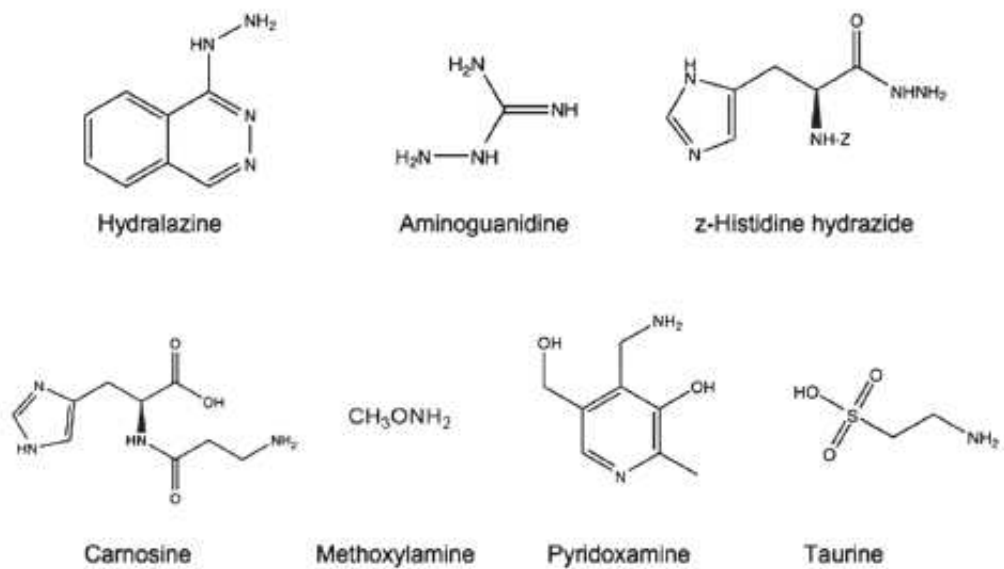


Figure A.1 - Chemical structure of the various carbonyl-trapping agents used in this study. z-, carbobenzoxy- .

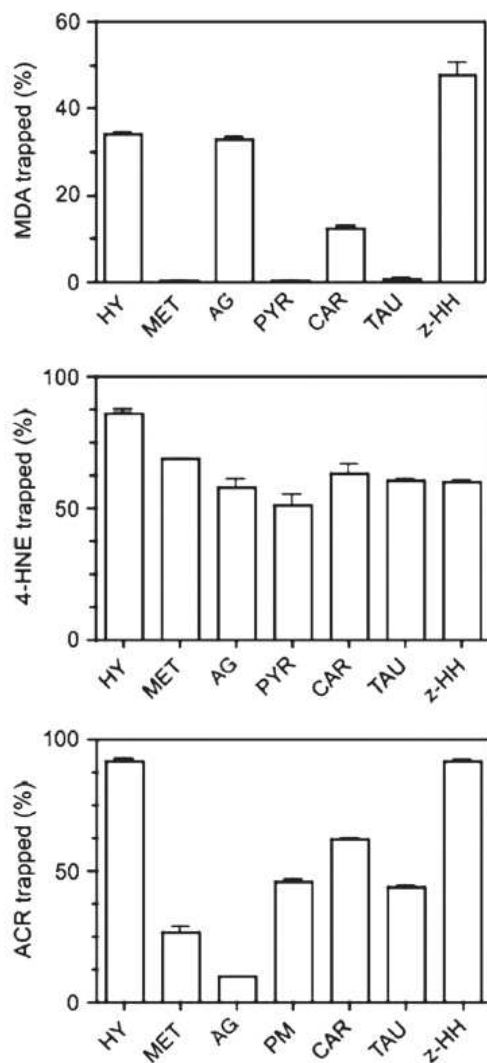


Figure A.2 - Ability of carbonyl scavengers to trap various RCS in a cell-free system. MDA (36 μ M), 4-HNE (25 μ M) and acrolein (100 μ M) were incubated for 2h at room temperature in the presence or absence of various carbonyl scavengers (1mM). After incubation, the amount of unreacted RCS was determined as described under Material and Methods. Values are expressed as the % of RCS trapped by the scavenger and represent the mean \pm SEM of three separate incubations. The concentration of acrolein in these experiments was 4-times higher than that of 4-HNE solely because the sensitivity of the assays for measuring each unsaturated alkenal is different. Abbreviations: HY, hydralazine; MET, methoxylamine; AG, aminoguanidine; PYR, pyridoxamine; CAR, carnosine; TAU, taurine; z-HH, z-histidine hydrazide.

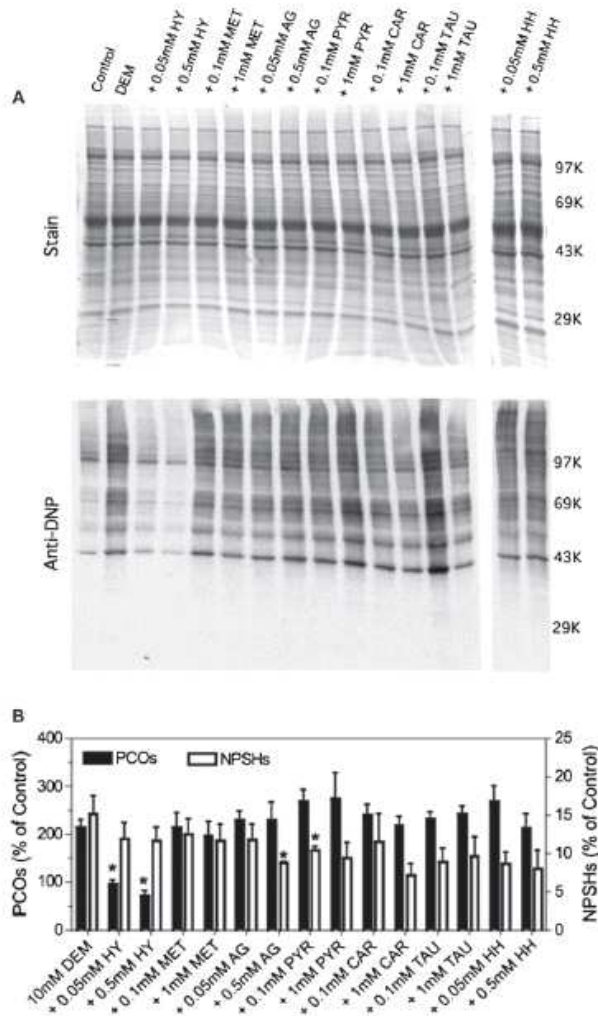


Figure A.3 - Effect of carbonyl scavengers on DEM-induced protein carbonylation. Rat brain slices were incubated with 10mM DEM in the absence or presence of two different concentrations of various carbonyl scavengers. After 2h, slices were homogenized in PEN buffer and aliquots of the homogenate were used to determine the PCOs by western blot as described under “Material and Methods”. Panel A shows a representative OxyBlot. The molecular weight markers are: phosphorylase b (97K), bovine serum albumin (69K), ovalbumin (43K), and carbonic anhydrase (29K). Other abbreviations are as in Figure 2. Panel B depicts protein carbonylation levels obtained from western blots and NPSH levels determined spectrophotometrically with 5,5'-dithiobis(2-nitrobenzoic) acid. Values are expressed as % of control and represent the mean \pm SEM of 3-4 experiments. Control values for carbonyls and NPSHs are 0.21 ± 0.02 nmol/mg protein and 10.8 ± 0.8 nmol/mg protein, respectively. Asterisks denote those numbers that are significantly different ($p < 0.05$) from DEM-treated slices.

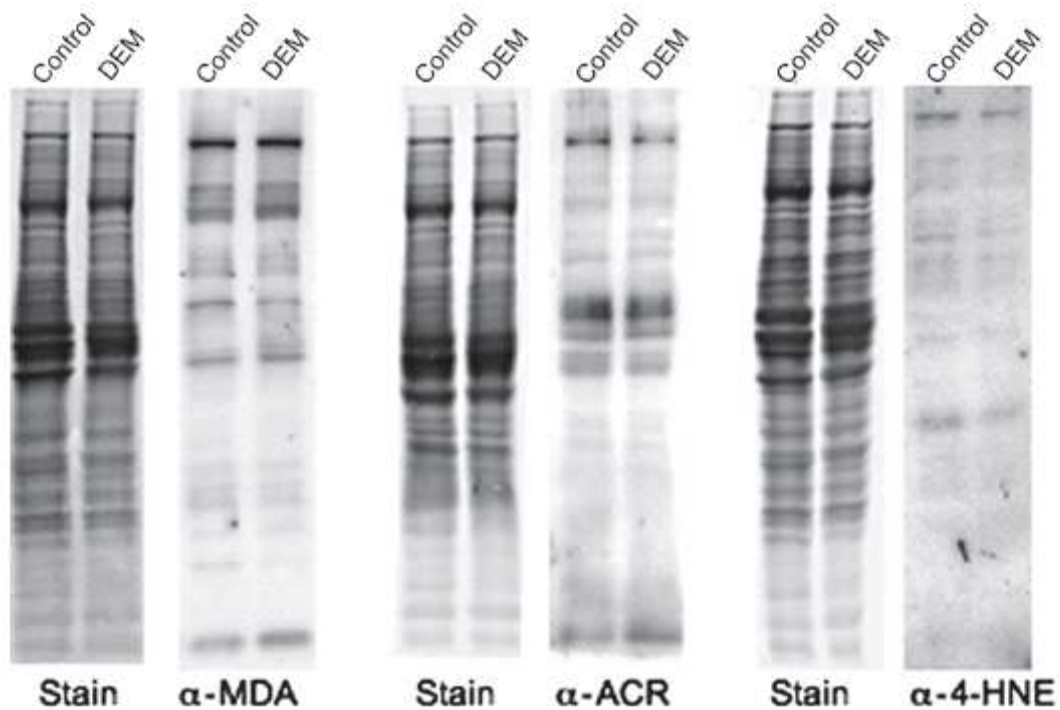


Figure A.4 - Detection of RCS-protein adducts in control and GSH-depleted brain slices. Rat brain slices were incubated in the absence (control) or presence of 10mM DEM. After 2h, slices were homogenized in PEN buffer and aliquots of the homogenate were analyzed by western blotting using antibodies against the various RCS as described in "Material and Methods".

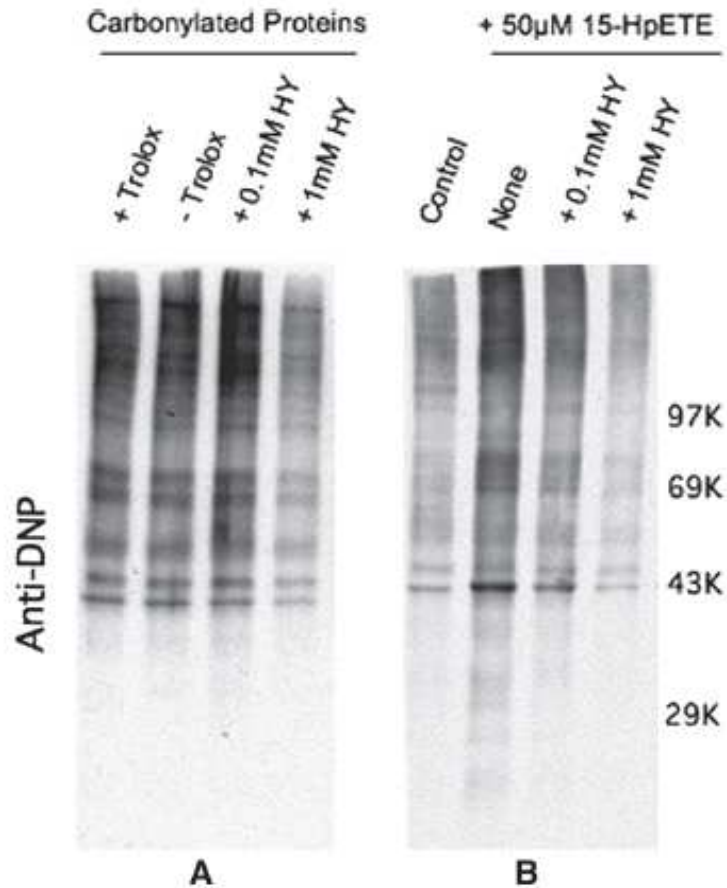


Figure A.5 A- Effect of hydralazine on protein-bound carbonyl groups. Oxidized proteins prepared from DEM-treated brain slices were incubated for 2h in the absence or presence of two different concentration of hydralazine as described in "Material and Methods". PCOs were derivatized with DNPH and analyzed by OxyBlot. The antioxidant trolox (1mM) was included in some samples to ascertain that further protein oxidation does not occur during the incubation period. B- Effect of hydralazine on lipid hydroperoxide-induced protein carbonylation in a cell-free system. Proteins prepared from control brain slices were incubated for 2h with 15-HpETE in the absence or presence of two different concentration of hydralazine. After incubation PCOs were derivatized with DNPH and analyzed by OxyBlot.

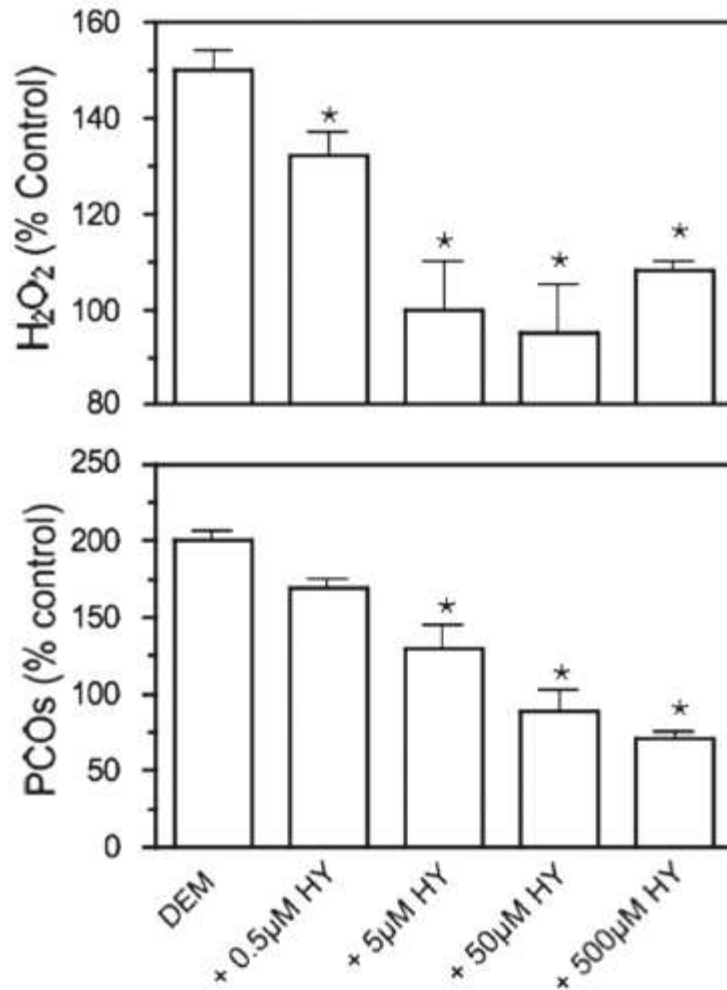


Figure A.6- Effect of increasing concentrations of hydralazine on DEM-induced protein carbonylation and hydrogen peroxide production. Rat brain slices were incubated with 10mM DEM in the absence or presence of increasing concentrations (0.5-500μM) hydralazine. After 2h, aliquots from the incubation media were removed and used to determine H₂O₂ levels using the FOX assay. Slices were homogenized in PEN buffer and aliquots of the homogenate were used to determine PCOs by OxyBlot. Values are expressed as % of control and represent the mean ± SEM of 3-4 experiments. Asterisks denote values that are significantly different (p<0.05) from DEM-treated slices.

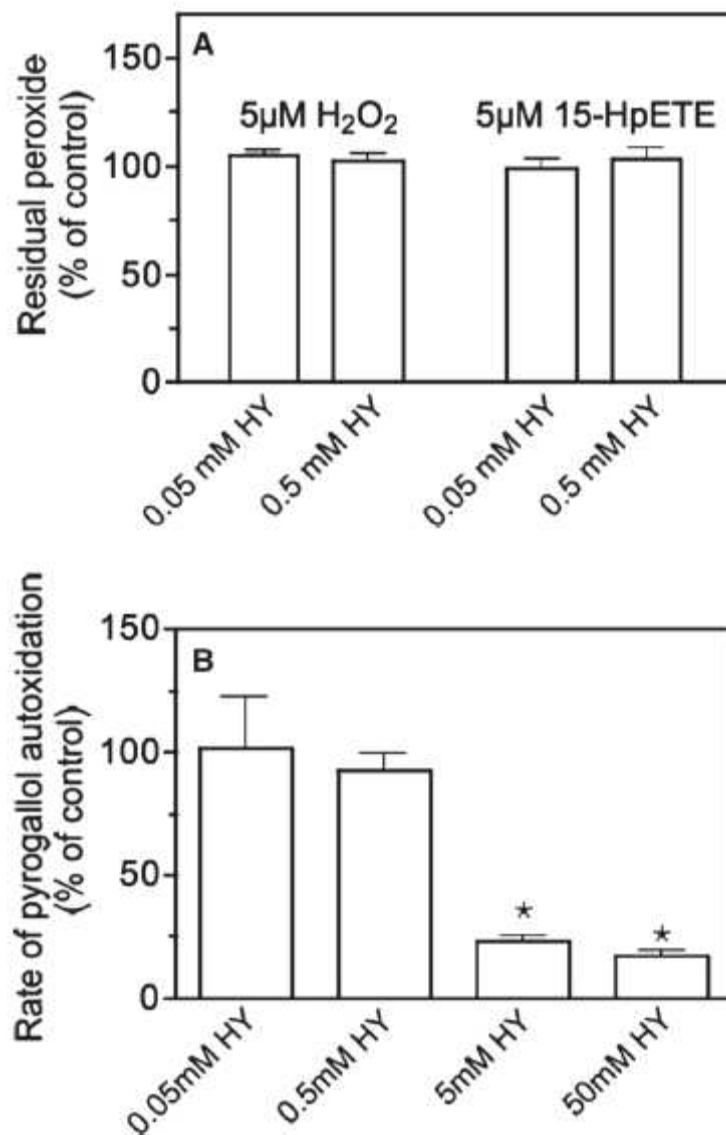


Figure A.7 A- Effect of hydralazine on hydrogen peroxide and lipid hydroperoxide stability. Hydrogen peroxide and the lipid hydroperoxide 15-HpETE were incubated in the absence or presence of two different concentrations of hydralazine. After 2h, residual peroxide levels were determined with the FOX assay as described under “Material and Methods”. B- Effect of hydralazine on the stability of pyrogallol-generated superoxide. Pyrogallol (0.2mM) was incubated in the absence or presence of two different concentrations of hydralazine, and the rate of autoxidation was determined as described in “Material and Methods”. Values are expressed as % of control (i.e. without hydralazine) and represent the mean \pm SEM of three experiments. Asterisks denote values that are significantly different ($p < 0.05$) from controls.

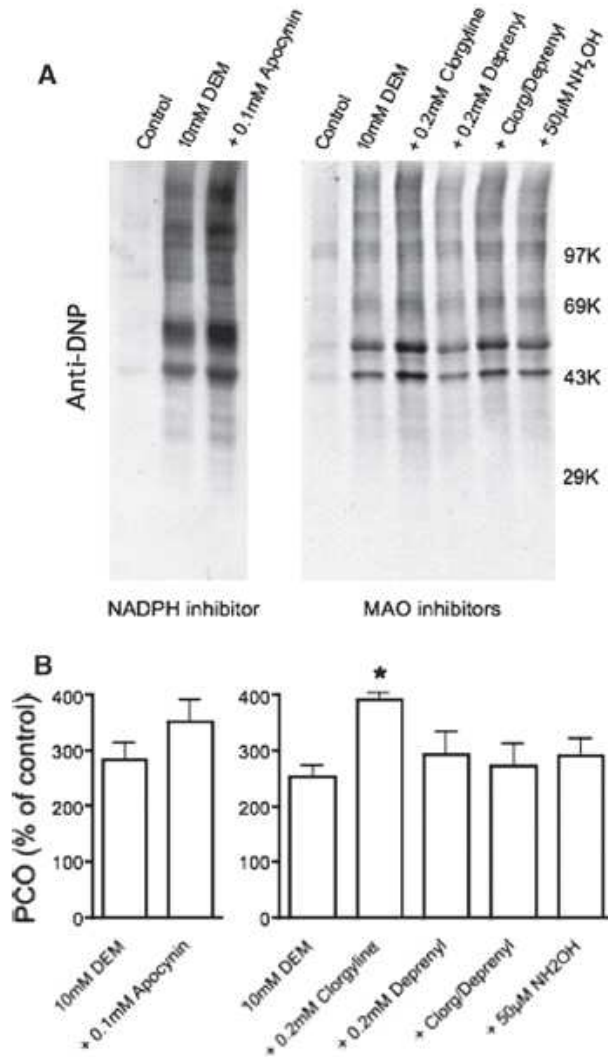


Figure A.8 - Effect of NADPH oxidase and MAO inhibitors on DEM-induced protein carbonylation. Rat brain slices were incubated with 10mM DEM in the absence or presence of a NADPH oxidase inhibitor (apocynin) or MAO inhibitors (clorgyline, deprenyl and hydroxylamine). After 2h, slices were homogenized in PEN buffer and aliquots of the homogenate were used to determine the PCOs by OxyBlot as described under "Material and Methods". Panel A shows representative OxyBlots. Panel B depicts protein carbonylation levels obtained from the western blots. Values are expressed as % of control and represent the mean \pm SEM of 3 experiments. Asterisk denotes the value that is significantly different ($p < 0.05$) from DEM-treated slices.

References

- [1] Stadtman ER, Berlett BS. Reactive oxygen-mediated protein oxidation in aging and disease. *Chem Res Toxicol* 1997; 10:485-494.
- [2] Levine RL. Carbonyl modified proteins in cellular regulation, aging, and disease. *Free Radic Biol Med* 2002; 32:790-796.
- [3] Aksenov MY, Aksenova MV, Butterfield DA, Geddes JW, Markesbery WR. Protein oxidation in the brain in Alzheimer's disease. *Neuroscience* 2001; 103:373-383.
- [4] Floor E, Wetzel MG. Increased protein oxidation in human substantia nigra pars compacta in comparison with basal ganglia and prefrontal cortex measured with an improved dinitrophenylhydrazine assay. *J Neurochem* 1998; 70:268-275.
- [5] Ferrante RJ, Browne SE, Shinobu LA, Bowling AC, Baik MJ, MacGarvey U, Kowall, NW, Brown RH, Beal MF. Evidence of increased oxidative damage in both sporadic and familial amyotrophic lateral sclerosis. *J Neurochem* 1997; 69:2064-2074.
- [6] Bizzozero OA, DeJesus G, Callahan K, Pastuszyn A. Elevated protein carbonylation in the brain white matter and gray matter of patients with multiple sclerosis. *J Neurosci Res* 2005; 81:687-695.
- [7] Adams S, Green P, Claxton R, Simcox S, Williams MV, Walsh K, Leeuwenburgh C. Reactive carbonyl formation by oxidative and non-oxidative pathways. *Front Biosci* 2001; 6:17-24.
- [8] Bizzozero OA, Ziegler JL, DeJesus G, Bolognani F. Acute depletion of reduced glutathione causes extensive carbonylation of rat brain proteins. *J Neurosci Res* 2006; 83:656-667.
- [9] Bizzozero OA, Reyes S, Ziegler JL, Smerjac S. Lipid peroxidation scavengers prevent the carbonylation of cytoskeletal brain proteins induced by glutathione depletion. *Neurochem Res* 2007; 32:2114-2122.
- [10] Zheng J, Reyes S, Bizzozero OA. Effect of hydralazine and other carbonyl scavengers at preventing the carbonylation of brain proteins induced by GSH depletion. *J Neurochem* 2008; 104 (Suppl.1): PTW06-15.
- [11] Nourooz-Zadeh A, Tajaddini-Sarmadi J, Ling KL, Wolff SP. Low-density lipoprotein is the major carrier of lipid hydroperoxides in plasma. *Biochem J*. 1996; 313: 781-786.
- [12] Riddles PW, Blakely RL, Zerner B. Ellman's reagent: 5,5'-dithiobis(2-nitrobenzoic acid)-a reexamination. *Anal Biochem* 1979; 94: 75-81.
- [13] Ohkawa H, Ohishi N, Yagi K. Assay for lipid peroxides in animal tissues by thiobarbituric acid reaction. *Anal Biochem* 1979; 95: 351-358.
- [14] Semsei I, Nagy K, Zs-Nagy I. In vitro studies on the OH and O₂- free radical scavenger properties of idebenone in chemical systems. *Arch Gerontol Geriatr* 1990; 11: 187-197.
- [15] Buchmuller-Rouiller Y, Corrandin SB, Smith J, Schneider P, Ransijn A, Jongeneel CV, Mauel J. Role of glutathione in macrophage activation: effect of cellular glutathione depletion on nitrite production and leishmanicidal activity. *Cell Immunol* 1995; 164:73-80.

- [16] Kaminskas LM, Pyke SM, Burcham PC. Strong protein adduct trapping accompanies abolition of acrolein-mediated hepatotoxicity by hydralazine in mice. *J Pharmacol Exp Ther* 2004; 310: 1003-1010.
- [17] Al-Abed Y, Bucala R. Efficient scavenging of fatty acid oxidation products by aminoguanidine. *Chem Res Toxicol* 1997; 10: 875-879.
- [18] Tang SC, Arumugam TV, Cutler RG, Jo DG, Magnus T, Chan SL, Mughal MR, Telljohann, RS, Nassar M, Ouyang X, Calderan A, Ruzza P, Guiotto A, Mattson MP. Neuroprotective actions of a histidine analogue in models of ischemic stroke. *J Neurochem* 2007; 101:729-736.
- [19] Burcham PC, Fontaine FR, Kaminskas LM, Petersen DR, Pyke SM. Protein adduct-trapping by hydrazinophthalazine drugs: mechanisms of cytoprotection against acrolein-mediated toxicity. *Mol Pharmacol* 2004; 65:655-664.
- [20] Voziyan PA, Metz TO, Baynes JW, Hudson BG. A post-amadori inhibitor pyridoxamine also inhibits chemical modification of proteins by scavenging carbonyl intermediates of carbohydrate and lipid degradation. *J Biol Chem* 2002; 277:3397-3403.
- [21] Hipkiss AR, Brownson C. A possible new role for the anti-aging peptide carnosine. *Cell Mol Life Sci* 2000; 57:747-753.
- [22] Devamanoharan PS, Ali AH, Varma SD. Prevention of lens protein glycation by taurine. *J Mol and Cell Biochem* 1997; 177: 245-250
- [23] Negre-Salvayre A, Coatrieux C, Ingueneau C, Salvayre R. Advanced lipid peroxidation end oxidative damage to proteins. Potential diseases and therapeutic prospects inhibitors. *Br. J Pharmacol* 2008; 153: 6–20.
- [24] Münzel T, Kurz S, Rajagopalan S, Thoenes M, Berrington WR, Thompson JA, Freeman BA, Harrison DG. Hydralazine prevents nitroglycerin tolerance by inhibiting activation of a membrane-bound NADH oxidase: A new action for an old drug. *J Clin Invest* 1996; 98:1465–1470.
- [25] Maher P, Davis JB. The role of monoamine metabolism in oxidative glutamate toxicity. *J Neurosci* 1996; 16: 6394-6401.
- [26] 't Hart BA, Simons JM, Knaan-Shanzer S, Bakker NP, Labadie RP. Antiarthritic activity of the newly developed neutrophil oxidative burst antagonist apocynin. *Free Radical Biol Med* 1990; 9:127–131.
- [27] Roh JH, Suzuki H, Azakami H, Yamashita M, Murooka Y, Kumagai H. Purification, characterization, and crystallization of monoamine oxidase from *Escherichia coli*. *Biosci Biotechnol Biochem* 1994; 58:1652-1656.
- [28] Kishi H, Kishi T, Folkers K. Bioenergetics in clinical medicine. III. Inhibition of coenzyme Q10-enzymes by clinically used antihypertensive agents. *Res Commun Chem Pathol Pharmacol* 1975; 12: 533-540.
- [29] Daiber A, Oelze M, Coldewey M, Kaiser K, Huth C, Schildknecht S, Bachschmid M, Nazirisadeh Y, Ullrich V, Mülsch A, Münzel T, Tsilimingas N. Hydralazine is a powerful inhibitor of peroxynitrite formation as a possible explanation for its beneficial effects on prognosis in patients with congestive heart failure. *Biochem Biophys Res Commun* 2005; 338: 1865–1874.

- [30] Refsgaard HF, Tsai L, Stadman ER. Modification of proteins by polyunsaturated fatty acid peroxidation products. *Proc Natl Acad Sci USA* 2000; 97: 611-691.
- [31] Pennathur S, Ido Y, Heller JI, Byun J, Danda R, Pergola P, Williamson JR, Heinecke JW. Reactive carbonyls and polyunsaturated fatty acids produce hydroxyl radical-like species. *J Biol Chem* 2005; 280: 22706-22714.
- [32] Bizzozero OA. Protein carbonylation in neurodegenerative and demyelinating CNS diseases. In *Handbook of Neurochemistry and Molecular Neurobiology - Brain and Spinal cord trauma*. (Lajtha, Banik and Ray, Eds) Springer, 2008 Chapter 23, pp. 543-562.
- [33] Smerjac S, Bizzozero OA. Cytoskeletal protein carbonylation and degradation in experimental autoimmune encephalomyelitis. *J Neurochem* 2008; 105: 763-772.
- [34] Requena JS, Chao CC, Levine R, Stadtman ER. Glutamic and aminoadipic semialdehydes are the main carbonyl products of metal-catalyzed oxidation of proteins. *Proc Natl Acad Sci USA* 2001; 98: 69-74.
- [35] Pamplona R, Dalfo E, Ayala V, Bellmunt MJ, Prat J, Ferrer I, Portero-Otin M. Proteins in human brain cortex are modified by oxidation, glycoxidation, and lipoxidation. *J Biol Chem* 2005; 280: 21522-21530.
- [36] Metha R, Wong L, O'Brien PJ. Cytoprotective mechanisms of carbonyl scavenging drugs in isolated rat hepatocytes. *Chemico-Biological Interactions* 2009; 178: 317-323.
- [37] Leiro JM, Alvarez E, Arranz JA, Cano E, Orallo F. Antioxidant activity and inhibitory effects of hydralazine on inducible NOS/COX-2 gene and protein expression in peritoneal macrophages. *International Immunopharmacol* 2004; 4: 163-177.
- [38] Svensson CK, Knowlton PW, Ware JA. Effect of hydralazine on the elimination of antipyrine in the rat. *Pharmaceutical Research* 1987; 4: 515-518.

Appendix B

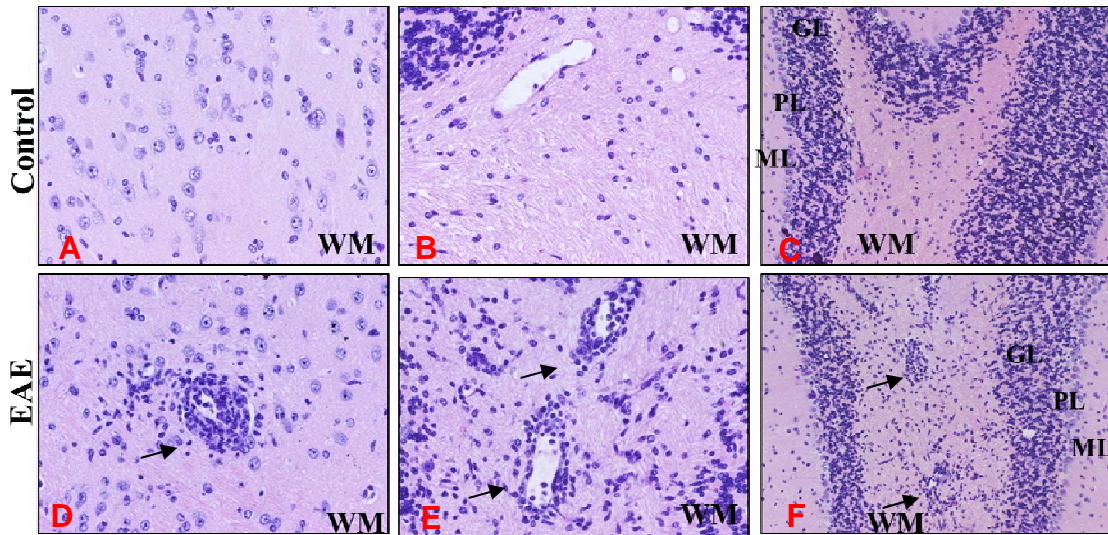


Figure B – Lymphocytes accumulate in cerebellar white matter of EAE mice. EAE was induced by active immunization with MOG35-55 peptide as described in Chapter 2. Upper Panels (A-C) and bottom panels (D-F) depict representative H&E-stained cerebellar sections from control and acute EAE, respectively. PL, purkinje cell laves; GL, granule cells layer; ML, molecular layer; WM, white matter. In panel D and E, arrows point to perivenular white matter lesions with abundant lymphocyte infiltration in the acute EAE. In panel F, arrows point to lymphocyte accumulation in the acute EAE.

Appendix C

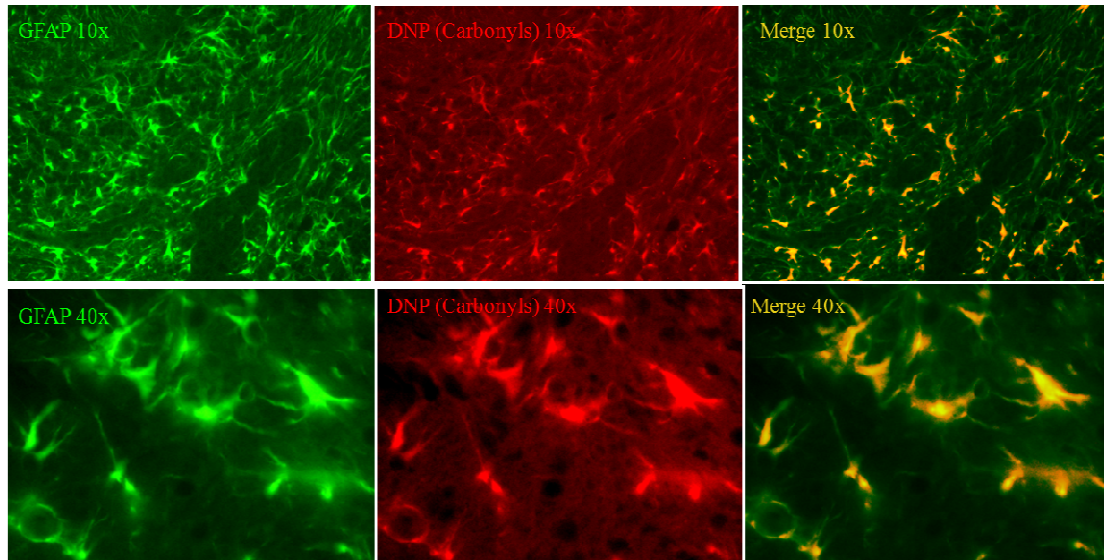


Figure C – Colocalization of carbonyls and GFAP in the cerebellum of acute EAE mice. Double immunofluorescence analysis was performed as described in Chapter 2. Green channel is for GFAP-positive astrocytes while red channel is for carbonyls. Immunofluorescent images show that cerebellar astrocytes have normal morphology and show colocalization of GFAP and carbonyl staining in their distal processes.

Appendix D

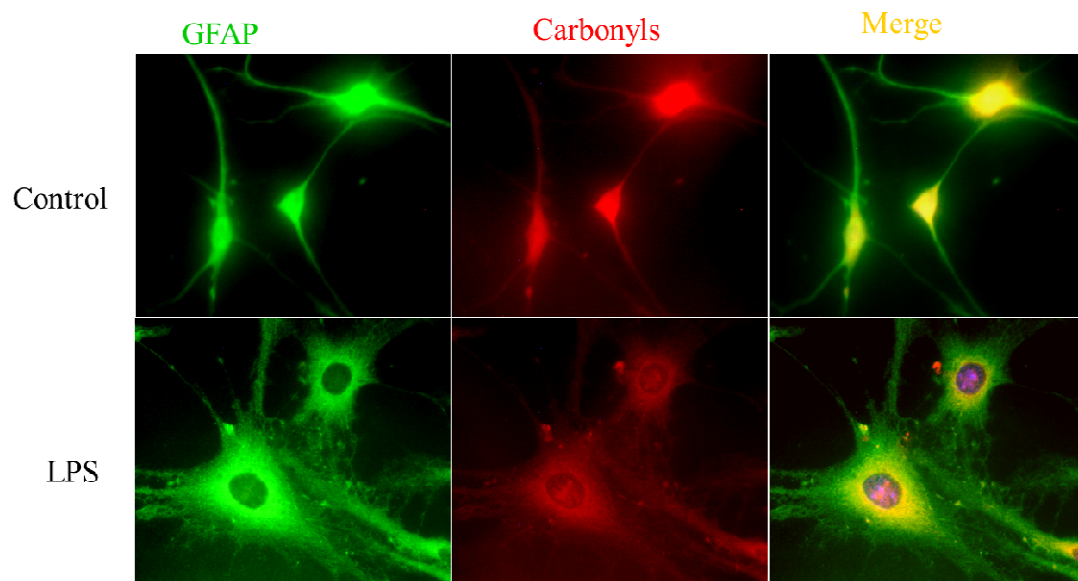


Figure D – Stimulation of astrocytes with LPS. Astrocytes were incubated with 1 $\mu\text{g/ml}$ of LPS for 24h as described in Chapter 3. Upper and lower panels depict representative a double immunofluorescence picture from untreated and LPS-treated astrocytes, respectively. GFAP, carbonyls and nuclear (DAPI) staining are shown in green, red and blue, respectively. Note the profound morphological changes of the astrocytes after LPS stimulation, including generation of dendritic processes and enlargement of cell bodies which is typical of activated astrocytes.

Appendix E

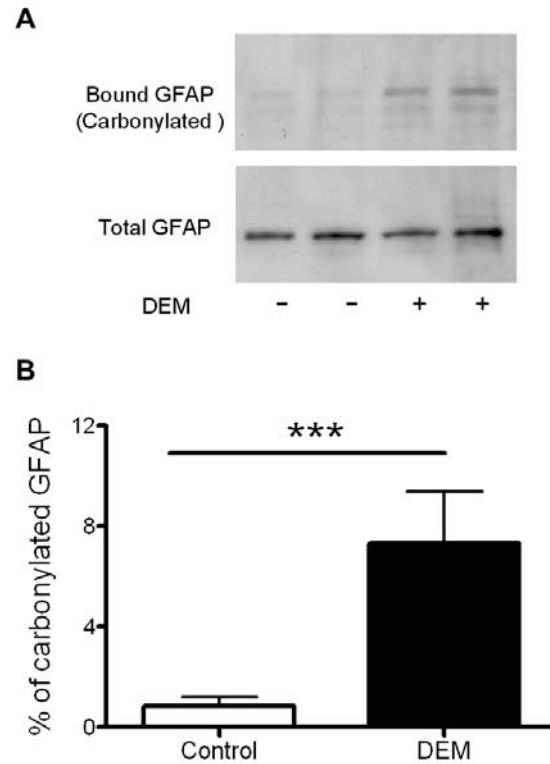


Figure E- The proportion of carbonylated GFAP in cultured astrocytes increases upon incubation with DEM. C6 cells were initially differentiated into astrocytes as described in Chapter 3. Astrocytes were then incubated with 10 μ M DEM. After 24 hours, carbonylated proteins were isolated and probed with antibodies against GFAP in Chapter 3. Densitometric scans were obtained to calculate the proportion of the carbonylated GFAP in two conditions (Panel B). Panel A is the representative blot. Values represent the mean \pm SEM of 3 experiments. * p <0.05.

Appendix F

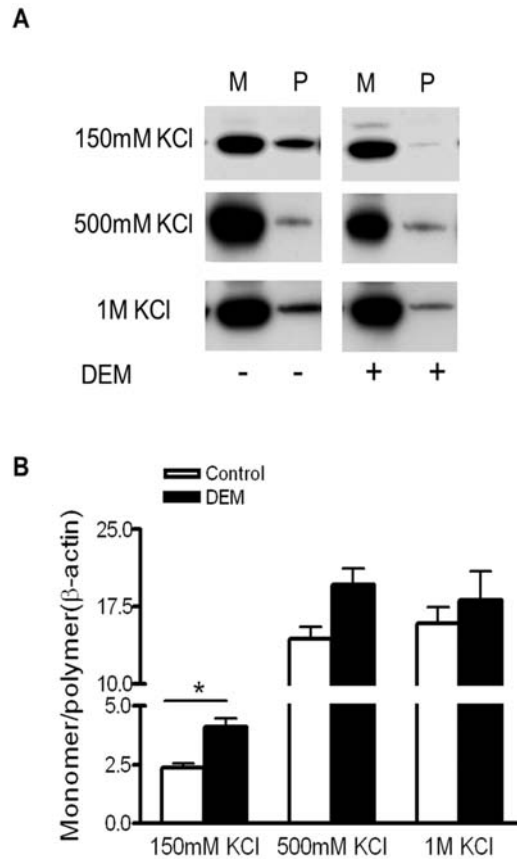


Figure F.1 The solubility of β -actin in DEM-treated astrocytes is elevated upon incubation of KCl. C6 cells were initially differentiated into astrocytes and then treated with DEM. Monomer and polymer were separated as described in chapter 5. The same volume of monomer and polymer was loaded and probed with antibodies against β -actin. Densitometric scans were obtained to calculate the ratio of monomer to polymer in β -actin under various conditions (Panel B). Panel A is the representative blot. Values represent the mean \pm SEM of 3 experiments. * $p < 0.05$. After 2 hours of incubation with 150mM KCl (an ionic strength close to a physiological medium), the ratio of monomer to polymer in β -actin is significantly elevated in the cell lysates from DEM-treated astrocytes, relative to the control. This data indicated that DEM increased the solubility or decreased the stability of β -actin under a physiological ionic strength.

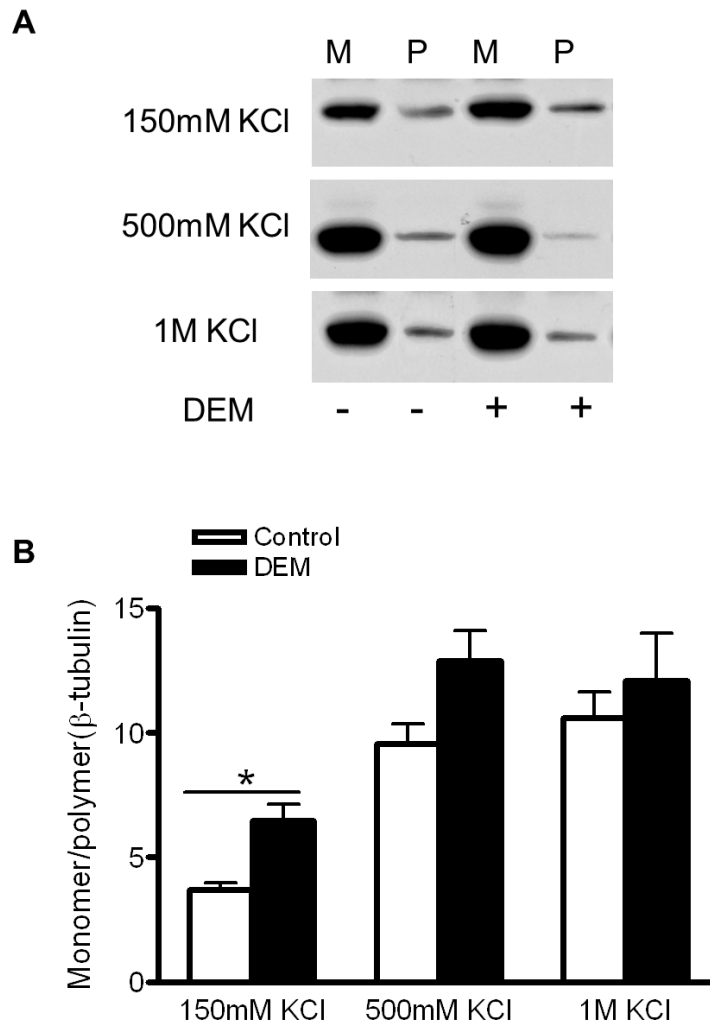


Figure F.2 The solubility of β -tubulin in DEM-treated astrocytes is elevated upon incubation of KCl. The solubility of β -tubulin to KCl upon DEM treatment is tested as described in above Figure F.1. Panel A is a representative blot while panel B shows the statistical results. Values represent the mean \pm SEM of 3 experiments. * $p < 0.05$. Similar to GFAP and β -actin, DEM increased the solubility or decreased the stability of β -tubulin under a physiological ionic strength.

Abbreviations

ACR: acrolein

AG: aminoguanidine

BSA: bovine serum albumin

CAR: carnosine

CFA: complete Freund's adjuvant

CNS: central nervous system

Cox-2: Cyclooxygenase-2,

DNP: 2,4-dinitrophenyl

DPI: days post-immunization

DTT: dithiothreitol

EAE: experimental autoimmune encephalomyelitis

ECL: enhanced chemiluminescence

ER: endoplasmic reticulum

GFAP: glial acidic fibrillary protein

GM: gray matter

GO: glyoxal

GSH: glutathione

HDJ1: DnaJ protein homolog 1

4-HNE: 4-hydroxynonenal

HY: hydralazine

HSC-71: heat shock cognate-71

IEF: isoelectric focusing

IHC: immunohistochemistry

LLVY-AMC: Suc-Leu-Leu-Val-Tyr-7-amido-4-methylcoumarin

LPO: lipid peroxidation

LPS: lipopolysaccharide

MAO: monoamine oxidase

MDA: malondialdehyde

MET: methoxylamine

MGO: methylglyoxal

MOG: myelin oligodendrocyte glycoprotein

MS: multiple sclerosis

PAC: proteasome assembling chaperones

PBS: phosphate-buffered saline

PCO: protein carbonyl

PGPH: peptidylglutamyl-peptide-hydrolyzing

POMP: proteasome maturation protein

PYR: pyridoxamine

RCS: reactive carbonyl species

ROS: reactive oxygen species

SDS: sodium dodecyl sulfate

TAU: taurine

UMP: ubiquitin-mediated proteolysis

WM: white matter

z-HH: z-histidine hydrazide

References

- Aksenov M. Y., Aksenova M. V., Butterfield D. A., Geddes J. W. and Markesbery W. R. (2001). Protein oxidation in the brain in Alzheimer's disease. *Neuroscience* 103, 373–383.
- Bizzozero O. A. (2009). Protein Carbonylation in Neurodegenerative and Demyelinating CNS Diseases. *Handbook of Neurochemistry and Molecular Neurobiology*, pp. 543-562
- Bizzozero O. A., DeJesus G., Callahan K. and Pastuszyn A. (2005). Elevated protein carbonylation in the brain white matter and gray matter of patients with multiple sclerosis. *J Neurosci Res* 81, 687–695.
- Bota D.A., Davies K.J. (2002). Lon protease preferentially degrades oxidized mitochondrial aconitase by an ATP-stimulated mechanism. *Nat Cell Biol* 4, 674-80.
- Bulteau A.L., Lundberg K.C., Humphries K.M., Sadek H.A., Szweda P.A., Friguet B. and Szweda L.I. (2001). Oxidative modification and inactivation of the proteasome during coronary occlusion/reperfusion. *J Biol Chem* 276, 30057-30063.
- Chondrogianni N. and Gonos E. S. (2008). Proteasome activation as a novel antiaging strategy. *IUBMB Life* 60, 651–655.
- Ciechanover A, Brundin P. (2003). The ubiquitin proteasome system in neurodegenerative diseases: sometimes the chicken, sometimes the egg. *Neuron* 40, 427-46.
- Dalle-Donne I., Aldini G., Carini M. (2006). Protein carbonylation, cellular dysfunction, and disease progression. *J Cell Mol Med* 10, 389-406.
- Das S., Powell S.R., Wang P. (2005). Cardioprotection with palm tocotrienol: antioxidant activity of tocotrienol is linked with its ability to stabilize proteasomes. *Am J Physiol Heart Circ Physiol*. 289, H361-7.
- Davies S.S., Amarnath V., Montine K.S., Bernoud-Hubac N., Boutaud O., Montine T.J., Roberts L.J. (2002). Effects of reactive gamma-ketoaldehydes formed by the isoprostane pathway (isoketals) and cyclooxygenase pathway (levuglandins) on proteasome function. *FASEB J* 16, 715-7.
- DING Q. (2003). Characterization of chronic low-level proteasome inhibition on neural homeostasis. *J Neurochem* 86,489–497
- Divald A. and Powell S.R. (2006). Proteasome mediates removal of proteins oxidized during myocardial ischemia. *Free Radic Biol Med* 40, 156–164.
- Dunlop, R. A., Brunk, U. T. and Rodgers, K. J. (2009) Oxidized proteins: Mechanisms of removal and consequences of accumulation. *IUBMB Life* 61, 522–527.
- Ehlers M.D. (2004). Deconstructing the axon: Wallerian degeneration and the ubiquitin-proteasome system. *Trends Neurosci* 27, 3-6.
- Farias A.S., de la Hoz C., Castro F.R., Oliveira E.C., Ribeiro dos Reis J.R., Silva J.S., Langone F., Santos L.M.B. (2007). Nitric Oxide and TNF α Effects in Experimental Autoimmune Encephalomyelitis Demyelination. *Neuroimmunomodulation* 14, 32-38.

- Farout L., Mary J., Vinh J., Szweda L.I. and Friguet B. (2006). Inactivation of the proteasome by 4-hydroxy-2-nonenal is site specific and dependent on 20S proteasome subtypes. *Arch Biochem Biophys* 453, 135-142.
- Fehlker M., Wendler P., Lehmann A., Enenkel C. (2003). Bln3 is part of nascent proteasomes and is involved in a late stage of nuclear proteasome assembly. *EMBO Rep* 4, 959–963
- Ferrante R. J., Browne S. E., Shinobu L. A., Bowling A. C., Baik M. J., MacGarvey U., Kowall N. W., Brown R. H. and Beal M. F. (1997), Evidence of increased oxidative damage in both sporadic and familial amyotrophic lateral sclerosis. *J Neurochem* 69, 2064–2074.
- Ferrington D.A., Husom A.D. and Thompson L.V. (2005). Altered proteasome structure, function and oxidation in aged muscle. *FASEB J* 19, 644-646.
- Floor E. and Wetzel M. G. (1998). Increased protein oxidation in human substantia nigra pars compacta in comparison with basal ganglia and prefrontal cortex measured with an improved dinitrophenylhydrazine assay. *J Neurochem* 70, 268–275.
- Friguet B. (2006). Oxidized protein degradation and repair in ageing and oxidative stress. *FEBS Lett* 580, 2910–2916.
- Gaczynska M. (2003). Proline- and arginine-rich peptides constitute a novel class of allosteric inhibitors of proteasome activity. *Biochemistry* pp. 8663–8670.
- Gilgun-Sherki Y., Melamed E. and Offen D. (2004). The role of oxidative stress in the pathogenesis of multiple sclerosis: the need for effective antioxidant therapy. *J Neurol* 251, 261–268.
- Glockzin S., von Knethen A., Scheffner M. and Brune B. (1999). Activation of the cell death program by nitric oxide involves inhibition of the proteasome. *J Biol Chem* 274, 19581–19586.
- Gold R., Hartung H. P. and Toyka K. V. (2000). Animal models for autoimmune demyelinating disorders of the nervous system. *Mol Med Today* 6, 88–91.
- Goldbaum O., Vollmer G. and Richter-Landsberg C. (2006). Proteasome inhibition by MG-132 induces apoptotic cell death and mitochondrial dysfunction in cultured rat brain oligodendrocytes but not in astrocytes. *Glia* 53, 891-901.
- Gonsette R.E. (2008). Oxidative stress and excitotoxicity: a therapeutic issue in multiple sclerosis? *Mult Scler* 14, 22-34.
- Grune T. Oxidative stress, aging and the proteasomal system. *Biogerontology*. 2000;1(1):31-40.
- Grune T., Shringarpure R., Sitte N., Davies K. (2001). Age-related changes in protein oxidation and proteolysis in mammalian cells. *J Gerontol A Biol Sci Med Sci* 56, B459-67.
- Hershko A., Ciechanover A. (1992). The ubiquitin system for protein degradation. *Annu Rev Biochem* 61, 761-807.
- Hoffman L, Rechsteiner M. (1994). Activation of the multicatalytic protease. The 11 S regulator and 20 S ATPase complexes contain distinct 30-kilodalton subunits. *J Biol Chem* 269, 16890-5.

- Hsiao V.C., Tian R., Long H., Der Perng M., Brenner M., Quinlan R.A., Goldman J.E. (2005). Alexander-disease mutation of GFAP causes filament disorganization and decreased solubility of GFAP. *J Cell Sci* 118, 2057-65.
- Husom A.D., Peters E.A., Kolling E.A., Fugere N.A., Thompson L.V., Ferrington D.A. (2004). Altered proteasome function and subunit composition in aged muscle. *Arch Biochem Biophys* 421, 67-76.
- James A.B., Conway A.M., Morris B.J. (2006). Regulation of the neuronal proteasome by Zif268 (Egr1). *J Neurosci* 26, 1624-34.
- Kapfahn R.J., Bigelow E.J., Ferrington D.A. (2007). Age-dependent inhibition of proteasome chymotrypsin-like activity in the retina. *Exp Eye Res* 84, 646-54.
- Keller J.N., Gee J., Ding Q. (2002). The proteasome in brain aging. *Ageing Res Rev* 1, 279-93.
- Keller J.N., Kindy M.S., Holtsberg F.W., St Clair D.K., Yen H.C., Germeyer A, Steiner SM, Bruce-Keller AJ, Hutchins JB & Mattson MP. (1998). Mitochondrial MnSOD prevents neural apoptosis and reduces ischemic brain injury: suppression of peroxynitrite production, lipid peroxidation and mitochondrial dysfunction. *J Neurosci* 18, 687–697.
- Kessova I.G. and Cederbaum A.I. (2005). The effect of CYP2E1-dependent oxidant stress on activity of proteasomes in HepG2 cells. *J. Pharmacol Exp Ther* 315, 304-312.
- Kloetzel P.M. (2004). Antigen processing by the proteasome. *Nat Rev Mol Cell Biol* 2, 179-87.
- Korhonen L. and Lindholm D. (2004). The ubiquitin proteasome system in synaptic and axonal degeneration. *J Cell Biol* 165, 27–30.
- Kornek B., Lassmann H. (1999). Axonal pathology in multiple sclerosis: a historical note. *Brain Pathol* 9, 651–656.
- Kuerten D., Kostova-Bales L., Frenzel J., Tigno M., Tary-Lehmann D., Angelov P. (2007). MP4- and MOG:35–55-induced EAE in C57BL/6 mice differentially targets brain, spinal cord and cerebellum. *J Neuroimmunol* 189, 31 - 40.
- Kurnellas M.P., Donahue K.C., Elkabes S. (2007). Mechanisms of neuronal damage in multiple sclerosis and its animal models: role of calcium pumps and exchangers. *Biochem Soc Trans* 35, 923-6.
- Lu X. (2001). Heat shock protein-90 and the catalytic activities of the 20 S proteasome (multicatalytic proteinase complex). *Arch Biochem Biophys* 387, 163–171.
- Mancuso M., Orsucci D., Coppedè F., Nesti C., Choub A., Siciliano G. (2009). Diagnostic approach to mitochondrial disorders: the need for a reliable biomarker. *Curr Mol Med.* 9,1095-107.
- Marques C., Pereira P., Taylor A., Liang J.N., Reddy V.N., Szweda L.I., Shang F. (2004) Ubiquitin-dependent lysosomal degradation of the HNE-modified proteins in lens epithelial cells. *FASEB J* 18, 1424-6.
- Martinez-Vicente M, Sovak G, Cuervo AM. Protein degradation and aging. *Exp Gerontol.* 2005 Aug-Sep;40(8-9):622-33.

- Mattson M.P., Furukawa K. (1998). Signaling events regulating the neurodevelopmental triad. Glutamate and secreted forms of beta-amyloid precursor protein as examples. *Perspect Dev Neurobiol.* 5, 337-52.
- Mayo I., Arribas J., Villoslada P., Alvarez DoForno R., Rodríguez-Vilariño S., Montalban X., De Sagarra M.R. and Castaño J.G. (2002). The proteasome is a major autoantigen in multiple sclerosis. *Brain* 125, 2658-2667.
- McCutchen-Maloney S.L. (2000). cDNA cloning, expression, and functional characterization of PI31, a proline-rich inhibitor of the proteasome. *J Biol Chem* 275, pp. 18557–18565.
- Rechsteimer M. and Hill C.P. (2005). Mobilizing the proteolytic machine: cell biological roles of proteasome activators and inhibitors. *Trends Cell Biol* 15, 27-33.
- Rechsteiner M. and Hill C.P. (2005). Mobilizing the proteolytic machine: cell biological roles of proteasome activators and inhibitors. *Trends Cell Biol* 15, 27-33.
- Reinheckel T., Ullrich O., Sitte N., Grune T. (2000). Differential impairment of 20S and 26S proteasome activities in human hematopoietic K562 cells during oxidative stress. *Arch Biochem Biophys* 377,65-8.
- Rockwell P., Yuan H., Magnusson R. and Figueiredo-Pereira M.E. (2000). Proteasome inhibition in neuronal cells induces a proinflammatory response manifested by upregulation of cyclooxygenase-2, its accumulation as ubiquitin conjugates, and production of the prostaglandin PGE(2). *Arch Biochem Biophys* 374, 325-333.
- Shringarpure R., Grune T., Mehlhase J. and Davies K.J. (2003). Ubiquitin conjugation is not required for the degradation of oxidized proteins by proteasome. *J Biol Chem* 278, 311–318.
- Sitte N., Huber M., Grune T., Ladhoff A., Doecke W., Von Zglinicki T. and Davies J.A. (2000) Proteasome inhibition by lipofuscin/ceroid during postmitotic aging of fibroblasts. *FASEB J* 14, 1490-1498.
- Smerjac S.M. and Bizzozero O.A. (2008) Cytoskeletal protein carbonylation and degradation in experimental autoimmune encephalomyelitis. *J Neurochem* 105, 763-772.
- Tanahashi N., Murakami Y., Minami Y., Shimbara N., Hendil K.B. and Tanaka K. (2000). Hybrid proteasomes: induction by interferon- γ and contribution to ATP-dependent proteolysis. *J Biol Chem* 275, 14336–14345.
- Trapp B.D., Syts P.K., (2009). Virtual hypoxia and chronic necrosis of demyelinated axons in multiple sclerosis. *Lancet Neurol* 8, 280-291.
- Troncoso J.C., Costello A.C., Kim J.H. and Johnson G.V. (1995). Metal-catalyzed oxidation of bovine neurofilaments in vitro. *Free Radic Biol Med* 18, 891-899.
- Ustundag Y., Bronk S.F., Gores G.J. (2007). Proteasome inhibition-induces endoplasmic reticulum dysfunction and cell death of human cholangiocarcinoma cells. *World J Gastroenterol.* 13, 851-7.
- Yan L.J., Sohal R.S. (1998). Mitochondrial adenine nucleotide translocase is modified oxidatively during aging. *Proc Natl Acad Sci* 95,12896-901.
- Zaiss D.M. (1999). The proteasome inhibitor PI31 competes with PA28 for binding to 20S proteasomes. *FEBS Lett* 457, 333–338.

Zheng J, Bizzozero OA. (2010) Traditional reactive carbonyl scavengers do not prevent the carbonylation of brain proteins induced by acute glutathione depletion. *Free Radic Res* 44, 258-66.